



**HAL**  
open science

## Chapter 1 - The Rare Earth Resources of Europe and Greenland - Mining Potential and Challenges

Nicolas Charles, Johann Tuduri, Gaëtan Lefebvre, Olivier Pourret, Fabrice Gaillard, Kathryn Goodenough

► **To cite this version:**

Nicolas Charles, Johann Tuduri, Gaëtan Lefebvre, Olivier Pourret, Fabrice Gaillard, et al.. Chapter 1 - The Rare Earth Resources of Europe and Greenland - Mining Potential and Challenges. *Metallic Resources 1: Geodynamic Framework and Remarkable Examples in Europe*, Wiley, pp.1-142, 2023, 10.1002/9781394264810.ch1 . hal-04394758

**HAL Id: hal-04394758**

**<https://normandie-univ.hal.science/hal-04394758>**

Submitted on 2 Jul 2024

**HAL** is a multi-disciplinary open access archive for the deposit and dissemination of scientific research documents, whether they are published or not. The documents may come from teaching and research institutions in France or abroad, or from public or private research centers.

L'archive ouverte pluridisciplinaire **HAL**, est destinée au dépôt et à la diffusion de documents scientifiques de niveau recherche, publiés ou non, émanant des établissements d'enseignement et de recherche français ou étrangers, des laboratoires publics ou privés.

# 1

## The Rare Earth Resources of Europe and Greenland: Mining Potential and Challenges

**Nicolas CHARLES<sup>1</sup>, Johann TUDURI<sup>1,2</sup>,  
Gaétan LEFEBVRE<sup>1</sup>, Olivier POURRET<sup>3</sup>,  
Fabrice GAILLARD<sup>2</sup> and Kathryn GOODENOUGH<sup>4</sup>**

<sup>1</sup>*BRGM, Orléans, France*

<sup>2</sup>*ISTO, CNRS, University of Orléans, France*

<sup>3</sup>*AGHYLE, UniLaSalle, Beauvais, France*

<sup>4</sup>*British Geological Survey, Edinburgh, United Kingdom*

### 1.1. Introduction

In the past few years, 17 metal elements have absorbed the principal attention of industrialized countries, which are now aiming for a digital transformation and energy transition. Rare earths, which were little used in industry at the outset, are strategic metals today, a kind of vitamin for digital and green technologies (Bru et al. 2015; EC 2019a, 2019b; Blengini et al. 2020; Dushyantha et al. 2020). Used anecdotally in the 1950s and 1960s within heavy mineral placers in Australia, India, South Africa or Brazil, their attractiveness grew, and the United States became their main producer from the 1970s to 1980s with its Mountain Pass deposit.

At the end of the 1980s, China then became the main global producer of rare earths. In 1992, the first secretary of the Chinese Communist Party, Deng Xiaoping, was pleased to say that “the Middle East has oil; China has rare earths”. This is still the case for China today with its hegemonic position, which it owes to the use of gigantic deposits such as Bayan Obo, but above all to its expertise in rare earth separation.

At the outset, everyone seemed to accommodate this situation, with importing countries benefiting from the low price, while also avoiding the environmental and social impacts of mining these metals on their own territory.

It took a diplomatic incident involving a small island in the East China Sea for the whole situation to change in September 2010. China declared an embargo on the export of rare earths to Japan, a major importer of rare earths and a country at the forefront of digital technologies. Then, the lowering of Chinese export quotas lit the keg in 2011, with the rapid increase in the price of rare earths (as much as 10,000% for dysprosium).

Many countries were already aware of the vulnerability of their supply chain, principally in Europe (EC 2011, 2017; Sebastiaan et al. 2017; Lauri et al. 2018; Blengini et al. 2020). Rare earths were already strategic raw materials, and their criticality for European industry was classed as a priority. Therefore, for some years mining for rare earths benefited from investments intended for finding alternatives to the Chinese deposits.

In addition to the study of primary deposits (Goodenough et al. 2016; EURARE 2017; Tuduri et al. 2020), the recycling path was also considered (Ahonen et al. 2015; Guyonnet et al. 2015). It transpired that Europe and Greenland (a constituent territory of Denmark) had real potential for rare earth mining that could support the needs of the Old Continent for several decades, or even beyond. Europe was the continent where rare earths were discovered in 1787, but to date, there is no mine for these metals, and 95% of their imports depend on China (Gislev and Grohol 2018).

Geological potential is not all, however, and an entire value chain must be developed, from the extraction of the minerals, or rather of rare earth minerals, which require processing techniques adapted for each of them, to their transformation into high added value products (Ahonen et al. 2015).

It is here that the challenges begin, because the investments to be considered are colossal. In addition, what about the environmental, social and societal acceptability of mining activity in Europe? Although Europe has remarkable rare earth potential, can we envisage exploiting it? This original summary provides a panorama of rare

earths in Europe through their physicochemical, mineralogical, socioeconomical, geodynamic and metallogenetic aspects.

## 1.2. The extreme diversity of rare earths

### 1.2.1. Rare earth elements

#### 1.2.1.1. Definitions

“Rare earths” is a collective name given, for historical and practical reasons, to a set of metal elements in the periodic table (Figure 1.1). Rare earth elements (REEs) are elements called “trace elements” in most natural environments. REEs are a group of 17 metal elements that are coherent in terms of ionic rays, charge and coordination. According to the definitions (Henderson 1984; Lipin and McKay 1989; Jones et al. 1996; Atwood 2012), the REEs include lanthanides (from  $^{57}\text{La}$  to  $^{71}\text{Lu}$ ), yttrium ( $^{39}\text{Y}$ ) and sometimes scandium ( $^{21}\text{Sc}$ ).

Scandium’s membership in this group has given rise to debate since its behavior in geological environments is generally different from that of the other REEs. Similarly, promethium ( $^{61}\text{Pm}$ ), with its extremely short half-life, is almost non-existent in nature.

Depending on the specific electron configurations within each atom, the REEs can be divided into two subgroups:

- the light rare earth elements (LREE) with La-Ce-Pr-Nd-Sm-Eu-Gd;
- the heavy rare earth elements (HREE) with Tb-Dy-Ho-Er-Tm-Yb-Lu-Y.

It should be noted, however, that the membership of some REEs to one of the two subgroups is still debated (Gupta and Krishnamurthy 2005; Chakhmouradian and Wall 2012; McLennan and Taylor 2012; Weng et al. 2013; Zepf 2013). There is therefore a classification specific to the mining industry that differs from that recommended by the International Union of Pure and Applied Chemistry (IUPAC). For economic reasons linked to geological abundance, to the costs of processing the ore, to separation techniques, etc., many actors in the mineral industry only consider these as LREE: La-Ce-Pr-Nd.

These same industrial actors separate and sell their concentrations of rare earths in the form of oxides, and it is usual to consider these elements in terms of rare earth oxides (REO). Thus, the terms light rare earth oxides (LREOs) and heavy rare earth oxides (HREOs) are generally considered over the course of any value chain, from mining exploration to their separation, by mining extraction.

1 H	Sc : scandium Y : yttrium La : lanthanum Ce : cerium Pr : praseodymium Nd : neodymium																Pm : promethium Sm : samarium Eu : europium Gd : gadolinium Tb : terbium Dy : dysprosium										Ho : holmium Er : erbium Tm : thulium Yb : ytterbium Lu : lutetium						2 He
3 Li	4 Be											5 B	6 C	7 N	8 O	9 F	10 Ne																
11 Na	12 Mg											13 Al	14 Si	15 P	16 S	17 Cl	18 Ar																
19 K	20 Ca	21 Sc	22 Ti	23 V	24 Cr	25 Mn	26 Fe	27 Co	28 Ni	29 Cu	30 Zn	31 Ga	32 Ge	33 As	34 Se	35 Br	36 Kr																
37 Rb	38 Sr	39 Y	40 Zr	41 Nb	42 Mo	43 Tc	44 Ru	45 Rh	46 Pd	47 Ag	48 Cd	49 In	50 Sn	51 Sb	52 Te	53 I	54 Xe																
55 Cs	56 Ba	57-71 Lanthanides	72 Hf	73 Ta	74 W	75 Re	76 Os	77 Ir	78 Pt	79 Au	80 Hg	81 Tl	82 Pb	83 Bi	84 Po	85 At	86 Rn																
87 Fr	88 Ra	89-103 Actinides	104 Rf	105 Db	106 Sg	107 Bh	108 Hs	109 Mt	110 Ds	111 Rg	112 Cn	113 Uut	114 Uuq	115 Uup	116 Uuh	117 Uus	118 Uuo																
										<b>Light Rare Earths (LREE)</b>								<b>Heavy Rare Earths (HREE)</b>															
		<b>Lanthanides</b> 57 La 58 Ce 59 Pr 60 Nd 61 Pm 62 Sm 63 Eu 64 Gd 65 Tb 66 Dy 67 Ho 68 Er 69 Tm 70 Yb 71 Lu																															
		<b>Actinides</b> 89 Ac 90 Th 91 Pa 92 U 93 Np 94 Pu 95 Am 96 Cm 97 Bk 98 Cf 99 Es 100 Fm 101 Md 102 No 103 Lr																															

**Figure 1.1.** Rare earth elements in the periodic table of elements

#### 1.2.1.2. The physical and chemical properties of the rare earths

The REEs have physical-chemical properties much sought after by manufacturers, thanks in particular to their internal electron structure linked to their 4f electron subshell. The REEs in neutral metallic form have fairly similar atomic radii, except for europium and ytterbium, whose larger atomic radii explain their lower densities. Their hardnesses are variable, ranging from soft (La, Nd, Yb) to hard (Ho, Er, Lu).

The REEs are moderately fusible, and their fusion temperatures range between 799°C (Ce) and 1,663°C (Lu). The spectral properties of REEs are most remarkable for absorption (coloration), as well as for transmission (luminescence), which explains their current use in phosphors and lasers. It is the electrons' level of mobility in the atoms' energy levels that forms the basis of this property. Subject to powerful rays (e.g. UV rays), an REE atom surrounded by ligands (oxides or molecules) will be excited electronically, and de-excitation of the REE atom will result in the emission of light with wavelength emission peaks specific to the REE element (e.g. Y and Eu: red and blue; Tb and Tm: green; Ce: yellow).

The other remarkable physical property of some REEs is their magnetism, which is the origin of their use for making high-performance permanent magnets (high magnetization and remanence). REEs paired with transition elements (Fe, Co) allow the creation of the most coercive magnets manufactured at the industrial scale (Sm-Co, Nd-Fe-B).

From a chemical point of view, REEs are reducing metals (deoxidation and desulfurization properties). Most take between a few days and a few months to oxidize rapidly in air and at ambient temperature (Eu, La, Ce, Pr, Nd). The HREEs resist oxidation for several years (Y, Dy, Ho, Er). Finely ground, Ce allied with Fe (ferrocium) burns in air. This was one of the first applications of REEs with flint-spark-lighters formed of ferrocium. In minerals, REEs are in trivalent cation form. Although the ionic radius varies from one rare earth to another, their chemical properties remain remarkably homogeneous, especially in solution. Although many substitutions between REEs are produced within the crystalline network of minerals, some mineral species are better adapted and more favorable to receiving a range of ionic radii. This is the case with “ceric earth” minerals, which are more inclined to incorporate Ce, La, Nd, Pr, (Sm), (Eu) and (Gd), such as monazite and bastnäsite. Other minerals called “yttric earths” are more favorable to Y, Tb, and Dy, such as xenotime and gadolinite.

#### 1.2.1.3. *A brief history of rare earths*

The discovery of rare earths began in 1787 in Sweden. Remember in passing that the word “earths” was the name given by chemists to the metal oxides supposed to be simple bodies. The epithet “rare” recalls the difficulties encountered by chemists in isolating them and their supposedly low concentration in ores. Carl Axel Arrhenius, a Swedish chemist, described for the first time a dense, black mineral in the pegmatites of Ytterby. They were sent for analysis to the Finnish chemist Johan Gadolin. In 1794, he discovered a new “earth” contained in this mineral, *yttria*, which would give its name to ytterbite, since it was known by the name gadolinite. However, a reddish mineral was discovered earlier, in 1751, by the Swedish mineralogist Axel Fredrik Cronstedt in the copper mine at Bastnäs. It was only in 1803 that the Swedish chemists Jöns Jakob Berzelius and Wilhelm Hisinger isolated a new “earth” with properties similar to *yttria*. This new earth was called *ceria*, a reference to the asteroid Ceres that had just been discovered, and would give its name to the mineral bastnäsite.

Throughout the 19th century, different chemists discovered that some previously isolated earths actually contained several other chemical elements with similar properties. For example, in 1839, Carl Gustaf Mosander discovered that cerium oxide is also formed of an oxide of another element that he would call lanthanum (from the Greek *lanthano*: to be hidden). In 1843, he discovered that ytterbium was in fact a mixture containing two other elements, terbium and erbium. The final REE element, lutetium, was discovered in 1907. Finally, it should be noted that promethium was discovered in 1947 in uranium fission products from the Oak Ridge reactor (United States).



in numerous primary deposits. Conversely, the HREEs are clearly less abundant, much like the rare metals (Sn, W, Ta) and are therefore much rarer, including in deposits of these elements (except Y). For this reason, HREEs are considered to be more strategically important than LREEs, hence their much higher market value. Thus, the HREO/LREO ratio is a critical parameter for evaluating a deposit.

In fact, it is the low quantity of natural minerals containing REEs that explains the term “rare”. Although more than 200 REE mineral species are known today (this number remains low), only some of them (Table 1.1) are of commercial interest (Gupta and Krishnamurthy 2005). In fact, although REEs are often incorporated into the crystal lattice of carbonates, oxides, silicates or even phosphates as a substitution for other more common chemical elements, the mineral industry values only a very small number of REE ores: bastnäsite (fluorocarbonate), monazite and xenotime (phosphates), and loparite (oxide). REEs have also been extracted from apatite in Russia and South Africa, but this production was extremely limited.

Except for xenotime, which is enriched with HREEs, all of these minerals are essentially characterized by their richness in LREEs. Since lanthanides share similarities with elements from the actinide group, the REE minerals also and almost systematically include radioactive elements (e.g. Th and/or U). Uraninite, as well as thorite may also accompany REE minerals. The presence of these radioactive elements is a restriction on mining project development. In fact, radioactivity accompanies every stage of the ore enrichment process, right up to metallurgy. These minerals and radioactive elements are a form of waste that must be managed rigorously. For these reasons, it is necessary to focus on the U and Th contents in deposits, particularly on the  $\text{ThO}_2/\text{REO}$  and  $\text{U}_3\text{O}_8/\text{REO}$  ratios of the minerals that form the ore.

Extracted from the main Chinese mines of Bayan Obo, Maoniuping Weishan and Dalucao, as well as from the Mountain Pass mine in the United States, bastnäsite is the main REE ore (Verplanck et al. 2016; Jia and Liu 2020). Since the 1970s, so-called ionic clays, or lateritic ion-adsorption clays, have formed an important source of HREEs (Bao and Zhao 2008). This production, located uniquely in southern China in Longnan (Jiangxi), but also in the provinces of Guangdong and Guangxi, is favored because of the low cost of labor and relatively simple extraction procedures using in situ lixiviation with neutral or acidic solutions.

However, with extremely low ore grades or 0.03–0.35% REO (Chi and Tian 2008; Zhou et al. 2017), such procedures question the balance between economic feasibility and protection of the environment. Nevertheless, the high proportion of HREEs coupled with the very low concentration of radioactive elements (U, Th) associated with this type of deposit make it an attractive challenge in mineral exploration.

Mineral	Chemical formula	Concentration (%)		
		RE <sub>2</sub> O <sub>3</sub>	ThO <sub>2</sub>	UO <sub>2</sub>
Allanite	([REE],Ca) <sub>2</sub> (Al,Fe) <sub>3</sub> Si <sub>3</sub> O <sub>12</sub> (OH)	2.5–17	<3	–
Ancylite	Si[LRREE](CO <sub>3</sub> ) <sub>2</sub> (OH).H <sub>2</sub> O	46–53	<0.4	<0.1
Apatite	Ca <sub>5</sub> (PO <sub>4</sub> ) <sub>3</sub> (F,Cl,OH)	<<2	–	<0.05
Bastnäsite	[LRREE]CO <sub>3</sub> (F,OH)	58–75	<2.8	<0.1
Clays	REE adsorbed on kaolinite/halloysite Al <sub>2</sub> Si <sub>2</sub> O <sub>5</sub> (OH) <sub>4</sub>	<<4	<0.01	<0.001
Eudialyte	(Na, <sub>2</sub> [REE]) <sub>15</sub> (Ca, <sub>2</sub> [REE]) <sub>6</sub> (Fe, <sub>2</sub> Mn) <sub>3</sub> (Si, <sub>2</sub> Nb) <sub>2</sub> (Zr, <sub>2</sub> Ti) <sub>3</sub> Si <sub>24</sub> O <sub>72</sub> (OH, <sub>2</sub> F, <sub>2</sub> Cl, <sub>2</sub> H <sub>2</sub> O) <sub>6</sub>	1–10	–	<0.1
Euxenite	([REE],U,Th)(Nb,Ta,Ti) <sub>2</sub> O <sub>6</sub>	16–30	<4.3	3–9
Fergusonite	[REE]NbO <sub>4</sub>	43–52	<8	<13.6
Gadolinite	[REE] <sub>2</sub> FeBe <sub>2</sub> Si <sub>2</sub> O <sub>10</sub>	45–54	<0.4	–
Loparite	(Na, <sub>2</sub> [LRREE],Ca,Sr,Th)(Ti,Nb,Ta)O <sub>3</sub>	28–37	1.6	0.03
Monazite	([LRREE],Th,Ca)(P,Si)O <sub>4</sub>	35–71	<20	<16
Parisite	Ca[LRREE] <sub>2</sub> (CO <sub>3</sub> ) <sub>3</sub> F <sub>2</sub>	50–59	<4	<0.3
Pyrochlore	(Ca, <sub>2</sub> Na, <sub>2</sub> U,[REE]) <sub>2</sub> (Nb,Ta) <sub>2</sub> O <sub>6</sub> (OH,F)	<22	<4	<27
Steenstrupine	Na <sub>14</sub> [LRREE] <sub>6</sub> Mn <sub>2</sub> Fe <sub>2</sub> (Zr,Th)(PO <sub>4</sub> ) <sub>7</sub> Si <sub>12</sub> O <sub>36</sub> .3(H <sub>2</sub> O)	<31	<6	<1
Thorite	(Th,U, <sub>4</sub> [REE])SiO <sub>4</sub>	<3	65–81	10–16
Uraninite	UO <sub>2</sub>	<1.5	<12.2	50–98
Xenotime	([HREE],Zr,U)(P,Si)O <sub>4</sub>	54–74	<8.4	<5.8
Zircon	(Zr, <sub>2</sub> [HREE],Th,U)SiO <sub>4</sub>	<19	0.01–0.8	0.01–4

Table 1.1. Minerals valued by the extraction industry (Tuduri et al. 2015)

The last decade has seen the emergence of a substantial market for the exploration of REEs, intended to find resources outside of China. Although different projects are in the process of valuation, many of them are innovative projects since they are not conventional and thus present economic risks. Some projects correspond to new deposit models, and others seek to develop new minerals: pyrochlore, fergusonite, oxides and numerous silicates (e.g. allanite, eudialyte, steenstrupine). These mineral stages, especially silicates, have the advantage of being enriched with HREOs.

### 1.3. The economy of rare earths in the world and their place in Europe

#### 1.3.1. The application domains for rare earths

The first use of REEs was attested in 1885, when cerium was used in gas sleeves in the city of Vienna. The usage of REEs was very limited until the 1960s (ferrocium in lighter flints), then more diversified with applications in technology from the 1970s (color cathode screens, lasers, phosphors, etc.) and 1980s (permanent magnets).

REEs have exceptional magnetic, electronic, optical and catalytic properties, and are particularly useful today for ever more diversified, well-developed technologies, especially in the defense industry, electronics and renewable energies (Figures 1.3 and 1.4) (Balaram 2019; Dushyantha et al. 2020). REEs are used in different chemical forms: metals, alloys, oxides and chlorides.

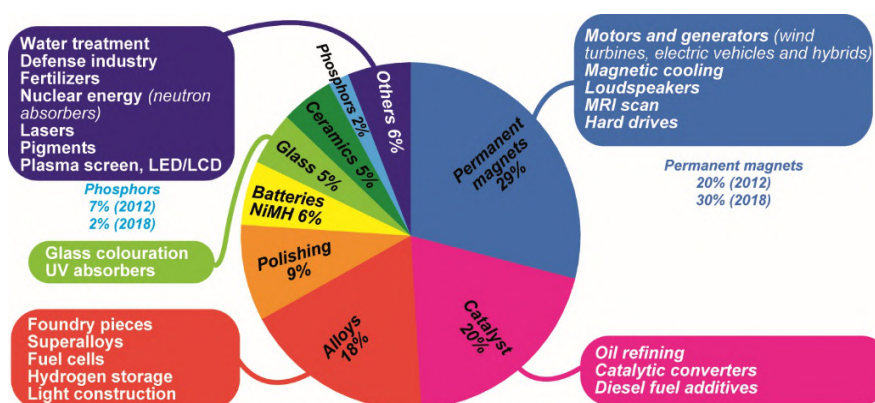


Figure 1.3. Global distribution of REE use by sector in 2018

Element	Applications
Y	Lighting, ceramics, metal alloys, lasers, catalysts
La	Catalyst for oil cracking, NiMH batteries, metal alloys, optics, lighting, mischmetal
Ce	Glass polishing, metal alloys, auto-catalysts, optics, lighting, mischmetal
Pr	Permanent magnets, lighting, ceramics, mischmetal, metal alloys, oxydation catalysts
Nd	Permanent magnets, ceramics, metal alloys, mischmetal, lighting, lasers
Pm	Nuclear batteries, defence, X-rays source in measurement instruments
Sm	Permanent magnets, optics, medicine, nuclear industry
Eu	Lighting, optics, nuclear industry
Gd	Permanent magnets, metal alloys, lighting, medical imaging, lasers
Tb	Lighting, permanent magnets, metal alloys, electronic components doping
Dy	Permanent magnets, metal alloys, optics, nuclear industry
Ho	Glass coloration, laser crystal doping
Er	Glass coloration, lighting, telecommunication optics, medical lasers
Tm	Laser fibres and lighting doping
Yb	Laser crystals component, seismic measurements, metals
Lu	Medical tomography, ceramics, metal alloys, lasers, catalyst

**Figure 1.4.** *The main applications for each REE (Bru et al. (2015) and references therein; Sebastiaan et al. (2017))*

REEs made it possible to increase the performance of technological products, while still ensuring miniaturization, such as with magnets, and they deserve the name “the vitamins of modern industry” (Balaram 2019). For some years, REEs have excited additional interest in their use in manufacturing green technologies (wind turbines, solar panels), which are indispensable for ensuring energy transition (Judge et al. 2017). Thus, the use of Pr, Gd, Eu and Er in nanoparticle form in solar panels makes it possible to improve the capacity to convert photons into energy. Pr, Nd, Tb and Dy are used in permanent magnets in wind turbines and allow them to be lightened drastically (a 100 g NdFeB magnet is equivalent to a 1 kg traditional magnet), also allowing the miniaturization of the engine, while still ensuring increased performance, even at low wind speeds, as well as reduced maintenance.

Nevertheless, the market volatility of REE has led substitution elements to be found (Bru et al. 2015; Pavel et al. 2017). Other less well-known REE domains are zootechnics and agriculture since REEs play an essential role in the working and structure of the molecules of biological systems, especially La and Ce (Abdelnour et al. 2019). REEs are thus incorporated into animal food and fertilizer. REEs can also be used for military purposes, in the form of effective permanent magnets

(SmCo, NdFeB), useful in guiding systems for missiles, fighter planes and drones, or for on-board electrical engines. Tb, Er and Gd are useful for night vision optical lenses. Y is used in the manufacture of highly resistant ceramics (tanks, bullet-proof vests). Eu and Lu allow radar signals to be amplified or are useful in sonar detection.

The sectors where REEs are used have evolved extensively since 2010, the year of the global crisis triggered by the restriction of Chinese exports and a momentary drop in global consumption (Bru et al. 2015). Since 2012, the growth of this consumption has resumed and exceeded 100,000 t REO (Figure 1.6), particularly due to the permanent magnet sector. The main technology used is NdFeB magnet technology, using Nd and Pr in particular and, to a lesser extent, Dy and Tb for high-performance applications. The application that consumes the most REEs globally is NdFeB magnets, with approximately 30% of REE use in tonnage in 2018 and nearly 53% of the total value of the REE market. This demand is increasing by 10% per year. There are multiple sectors for the use of these magnets, such as the domain of high-efficiency electrical engines, where they allow miniaturization (electronics, robotics), and lightning of equipment (offshore wind farms, electrical vehicle engines, etc.)

Other sectors using REEs are becoming a minority in proportion (Bru et al. 2015), either due to restricted or specific uses (the defense industry, medical lasers, etc.), or on the contrary, usage with low added value for applications where performance is of less importance (polishing powders catalysts in cars, metallurgical alloys).

### **1.3.2. The evolution of prices**

There is a great disparity between the price of LREEs, which are very abundant, and that of HREEs, which are reserved for niche applications because of their rarity. These prices thus range from single to triple digits or more depending on the elements (Figure 1.5).

These prices have also varied greatly over time, with prices multiplying by several dozen between 2002 and 2003, reaching a peak in July 2011, before a great drop, then a new and relative equilibrium after 2015. The very sharp rise in the prices of all REEs began at the start of 2010, was amplified after February 2011, and reached its height in mid-July 2011. On July 14, 2011, the price of dysprosium-metal reached 3,410 US\$/kg, a multiplication by a factor of 106 compared to the average price of this metal from 2002–2003 (then, it was 32.1 US\$/kg), which is an increase of 10,500%, which is probably an absolute record for all raw materials combined.

The sky-rocketing of prices in 2010–2011 was triggered by the conjunction of two main factors:

- the decision to reduce Chinese export quotas considerably (these exceeded approximately 60 kt from 2006–2007, 57 kt in 2008, 50 kt in 2009 and then 30 kt/year from 2010);

- the increase in demand (after a marked drop in 2009 in the context of the slump following the economic crisis) and in anticipation of furthering this increase, particularly for permanent magnets (the push for renewable energies, including wind power; anticipating, at that time, the striking take-off of the electric vehicle market, etc.), and phosphors (the increasingly widespread replacement of incandescent bulbs by compact fluorescent bulbs).

The incident at the Senkaku/Diaoyu Islands, in September 2010 between China and Japan, led China to declare an embargo on the export of REEs to Japan in October 2010. Cited by many as the trigger for the spike in the price of REEs, this event, in reality, only accentuated the rise in prices that had already begun several months before and that continued for several months afterwards. Threats to world supplies outside China following this event led manufacturer-users to buy to create preventive stocks, thus contributing to a price increase, the whole accentuated by a speculative factor. Following a classical “bubble” mechanism, soaring prices led to a drop in demand (Figure 1.6). This drop in consumption led to the “bursting” of this bubble and a near-continuous fall in prices for two years (between mid-2011 and mid-2013).

After occasional rises in 2014 and 2017 linked to imbalances in supply and demand and the effect of advertising (Lefebvre 2017), the prices of different REEs remained at almost unchanged levels until 2020. Expressed in metal form at 99% FOB China, La and Ce remained at almost unchanged levels in 2018 and 2019, at 6 \$/kg on average. The price of Tb, then more expensive than REEs, became established at approximately 600 \$/kg, whereas Dy is exchanged at 250 \$/kg on average. Finally, the prices of Nd and Pr have stabilized today at 55 \$/kg and 100 \$/kg, respectively (compared to 85 \$/kg on average from 2016 and 2017 for Pr, illustrating its growing role in permanent magnets).

The health crisis linked to the global Covid-19 pandemic had a limited impact on the rare earths market in China. Although 70–80% of rare earth transformation capacities underwent temporary interruptions in January and February 2020, linked to lockdown (in particular, capacities for processing HREEs in the southern regions, of the provinces of Jiangxi and Guangdong, close to the city of Wuhan), most of them were already functioning at less than full capacity or involved illegal or

obsolete sites. There was therefore excess capacity in the country for the production of rare earths, which limited the impact of the health crisis on the sector. Only dysprosium and terbium, the HREE elements involved in high-performance, permanent NdFeB magnets (in temperature conditions higher than 200°C), saw high prices between January and March 2020: 15.5% for metal terbium (762 \$/kg) and 20% for metal dysprosium (372 \$/kg), respectively, reflecting the low stocks available rather than an underlying trend.

The increase in demand linked to the take-off in sales of electrical vehicles and renewable energies, faced with limitations mine in Chinese production capacities (Figure 1.6), could lead to a new rise in prices between now and 2025. On average, demand for REEs is progressing from 8 to 10% per year and should continue at this rate, driven by the rise in electrical vehicles, as well as by the rise in electronics and robotics. At such a rate, global REE consumption could double in less than 10 years.

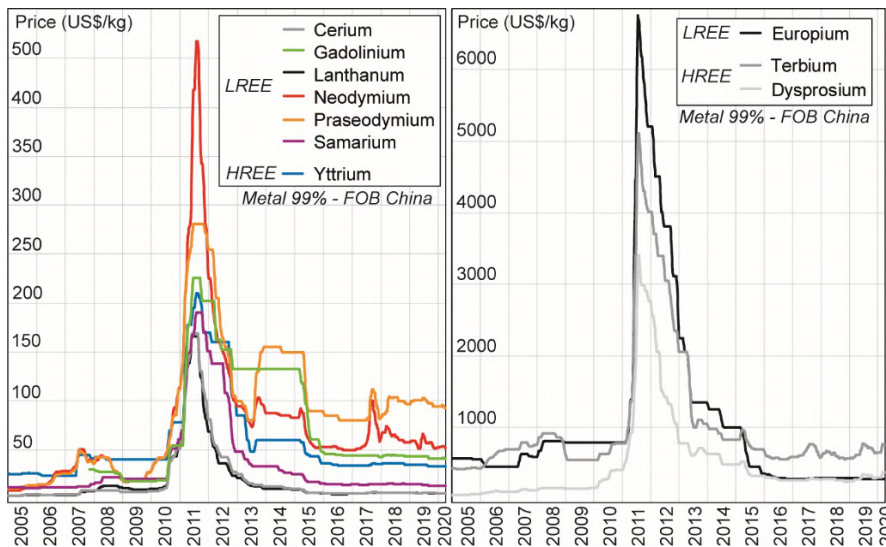


**Figure 1.5.** Evolution of prices for the main REEs (source: BRGM)

The case of electrical vehicles is eloquent. Although sales were in the order of two million units in 2018, many scenarios predict an exponential increase in 2030 between 20 and 38 million/year, as estimated by the International Energy Agency (New Policies Scenarios and EV30). Indeed, according to data from the consultant Roskill (2018), 90% of new electric vehicles are equipped with engines using permanent REE magnets (dominated by Chinese models, but also Tesla for its Model 3 Long Range) compared to induction motor technology, chosen especially

by BMW to eliminate the need for REEs. Consequently, with an average value of 2 kg of permanent magnets mounted on each vehicle, which is 750 g of Nd-Pr alloy, this new market would reach between 15,000 and 28,500 tons of Nd-Pr allowance, compared to 3,000 tons in 2018.

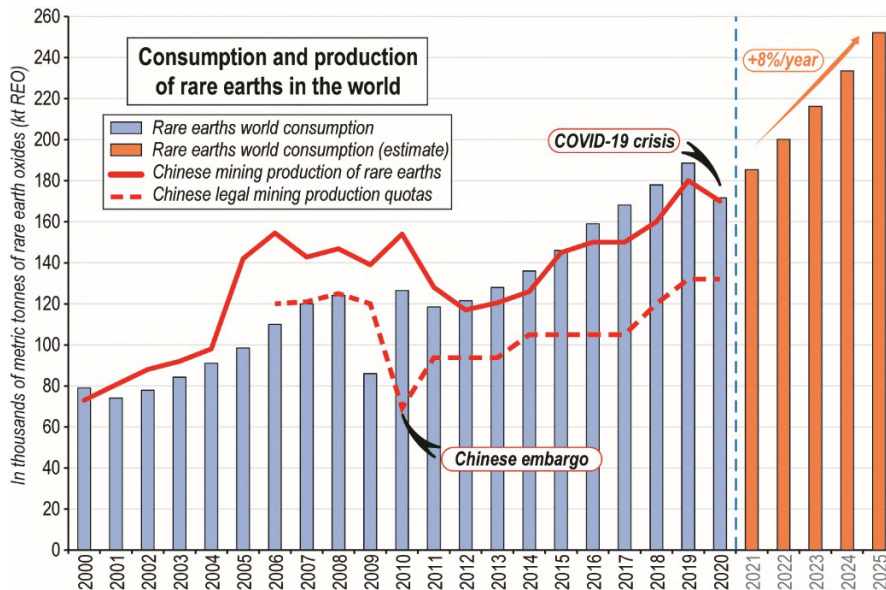


**Figure 1.6.** Global consumption and production of REEs between 2000 and 2020 and estimates between 2021 and 2025 (source: BRGM)

### 1.3.3. Europe in the rare earth economy

Europe consumes 10% of the REEs produced in the world. Moreover, this is one of the most promising markets for the development of electrical mobility and for the installation of offshore wind farms. Legitimate questions arise about potential sources of REEs to ensure their needs. In 2018, global production was estimated at 170,000 t REO. This figure represents a low range, since only official Chinese government quotas are considered (120,000 t in 2018, an increase of 14% compared to 2017), and not the country's illegal production (estimated between 40,000 and 50,000 tons). China's contribution to global production should comprise between 70 and 90% according to estimates.

Vertical integration of the whole REE production chain up to permanent magnets is one of China's major competitive advantages and raises the important question of

the vulnerability of supplies for the European industry (Figure 1.7), not only of the raw material, but also of the products that are derived from it (Figure 1.8). To attenuate the concomitant industrial risks, the EU is encouraging the United States to develop and diversify their supply sources, whether primary (mining) or secondary, thanks to reuse, recycling and waste reduction (Guyonnet et al. 2015; Rollat et al. 2016).

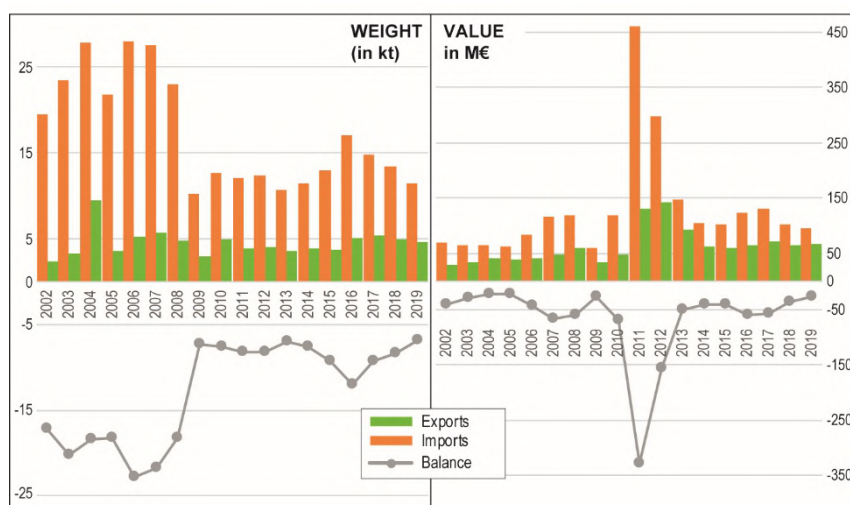


**Figure 1.7.** Imports, exports and trade balance of the European Union for REEs (metals, alloys and compounds) expressed in weight (kt-thousands of tons) and in value (M€-million euros) between 2002 and 2019 (source: Eurostat). Codes CN8 no. 2846 and 280530

One of the main challenges for the European continent, beyond commissioning these deposits, is to develop expertise in transforming REEs at the separation and refining stages, inspired by recent dynamics from Australia and the United States.

Thus, the Australians declared some projects as being of “national interest” and confirmed in March 2020 the desire to form part of a financial consortium for the development of the Dubbo project in New South Wales (Alkane 2020). In July 2020, via the Pentagon, Americans announced 40 million US\$ worth of financial assistance to build two heavy rare earth separation factories on American soil (Scheyder 2019, 2020).

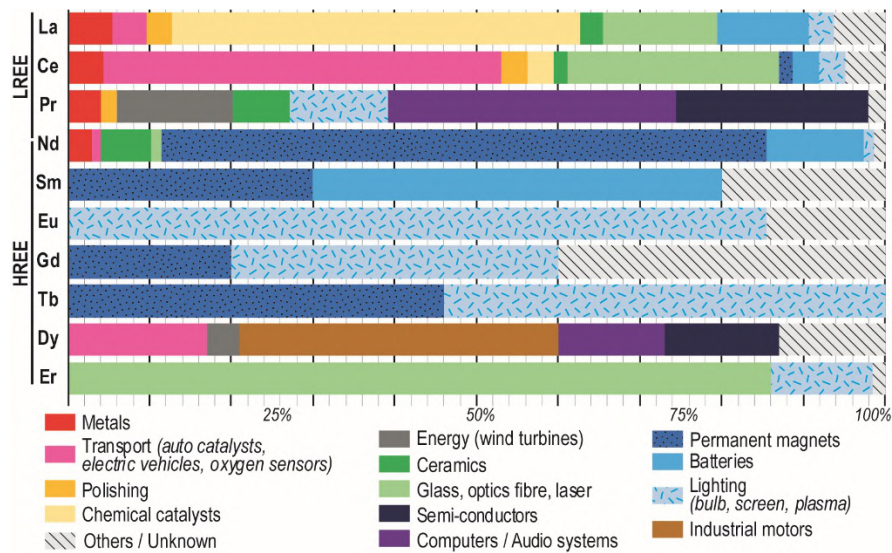


**Figure 1.8.** Use of REEs in the European Union in 2016  
(Sebastiaan et al. (2017) and references therein)

#### 1.4. Classification of rare earth deposits

REE deposits can be divided into two major categories (Figure 1.9):

– primary or endogenous deposits associated with magmatic and hydrothermal processes;

– secondary exogenous deposits linked to sedimentation and/or climatic processes (Walters et al. 2011; Chakhmouradian 2012a, 2012b; Charles et al. 2013; Tuduri et al. 2015; Goodenough et al. 2016; Dushyantha et al. 2020). Despite the great variety of deposits, only three types are in use:

- carbonatites (48% of production globally),
- alkaline magmatism deposits (2%),
- ionic clay deposits (36%),
- lateritic deposits (12%),
- placers (2%).

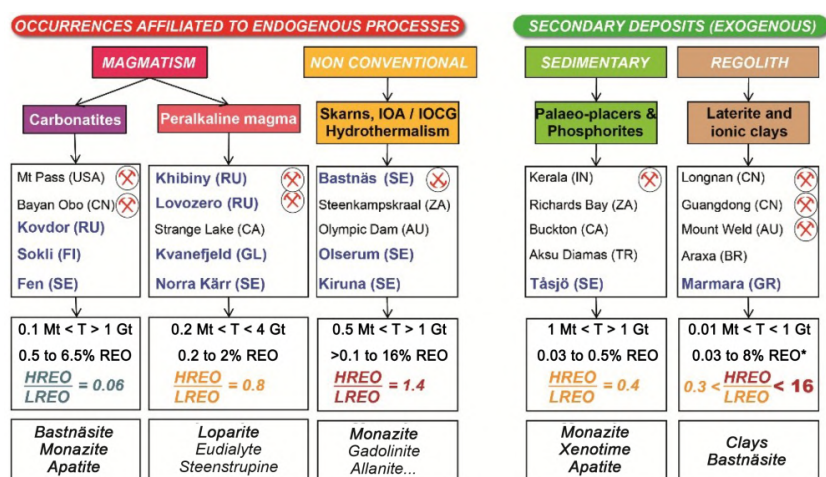


Figure 1.9. Characteristics of the main deposit models

COMMENT ON FIGURE 1.9.– In blue, the major deposits located in Europe or Greenland. T: tonnage; \*the 8% value corresponds to the Mount Weld deposit, and the corresponding HREO/LREO ratio is 0.3. Active mines are marked with a mining symbol. Bastnäs is a part of mining heritage. Abbreviations: AU (Australia), BR (Brazil), CA (Canada), CN (China), FI (Finland), GL (Greenland), GR (Greece), IN (India), RU (Russia), SE (Sweden), TR (Turkey), US (United States), ZA (South Africa).

#### 1.4.1. Primary endogenous deposits

REE carbonatites are characterized by intrusive bodies formed of carbonate rocks that are low in silica (< 10% weight SiO<sub>2</sub>), but often enriched in REEs and accompanied by additional Nb, Ba, Sr, F, U, Th, Ti, Zr, and P minerals, as well as base metals (Cu, Pb, Zn). The carbonatites generally have REO levels above 1% and may exceed 5%, as in Bayan Obo (China) or the Mountain Pass mine (United States). Enrichment with REEs is marked by LREE levels in bastnäs, monazite, apatite and allanite. The HREO/LREO ratio is low and generally below 0.1 (Figure 1.9).

REE deposits may also be associated with the alkaline complexes formed by magmatic alkaline rocks, generally undersaturated and moderately enriched with silica (35–60% weight SiO<sub>2</sub>). These types of rocks (e.g. nepheline syenite) are characterized by an abundant and rich mineralogy that, in addition to REEs and Nb, are enriched with Zr, Ta, Be, Ti, Li, U and Th.

In contrast, REE levels associated with alkaline complexes are lower than those in carbonatites and generally <2% (e.g. Norra Kärr in Sweden and Kringlerne in Greenland at 0.6% REO). These types of deposits are frequently enriched in HREEs (in comparison to carbonatites). Therefore, the HREO/LREO ratio, although it is generally very variable, is generally > 0.15 and sometimes > 1. The main, useful minerals are loparite, eudialyte, gadolinite or even steenstrupine and are often associated with the names of “exotic” rocks (ijolites, lujavrites, kakortokites, urtites or melteigites, etc).

Rifts in cratonic domains are zones with great economic potential, such as the Baltic shield, which includes the Kola Peninsula in Russia and Greenland (Goodenough et al. 2016). Only the loparite alkaline complexes of the Kola Peninsula are exploited today for their REEs and represent only 2% of global production. Although they are underused, alkaline complexes are the essence of new projects for exploring REEs. In 2015, Norra Kärr (Sweden) was the first deposit situated in the EU to certify resources and reserves evaluated at almost 55 Mt at 0.55% REO. Other deposits linked to alkaline intrusions show great potential. Moreover, the Khibina and Lovozero complexes in the Kola Peninsula include reserves estimated at more than 2 Gt at 0.6% REO. In southern Greenland, the magmatic province of Gardar is probably the most extraordinary. It is an ancient rift (1.35–1.12 Ga) over which a large number of alkaline complexes have been made (Grønnedal-Ika, Igaliko, Ilímaussaq, Nunarssuit or Tugtutôg) and has great potential since all have REE minerals, but also Nb and Zr ± U. Each intrusion contains a potentially world-class deposit such as the Ilímaussaq complex, including the Kvanefjeld and Kringlerne deposits. These alkaline complexes are mainly formed of nepheline syenite, associated locally with carbonatites. Concerning deposits associated with carbonatites, Norway, Finland and the Kola Peninsula in Russia have the greatest potential. The main REE-bearing minerals are apatite, bastnäsite, monazite and pyrochlore, and sometimes allanite, parisite and ancylite. The main targets are Fen in Norway (83.7 Mt at 1.08% REO), and there are many occurrences in the Kola Peninsula in Russia, such as Kovdor, which includes REO levels between 0.001 and 0.09% for an average tonnage of 500 Mt. In some deposits, substantial accumulations of apatite can form massive (apatite) bodies within carbonatites. This is the case with the carbonatites at Siilinjärvi and Sokli (Finland), which, with 200 Mt of apatite reserves, could also form an important target for prospecting REEs. Indeed, Decrée et al. (2020) have recently demonstrated that the extraction of the rare earths contained in apatite from carbonatite at Siilinjärvi (Finland) would represent a tonnage of between 133,000 and 161,000 tons REO.

In less conventional form, the famous mine at Ytterby in Sweden (Romer and Smeds 1994) belongs to the NYF pegmatite model (Nb, Y, F). Similarly, it makes sense to distinguish deposits associated with skarns (e.g. Bastnäs).

### 1.4.2. Secondary exogenous deposits

Secondary deposits represented the major part of REE production before the 1970s, with the exploitation of monazite placers. Today, secondary deposits can be subdivided into two groups: deposits associated with surface processes and belonging to the regolith type and basin deposits associated with sedimentary environments (Figures 1.9 and 1.10).

Surface processes, including hydrolysis, oxidation, hydration, or indeed decarbonation reactions, trigger a chemical change in rocks and minerals in addition to physical phenomena. Thus, the soluble elements (Mg, Ca) are partly or sometimes entirely leached in very aggressive climates. The insoluble elements (Fe and Al, which form part of the REE group) remain in place to recombine into neoformed minerals, mainly clays, hydrophosphates or carbonates. In the context of laterite, the weathering of rocks initially rich in REEs (e.g. carbonatite) will therefore produce secondary, still richer REE deposits. This is the case with the REE laterite deposit at Mount Weld (Australia), which developed at the expense of a carbonatite deposit, the exploited content of which is higher than 8% (Lottermoser 1990). Ionic clay deposits (ion-adsorption laterite clays) are associated with the weathering of granites. REEs with weak solubility are adsorbed to the surface of neoformed clays (halloysite/kaolinite). These deposits are certainly numerous, but they are very small in size (some tens of thousands of tons) and are exploited despite their very low content levels. Southeastern Europe has many REE occurrences associated with weathering processes and linked to bauxites and laterites. These occurrences offer potential that remains to be ascertained in the Balkans and in Greece (Grebnik, Nazda-Vlasenica, Marmara).

Sedimentary basins, placer-type deposits, are accumulations of heavy minerals in sand and gravel separated by the process of gravity during their transportation by water or wind. Diagenesis consolidates these placers, transforming them into paleoplacers. The main REE-bearing minerals are monazite, xenotime, fergusonite, euxenite and allanite. These deposits represented the greater part of REE production before the 1970s, in particular through the exploitation of monazite placers. They are still exploited (2% of global production in 2018). Another accumulation process of microorganisms and algae in a marine setting at this time can, via diagenesis, produce concentrations of phosphates called phosphorites. These rocks, enriched with apatite can, in some settings, include REEs (e.g. Tåsjo in Norway). Finally, concerning authigenic deposits, the diagenesis of some silico-clastic rocks enriched with organic matter can in some cases, under the effect of a raised temperature, produce notable concentrations of REEs (Donnot et al. 1973; Pourret and Tuduri 2017).

In Europe, secondary paleoplacer-type deposits are generally of Cenozoic age, even though some date back to the Precambrian (e.g. the Nordkinn Peninsula in Norway). The main mineral encountered is monazite, sometimes with xenotime, allanite, apatite, euxenite, fergusonite, loparite and zircon. In Western Europe, these paleoplacers are mainly characterized by gray monazite enriched with intermediate REEs (Sm-Eu-Gd) and with very low concentrations of U and Th. These monazites result from the erosion of sedimentary rocks from the ancient basins of the Lower Paleozoic in Western Europe (France, Wales, Belgium, Czech Republic, Iberia). They remain small in size and without economic interest (Donnot et al. 1973; Tuduri et al. 2013). The phosphate sandstones of the Ordovician are also interesting targets, for example, Tåsjö (Sweden).

Like some deposits of sedimentary phosphates in the United States (Emsbo et al. 2015), deposits of oolitic iron and phosphate ooids in Norway, Sweden or Estonia (Sturesson 1995) and phosphate chalk at Ciply in the Mons basin in Belgium (Jacquemin 2020) may also form potential targets for the exploration of rare earths in Europe (see Decrée et al. (2017) and references therein).

### **1.5. Rare earths deposits in Europe**

From analyzing the geographical distribution of REE deposits, it seems that they are present at all stages of the rock cycle. Indeed, REEs are often associated with metamorphism, plutonism, metasomatism, hydrothermal processes and sedimentary environments. Moreover, Fedele et al. (2008) argue that the large-scale distribution of REE deposits across Europe has a geogenic origin as their source. Goodenough et al. (2016) argue that the main economic REE deposits in Europe are linked to areas of intracontinental rifting. Their varied geological settings are the result of a region's evolution through geological time periods.

Thus, Europe and Greenland display extremely varied geological settings and include lithospheric blocks of varied nature that were assembled over the course of a geological history stretching back 3.8 billion years (see Choubert and Faure-Muret 1976; Ager 1980; Auboin 1980; Ziegler 1990; Asch 2003; Plant et al. 2005; Gee et al. 2008; Henriksen et al. 2009; Cloetingh et al. 2010 and references therein for a review).

The European continent has resulted from a long geological history over 3.6 billion years, with the assembly of many continental blocks. The European lithosphere can be divided into two distinct parts:

– an ancient cold craton (the East European craton, EEC) partially covered by a weakly deformed covering from the Phanerozoic and strewn with rifts from the Meso-Neoproterozoic in Eastern Europe;

– a thinner and cooler lithosphere dating mainly from the Phanerozoic and accreted to the craton during the course of the Paleozoic, including younger orogens in Western Europe (Figure 1.10) (Gee et al. 2008).

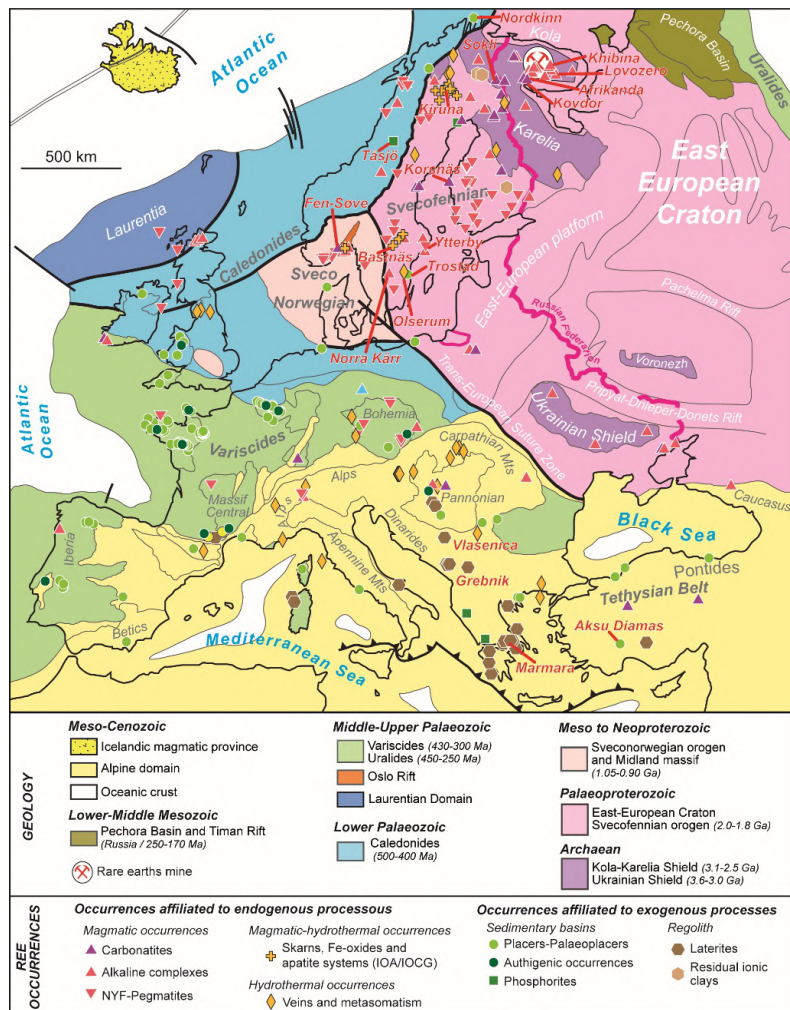


**Figure 1.10.** Distribution of different occurrences of REEs affiliated with endogenous and exogenous processes in Europe (Charles et al. 2013; Goodenough et al. 2016; EURARE 2017; Tuduri et al. 2020)

On the eastern flank of the craton, the Paleozoic orogeny of the Ural Mountains marks the boundary with Asia. To the north of Europe, the craton is surrounded by the Caledonids and the Timanids. Conversely, the southern border of the craton is less well defined since the evidence of accretions from the Neoproterozoic and the Paleozoic is partially obliterated by Alpine deformations and uplift, particularly well expressed in the Caucasus.

Finally, the western border of the craton is characterized by a major boundary of lithospheric scale, called a “Trans-European Suture Zone, TESZ” (Teisseyre 1903; Tornquist 1908; Thybo et al. 1999, 2002), stretching from the Black Sea to the North Sea. Thus, the TESZ separates the Precambrian lithosphere (EEC) to the east (e.g. the Baltic or Fennoscandian shield, the Ukrainian shield, and the Voronech massif) from the Phanerozoic lithosphere to the west. The latter is formed of land accreted during the Caledonian orogeny (e.g. Scandinavian, Irish-Scottish, German-Polish Caledonides) to the north, the Variscan orogeny (e.g. the French Massif Central, Bohemian massif, Armorican massif, Iberian massif) in the center, and the Alpine orogenies (e.g. the Alps, Pyrenees, Carpathians, Dinarides, Apennine, Betics) to the south.

### **1.5.1. Rare earth indices in the Baltic shield**

#### **1.5.1.1. Kola-Karelia Peninsula**

The Kola-Karelia Peninsula includes a remarkable set of alkaline and hyperalkaline rocks (Figure 1.11) (Kogarko 1987). This area can be subdivided according to:

- rocks from the Neoproterozoic age (2,750–2,600 Ma), including the Keivy complex;
- rocks from the Paleoproterozoic age (1,900–1,600 Ma), including the Gremyakh-Vyrmes and Yeletozero intrusions (Arzamastsev et al. 2005);
- rocks from the Paleozoic age (370 Ma), such as the Khibina, Lovozero or Sokli massifs (Vartiainen and Woolley 1976; Kramm and Kogarko 1993; Arzamastsev et al. 2008).

All these massifs are composed of rocks that contain REE minerals (e.g. apatite, loparite, eudialyte and ancylite) and can constitute future deposits.

1.5.1.1.1. Neoproterozoic Keivy province (2,750–2,600 Ma)

The alkaline intrusions from the Neoproterozoic are situated in the western part of the Keivy greenstone belt. The alkaline province of Keivy is formed by six hyperalkaline granite laccolites that date back to 2,750 to 2,600 Ma for a surface of approximately 2,500 km<sup>2</sup> and two massifs of nepheline syenite injected along a fault on the border of the Keivy “terrane” (Mitrofanov et al. 2000; Zozulya et al. 2005, 2013).

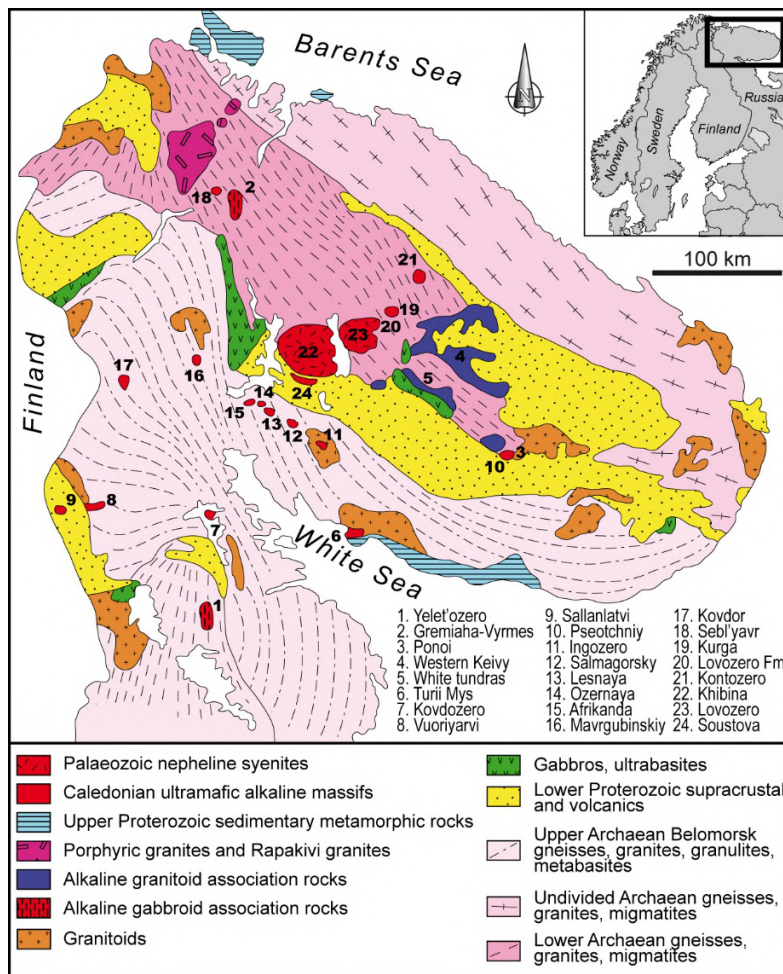


Figure 1.11. The alkaline complexes of Kola-Karelia (Kogarko 1987)

These massifs include six lithological groups: aegirine-arfvedsonite granites, ænigmatite-arfvedsonite granites, lepidomelane-arfvedsonite granites, lepidomelane granites, aegirine-magnetite granites and ferrohastingsite-lepidomelane-aegirine-augite syenogranites. The granites are enriched with Zr, REE, Nb and Ga, the main bearing minerals of which are zircon, monazite, britholite-(Y) and fergusonite. The known occurrences are pegmatitic veins (*elskoozerskoe*) present in microcline-albite-quartz mineralized zones within alkaline granites (*junperuiv*) and in albitized and zeolite zones in contact with nepheline syenites (Sakharjok 1984; Belolipetskyi et al. 1992; Korsakova et al. 2012; Zozulya et al. 2012). Little exploration work has yet been done, but – given the surface of this province – the potential for mining discovery is real (Korsakova et al. 2012).

#### *Zr-REE alkaline complex at Sakharjok (Russia)*

The mineralized zone at Sakharjok (5–6 km<sup>2</sup>) is situated in the center of a hyperalkaline complex at western Keivy formed of a nepheline and phlogopite gabbro, a ferrohastingsite-lepidomelane syenite and an aegirine-lepidomelane nepheline syenite (Batieva and Bel'kov 1984; Zozulya et al. 2012). The ferrohastingsite-lepidomelane syenite is situated to the west and southwest of the complex, while the nepheline syenite occupies the eastern part. Zr-REE mineralization is linked to these two intrusions, which date back to between 2,682 and 2,613 Ma. The Sakharjok index consists of parallel veins within albitized nepheline syenite (Batieva and Bel'kov 1984). These mineralized bodies have lengths of 400–1,540 m, widths of 10–300 m and thicknesses of 15–100 m, with contents of 0.614–1.074% ZrO<sub>2</sub>, 0.023–0.031% Y<sub>2</sub>O<sub>5</sub> and 0.051–0.065% Nb<sub>2</sub>O<sub>5</sub>. The resources of the Sakharjok occurrence have been estimated at 35.8 Mt to 0.16% REO, 0.62% Zr and 0.041% Nb (Batieva and Bel'kov 1984; Pozhilenko et al. 2002; Korsakova et al. 2012).

#### *Lesnoe alkaline intrusion (Russia)*

The alkaline intrusion at Lesnoe forms part of the western Keivy alkaline complex, but the reading list for this area is both sparse and written in Russian (Korovkin et al. 2003). The Nb-REE-Zr Lesnoe occurrence is situated in a nepheline syenite, and the main REE-bearing minerals are fergusonite and britholite-(Y). The estimated resources range between 1.511 Mt and 0.22% REO, 1.21% Zr and 0.31% Nb (Korovkin et al. 2003; Korsakova et al. 2012).

#### 1.5.1.1.2. Paleozoic alkaline province (370 Ma)

##### *Khibiny and Lovozero Nb-P-REE alkaline intrusions (Russia)*

The Khibiny and Lovozero massifs are the most substantial apatitic nepheline syenite intrusions in the world.

The Khibiny intrusion (67°74'N; 33°72'E, Russia) covers a surface area of 1,330 km<sup>2</sup> and measures nearly 40 km in diameter. It is a massif with concentric intrusions of agpaitic nepheline syenite and alkaline and ultrabasic rocks (Figure 1.12) (Arzamastsev et al. 2008; Kalashnikov et al. 2016). The alkaline rocks of Khibiny have been dated back to  $367.5 \pm 5.5$  Ma using the Rb–Sr method on whole rock (Kramm and Kogarko 1994). Although the size of this intrusion is incomparable, the alteration halo (finitization) is nonetheless not very broad, not exceeding 50 m. Its main economic interest lies in the exploitation of phosphorus deposits from apatite, spatially associated with urtite and lujavrite. The most substantial deposits are situated along a narrow band to the south of the massif (e.g. Rasvumchorr, Kukisvum-chorr, Yuksporr, Koashva, Niorkpakhk, Oleny Ruchey, Partomchorr). Apatite, the main mineral of the exploited ore, contains 40–41 wt.% P<sub>2</sub>O<sub>5</sub>, 1.8–3.5 wt.% SrO, 9,000–11,000 ppm REE and 500–900 ppm Y. The resources measured for the deposits of the Khibiny intrusion are estimated at almost 3,200 Mt to 0.36% REO and 14.87% P<sub>2</sub>O<sub>5</sub> (Eilu et al. 2013; Weihed et al. 2013; Kalashnikov et al. 2016). Many REE minerals have been identified: eudialyte, loparite, fluorapatite, ancylyte-(Ce), belovite-(Ce), etc. (Arzamastsev et al. 2008).

The Lovozero intrusion (67°82'N; 34°75'E, Russia) covers a surface of 650 km<sup>2</sup> and measures approximately 25 km in diameter (Figure 1.13). The alkaline rocks of Lovozero have been dated back to  $370.4 \pm 6.7$  Ma using the Rb–Sr method on whole rock (Kramm and Kogarko 1994). The massif intrudes garnet-biotite gneisses dating from the Archean. The Lovozero complex is often described as having four stages of intrusion (Eliseev and Fedorov 1953; Gerasimovsky et al. 1966; Kogarko et al. 1995; Kalashnikov et al. 2016):

- nepheline syenite with uniform grain, nosean nepheline syenite, metamorphosed nepheline syenite and poikilitic nosean syenite;
- embedded lujavrite-foyaite-urtite complex;
- layered urtite, lujavrite-eudialyte and foyaite-eudialyte complex;
- alkaline lamprophyre dykes (minchiquite, fourchite, tinguaitite).

Moreover, the finitized zone has a width of between 50 and 200 m. Many nepheline syenite and alkaline pegmatite veins intersect the host rocks and extend for more than 100 m around the contact. Surrounding the core of the massif, the lujavrite-foyaite-urtite layered sequence contains layers of loparite.

Loparite has been exploited episodically for 50 years for niobium and contains 30–36% REO. Loparite is present in submillimeter grains (0.2–0.6 mm) and more rarely in the form of large crystals (Vlasov et al. 1966; Smirnov 1977), with higher

content levels in rocks enriched with nepheline. It is found mainly in porphyry rocks associated with concentrations of urtite and homologs containing aegirine in juvite and of malignite. The mineralization consists of banded horizons of some centimeters to some meters in thickness, with 2-3% loparite (Hedrick et al. 1997). The measured resources are estimated ca. 1,020 Mt to 0.75% REO (Kalashnikov et al. 2016).

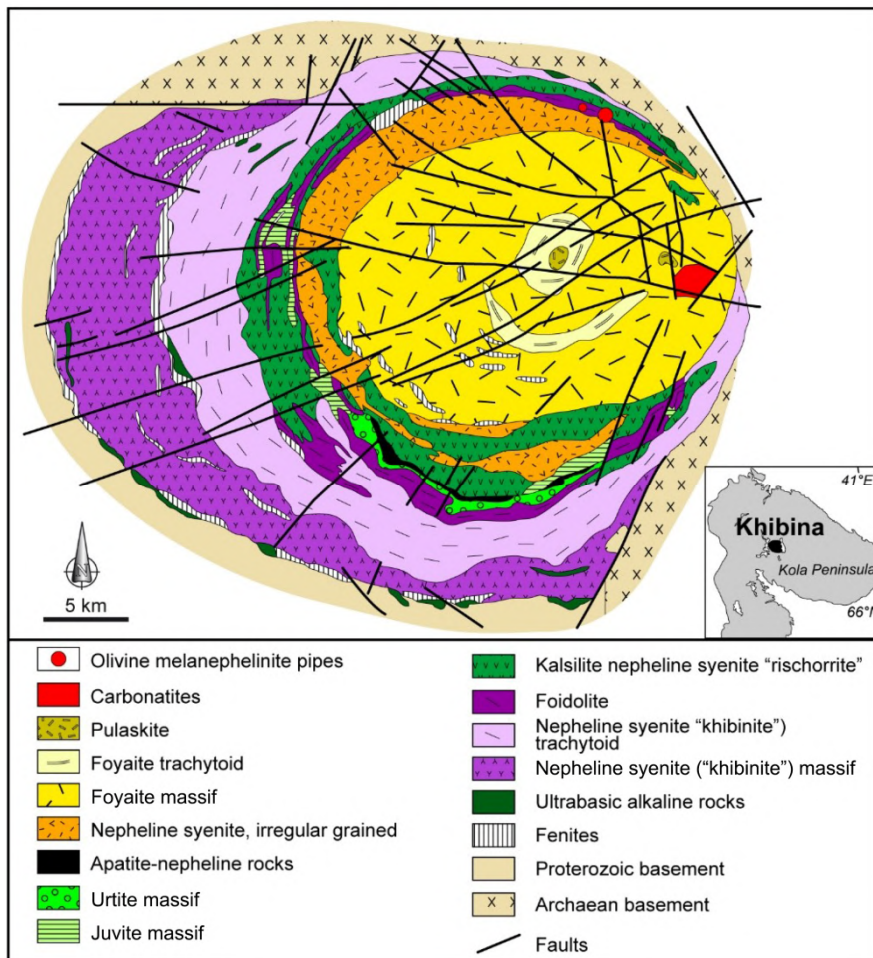


**Figure 1.12.** Khibiny alkaline intrusion (Arzamastsev et al. 2008)

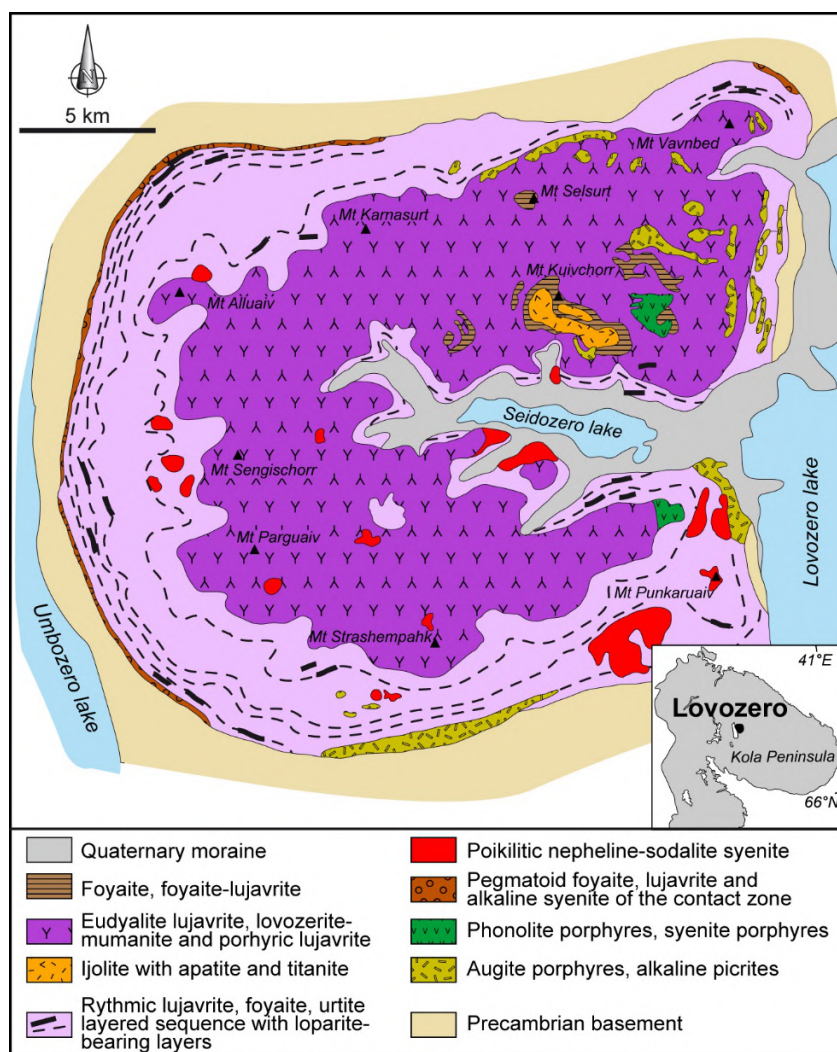


**Figure 1.13.** Lovozero alkaline intrusion (Arzamastsev et al. 2008)

#### *Kovdor ultrabasic alkaline complex (Russia)*

The Kovdor massif (Russia, 50 km SE of the Sokli carbonatite), with an area of 40 km<sup>2</sup>, is an alkaline complex of multiple concentric intrusions (Kogarko et al. 1995; Kalashnikov et al. 2016) that has been dated back to  $380 \pm 4$  Ma using the U/Pb method on baddeleyite (Bayanova et al. 1997). The formations, from the most ancient to the most recent, are ultrabasic rocks (dunite and clinopyroxenite), turjaites

and melilitolites, an ijolite-melteigite series, a mineralized complex of apatite-forsterite-magnetite phosphorites, nepheline syenites and carbonatites (Figure 1.14). It appears that apatite from phosphorites is enriched with REEs (2,720 ppm). Moreover, REEs are present in calcite from carbonatites and in melilite from melteigites with levels of 886 ppm and 914 ppm, respectively (Verhulst et al. 2000).

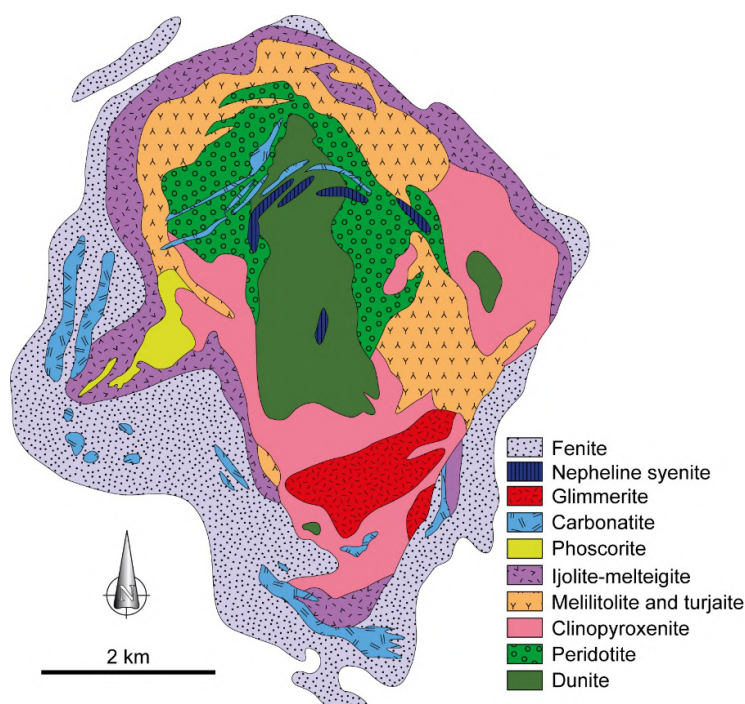


**Figure 1.14.** Kovdor alkaline intrusion (Verhulst et al. 2000)

#### *Sokli Nb-REE carbonatite (Finland)*

The Sokli carbonatite is situated to the northeast of Finland, 90 km from Savukoski, and forms part of the Kola alkaline province (Figure 1.15). This massif was discovered in 1967 during an airborne geophysics program (Paarma 1970) and described by Vartiainen and Woolley (1974, 1976), Vartiainen (1980, 2001), and Vartiainen and Vitikka (1994). This polyphase intrusion (~5 km in diameter) has a carbonatite core (phoscorites, sovite, silicosovite and rauhaugite) surrounded by a metacarbonatite and a broad fenite halo. The Sokli carbonatite dates back to the Devonian (360–380 Ma, (Vartiainen and Woolley 1974; Kramm et al. 1993)) and includes a deposit, which has still not been exploited, of P, Nb, Ta, Zr, REEs and U

(Korsakova et al. 2012; Sarapää et al. 2013). The most substantial REE potential occurs in the fenite halo and in the late carbonatite dykes intersecting the massif. In 2006, GTK (Finnish geological service) carried out a mineralogical and geochemical study on drill cores in carbonatites and reported a high total content (0.5–1.83% weight, including 0.11–1.81% weight LREEs and 0.01–0.041 wt. % HREEs; Kontio and Pankka 2006; Sarapää et al. 2013). The REE-bearing minerals are fluorapatite, apatite-Sr, monazite, bastnäsite-(Ce), ancylite-(Ce), strontianite, barite and brabantite (Al-Ani and Sarapää 2009, 2013). Finally, hydrothermal circulations are probably at the origin of the secondary monazite alteration. The Sokli phosphorus deposit displays substantial resources, with 190 Mt of ore in altered rock and 12,200 Mt of non-weathered rock ore (GTK).

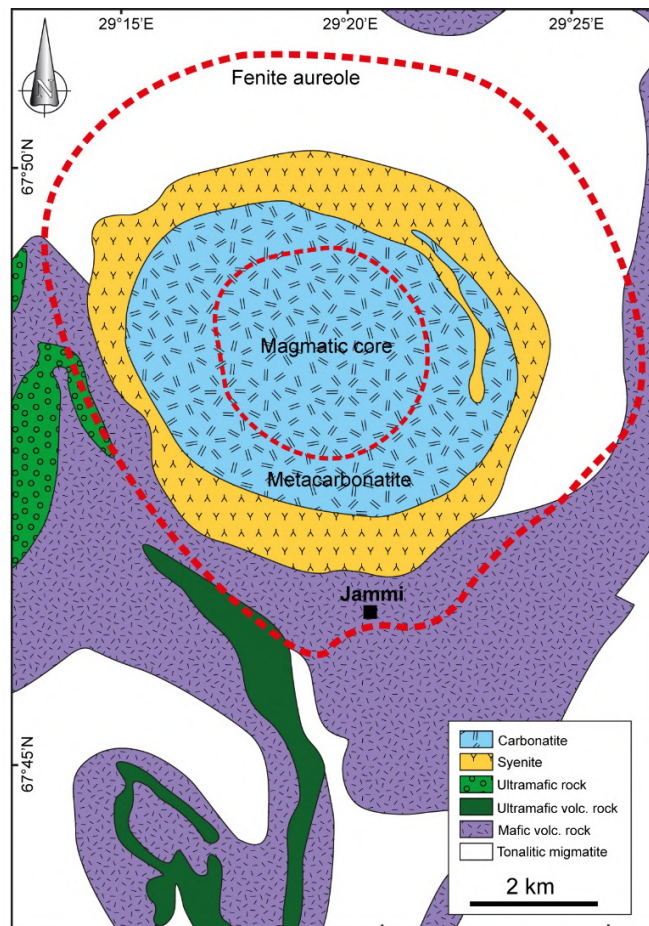


**Figure 1.15.** Sokli massif in Finland (modified from Browne (2008))

### *Iivaara alkaline complex (Finland)*

The Iivaara massif is an alkaline complex situated to the northeast of Finland and forms one of the most western intrusions of the Devonian Kola alkaline province (Kramm et al. 1993; Sarapää et al. 2013). This complex is an oval intrusion ( $> 10 \text{ km}^2$ ) that can be subdivided into three parts, from the center to the rims: alkaline rocks (nepheline and clinopyroxene urtite, ijolite, melteigite), a transition zone, and a fenitized zone up to 1,000 m in width (Lehijärvi 1960). The Iivaara alkaline complex has been dated back to between  $367.4 \pm 4.9$  and  $373.3 \pm 8.1$  Ma using the Rb–Sr method on whole rock (Kramm et al. 1993). Note that Iivaara is the type locality of ijolite, a fairly widespread rock in alkaline complexes. A mineralogical study of GTK has demonstrated the presence of REE-bearing minerals within nepheline syenites, mainly with apatite and allanite to a lesser degree. The samples analyzed contain  $< 200$  ppm REE and 1–5%  $\text{P}_2\text{O}_5$ , leading to a lack of economic interest where REEs are concerned (Sarapää et al. 2013). However, the fenitized zone of the Iivaara complex is still being studied, and the most optimistic results remain possible in terms of REE content.

#### 1.5.1.2. *Svecofennian domain*

##### 1.5.1.2.1. The Appinitic intrusions at Suhuvaara, Lehmikari and Vanttaus (Finland)

In the Lapland granulitic belt, to the north of Finland, the Suhuvaara massif is an intrusion formed mainly of syenitic to dioritic rocks (Sarapää et al. 2013). Similar appinitic intrusions have been identified further to the south in the central Lapland granitic complex with the Lehmikari and Vanttaus massifs (Mutanen 2011; Sarapää et al. 2013). High Ba, Sr, Zr, P and REE levels have been detected in these rocks. For syenitic rocks, the REE levels are above 1,300 ppm.

##### 1.5.1.2.2. REE-Nb-Zr sheared gneiss at Otanmäki (Finland)

In central Finland, to the south of Lake Oulujärvi, the Otanmäki-Katajakangas region contains REE-Nb-Zr within an alkaline granitic gneiss (Figure 1.16) (Hugg 1985; Hugg and Heiskanen 1986; Sarapää et al. 2013 and references therein). The region is formed mainly of gneiss of Archean age, intruded by gneissic granites and gabbro-anorthosites dating back to approximately 2.50 Ga. The Otanmäki area was exploited in the 1950s and 1980s by the Otanmäki Oy company for its deposits of Fe-Ti-V gabbro-anorthosites. Since 2010, the region has been explored by Tasman Metals for REEs through two licenses, those of Katajakangas and Kontioaho.

REE-Nb-Zr mineralization at Katajakangas was discovered by GTK in 1982. It is located at the contact between gneiss and metasediments (turbidites) in the form

of intrusive bodies of some meters in thickness (Kärenlampi et al. 2020). This main lens is greatly deformed. It is formed of a fine-grained gneiss (mylonite), reddish to gray, with quartz-feldspar, riebeckite and alkaline pyroxene. The main REE-bearing minerals are as follows: fergusonite, allanite, bastnäsite, and to a lesser extent columbite, thorite and xenotime (Marmo et al. 1966; Hugg and Keiskanen 1986; Äikäs 1990; Tasman Metals Ltd. 2010a). In 1985, an initial estimate of resources for Katajakangas yielded 0.46 Mt to 2.71% REO, 0.76% Nb<sub>2</sub>O<sub>5</sub> and 1.13% ZrO<sub>2</sub> (Hugg 1985). This estimate was based on an analysis of 14 core drillings carried out over seven profiles with a total length of 850 m and was calculated for a vertical depth of 150 m. More recently, Sarapää et al. (2013) again analyzed some samples of alkaline gneiss from cores from the 1980s. Analyses have demonstrated high REE contents (2.4 wt. % at most), with LREE/HREE ratios ranging from 8.82 to 9.77.

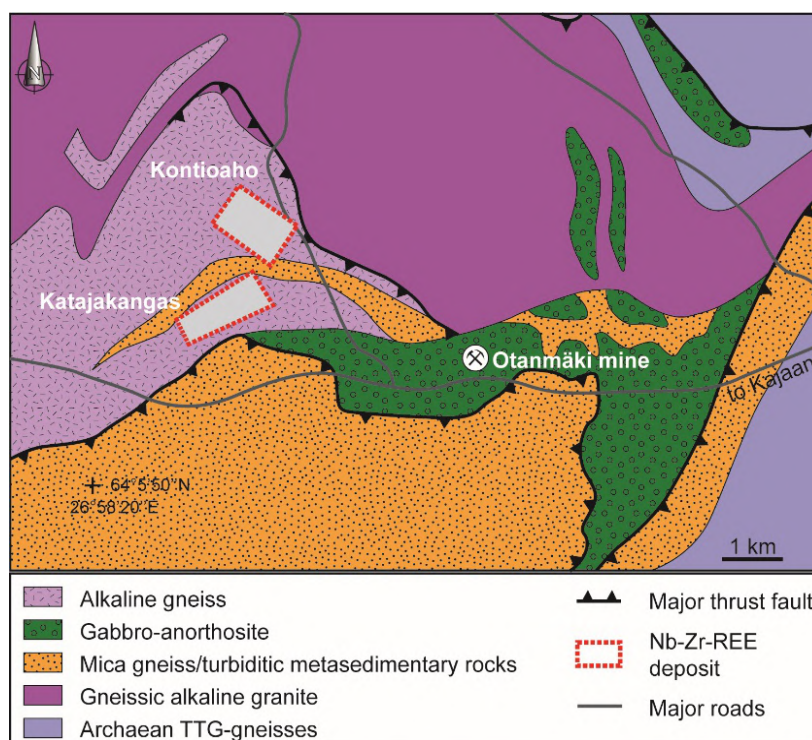


**Figure 1.16.** Shear gneiss with REE-Nb-Zr at Otanmäki-Katajakangas, Finland (Sarapää et al. 2013)

The permit at Kontioaho is situated 1.3 km to the northeast of the Katajakangas permit. REE mineralization was discovered within an altered area formed of

intrusive bodies 7–12 m in width, oriented northwest, and formed of quartz, microcline, plagioclase, zircon and magnetite within quartzo-feldspathic schists. The mineralized horizon is characterized by a strong magnetic anomaly oriented NW–SE over more than 400 m. The main REE-bearing minerals are allanite, fergusonite and xenotime (Tasman Metals Ltd. 2010a). The REO total content was estimated, on the basis of new drill core data, to be 0.59%.

The intrusive bodies of the permits at Kontioaho and Katajakangas carry a complex mineralization of Ti, Zr, Nb, REE, Th and U. This alkaline magmatism has been dated back to 2.04–2.05 Ga and then deformed over the course of the Svecofennian orogen approximately 1.9–1.8 Ga (Kärenlampi et al. 2020).

#### 1.5.1.2.3. Albite and felsite Sc-REE-U at Biggejav'ri (Norway)

The Sc-REE-U albitite at Biggejav'ri is situated in the volcano-sedimentary belt at Kautokeino, of Early Proterozoic age, in the extreme north of the county of Finnmark, in Norway. The rocks date back to 1,890–1,750 Ma (Statherian to Orosirian) and are mainly represented by Sc-U-REE-enriched albite felsites (Olerud 1985, 1988; NGU 2013). Felsite contains calcite, quartz, muscovite and rutile, but also minerals rich in Cr and V, such as davidite-loveringite and chromite. Additional minerals include La-Ce-bearing carbonates, monazite, orthite, thortveitite, coffinite, uranophane, brannerite, zircon, pyrite, sphalerite, galena, chromium chlorite and an unidentified REE-bearing mineral. The rock's total Sc content, and perhaps REE content, could present economic benefit (e.g. 122 ppm Sc, 1 027 ppm La, 605 ppm Ce, 248 ppm Y) (Olerud 1988).

#### 1.5.1.2.4. Kiruna-type iron ores with magnetite and apatite REEs (Sweden)

To the north of Sweden, close to Kiruna (67.85°N–20.22°E, Norrbotten region), Kiruna type P-Fe-apatite-REE iron ores form part of a group of occurrences formed by a magnetite-hematite-apatite assemblage, with rocks from the Paleoproterozoic from the Fennoscandian shield (Geijer 1931; Frietsch 1977; Frietsch and Perdahl 1995) (Figure 1.17). These surrounding rocks are alkaline rhyolites, trachytes and trachyandesitic lava flows with intrusive rocks and a sedimentary sequence (Geijer 1931; Geijer and Ödman 1974).

It is important to note that the deposits are directly associated with sodium and potassium alterations (Frietsch et al. 1997; Martinsson 1997). The ore is formed of a magnetite-apatite assemblage that contains nearly 30% apatite (mainly fluorapatite) and some additional minerals (i.e. actinolite, calcite, quartz, sphene, talc, albite). The mineralized bodies are massifs, forming stockworks and irregular, bulbous, but sometimes also concordant masses. The mineralization dates back to between 1.88 and 1.90 Ga (Cliff et al. 1990). Discovered in the 17th century, the apatite iron ores

of Kiruna are the subject of intense discussion (Cliff et al. 1990; Hitzman et al. 1992; Evans 2000; Harlov et al. 2002). Two main hypotheses are still discussed to explain the origin of the mineralizations:

- immiscibility between an iron-rich magmatic fluid and hydrothermal remobilization (Botke 1981; Harlov et al. 2002);
- or an exhalative hydrothermal process (Cliff et al. 1990; Evans 2000).

More broadly, according to Hitzman et al. (1992) and Barton and Johnson (1996), Kiruna-type mineralization forms a subclass of IOCG (iron-oxide copper gold) type deposits from the Proterozoic: IOA (iron-oxide apatite) type deposits.

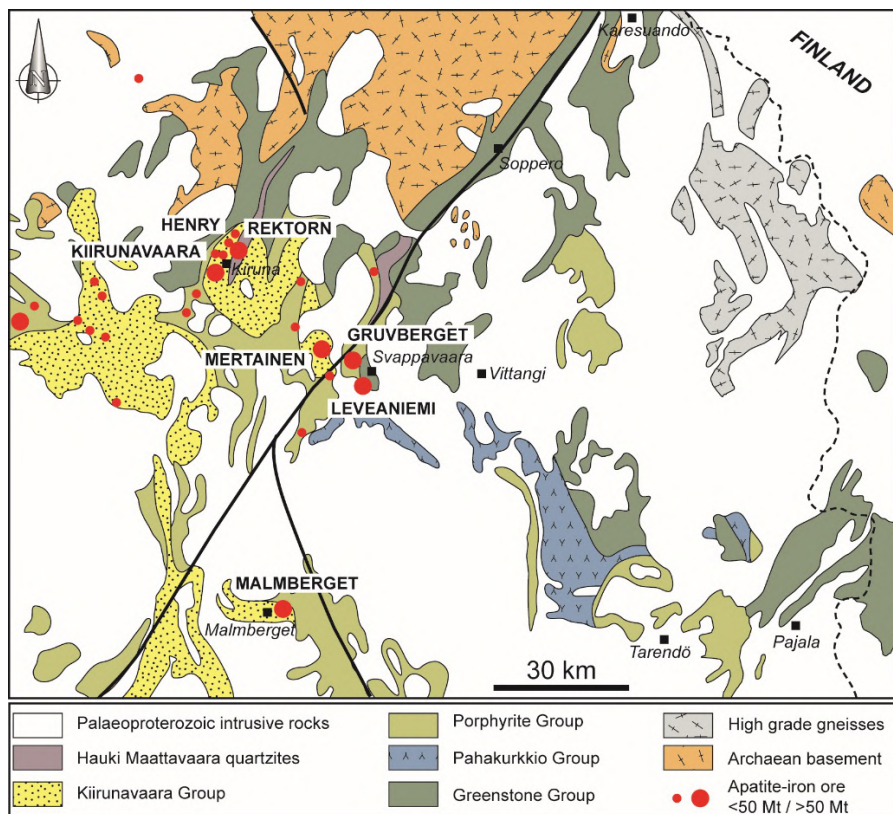


**Figure 1.17.** REE magnetite-apatite iron ores of the type found in Kiruna (Sweden), modified from Martinssen (2007)

The peculiarity of Kiruna-type iron mineralizations is their relatively high REE content (Parák 1973, 1975, 1985; Frietsch and Perdahl 1995). These significant REE contents in ores were first mentioned by Geiser (1931). The district of the first Kiruna-type iron deposits has an average content of 0.7% REO, mainly carried by apatite. The REEs are contained in apatite and to a lesser extent in monazite, which is not homogeneously present in the mineralizations. Moreover, the hematite ores of Kiruna have an average content of 0.5% REO and are still mainly contained in apatite. In a more precise fashion, Parák (1973) analyzed the REE content of apatite iron ores from several deposits from the Kiruna district: Kiirunavaara (6,560 ppm), Malmberget (5,760 ppm), Leveaniemi (1,545 ppm), Rektorn (3,275 ppm), Haukivaara (5,295 ppm), Henry (5,210 ppm), Nuku-tusvaara (6,730 ppm) and Lappmalmen (5,890 ppm).

The Swedish LKAB (Luossavaara-Kiirunavaara AB) company has extracted more than 950 Mt of ore since the start of exploitation a century ago, and only a third of the mineralized body was initially exploited. Recently, LKAB has sought to extract REE from the apatite present in tailings because of the ReeMAP research project (LKAB 2018). Tailing ponds that contain apatite represent a substantial volume with a relatively low REE content. These tailing ponds at Kiruna represent approximately 8 Mt/year and contain 4–8% apatite and 1,200–1,500 ppm REEs, which would represent 10–15 kt REEs per year (Renberg 2014). Industrial production of REE concentrate is predicted for 2021 and would represent more than 500% of Sweden's demand for REEs.

#### 1.5.1.2.5. Albitites at Uuniniemi, Honkilehto and Palkiskuru-Palovaara (Finland)

In the north of Finland, three small areas of hydrothermal alteration are presented as showing REE anomalies: Uuniniemi, Honkilehto and Palkiskuru-Palovaara (Sarapää et al. 2013). The Uuniniemi area (near Kuusamo, 680 km to the north of Helsinki) is formed of albitites, syenites and carbonatite veins (Mutanen 2011). The carbonatite has been sampled and analyzed, revealing levels of 2.80% P<sub>2</sub>O<sub>5</sub>, 0.43% REE and 256 ppm Nb (Sarapää et al. 2013). Moreover, the REE content is 0.1% in the albitite and carbonates and albite rocks. REE-bearing minerals have been identified through analyses using electron probes (monazite-Ce, colombite, ferro-columbite, euxenite-Y, zircon, Fe-thorite, britholite and bastnäsite in minority quantities).

In the central part of the Kuusamo belt (Vanhanen 2001), Au-Co mineralization at Honkilehto, surrounded by sericite and sulfide schists, also includes uranium

minerals (davidite), Pb-U and U-Si minerals. Bastnäsite and allanite are always associated with these anomalies. Analyses of drill core samples (e.g. DH398, 81–93 m intersection) by Sarapää et al. (2013) have revealed the following average levels: 1,552 ppm REE (maximum 3,442 ppm), 1,472 ppm Co (maximum 3,410 ppm), 175 ppm U (maximum 430 ppm) and 6.1% S (maximum 13.9%).

Finally, to the northeast of Finland, the Palkiskuru-Palovaara area shows albitites formed of REE-bearing minerals with bastnäsite, monazite, allanite and xenotime (Sarapää et al. 2013). The uranium minerals are davidite, masuyite and sayrite. The highest REE content is 0.4%, with levels of 209 ppm Th and 3,570 ppm U.

#### 1.5.1.2.6. Kaolinic weathering profiles at Virtasalmi and Mäkärä-Vaulo (Finland)

Laterization processes lead to the partial or total leaching of metals such as Al, Mg, Fe, Cu, Ni and REE from the bedrock and are then accumulated within a weathering profile between laterite and saprolite (Morteani and Preinfalk 1996).

To the southeast of Finland, the kaolin deposits of the Virtasalmi region (from 0.5 to 2 km in length and 50–400 m in depth, such as those of Litmanen, Eteläkylä, Vuorijoki and Montola) are covered by 20–30 m of formations from the Quaternary. Kaolin presents over an average thickness of 30–40 m, indeed up to 100 m, and contains 40–75% weight kaolinite, 20–30% quartz and some grains of potassium feldspar and muscovite. An area of transition is observed between the kaolin and the surrounding rocks (gneiss and tonalite), which present well-preserved structures. The kaolin deposits at Virtasalmi have been dated back to 1,180 Ma using the K/Ar method on authigenic illites from the Litmanen deposit (Sarapää 1996). Sarapää et al. (2013) selected some samples of drill cores to carry out mineralogical and chemical studies to estimate their REE potential. The kaolins show REE enrichment with LREE/HREE ratios between 6 and 19, (La/Yb)<sub>n</sub> between 6 and 66, and Ce/Ce\* equal to 1 (Al-Ani and Sarapää 2009). At the base of the kaolinic weathering profiles of the deposits at Litmanen and Eteläkylä, the total REE content may reach at most 0.1–0.2% (Sarapää et al. 2013).

To the north of Finland, near Sodankylä (Laponie), the region of Mäkärä-Vaulo forms part of the Tana belt (the southern part of the Lapland granulitic belt). It has been subject to exploration for gold, which had previously been detected through geochemical anomalies in REEs (anomalies strongly positive in La and Y). The Tana belt is a strongly tectonized area formed of amphibolites, from gneiss to garnet-biotite and arkosic gneiss. The whole area overlaps the central Lapland

greenstone belt at approximately 1.91 Ga (Tuisku and Huhma 2006). In the areas of Mäkärä and Vaalo, a thick kaolin profile is developed at the expense of basement rocks, the whole covered by glacial clay deposits (tills) rich in La and Y (Sarapää and Sarala 2011, 2013).

The Mäkärä profile shows levels of approximately 0.05% REE (maximum 0.1%), LREE/HREE ratios between 2.7 and 15.1 and Ce/Ce\* between 0.7 and 0.9. The profile of Vaalo shows a level of 0.40 to 0.45% REEs in the fine fraction of glacial deposits. The REE-bearing minerals are monazite, rhabdophane and xenotime. The REE potential of the Tana belt could be interesting since only the Mäkärä-Vaalo region has been explored (Sarapää et al. 2013).

#### 1.5.1.2.7. REE mineral pegmatites (Sweden)

The Svecokarelian orogeny includes some pegmatites that contain uranium- and REE-bearing minerals (Sadeghi et al. 2013). Allanite is the main REE-bearing mineral in pegmatites with high LREE/HREE ratios (Castor and Hedrick 2006). In Sweden, pegmatites have been classified into two categories following the study of additional minerals carried out by Smeds (1990):

- tourmaline pegmatite ± Li-bearing mineral (rocks with low to moderate metamorphic facies);
- pegmatites with REE-Y minerals (various geological settings).

Unfortunately, the pegmatites are generally too small or present contents too low to be of economic interest. Nevertheless, for pegmatites already exploited for feldspar and mica, the exploitation of the REEs contained in other minerals would be possible.

#### 1.5.1.2.8. P-REE and carbonatite complex at Siilinjärvi (Finland)

The carbonatite complex at Siilinjärvi is situated in eastern Finland (Figure 1.18), near Kuopio (380 km to the north of Helsinki). It is a steeply dipping lenticular body approximately 16 km long and 1.5 km broad (Pusstinen 1971). The calcite, dolomite and phlogopite rocks of this complex form a tabular body 600 to 700 m in width surrounded by a fenitized area. White to greenish medium-grained carbonate rocks are rarely present at Siilinjärvi, and carbonatite is not very widespread. The majority of the central body are rocks rich in phlogopite, ranging from pure glimmerite to silicocarbonatite, followed by some carbonatites. Dating using the U/Pb method on zircon has given an age of  $2\,610 \pm 10$  Ma (Tichomirowa et al. 2013), which makes the carbonatite from Siilinjärvi one of the oldest in the world.

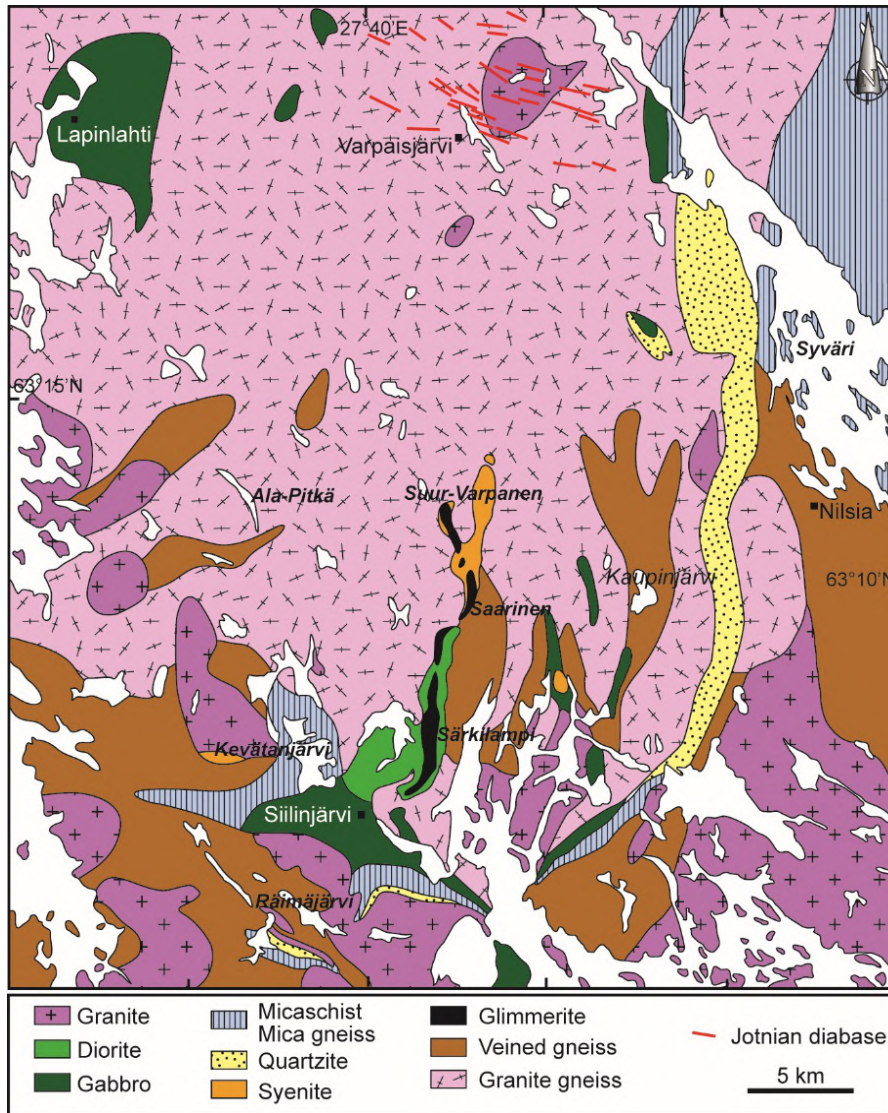


**Figure 1.18.** P-REE and carbonatite complex in Siilinjärvi, Finland (Pusstinen 1971)

Apatite is situated in the central part of the magmatic body in the form of gray to greenish-yellow prisms and irregular grains in glimmerite-carbonatite-type rocks. Apatite shows no inclusion in the thin sheets. It is fluorapatite with an average

content of 1.2% Sr and 0.4% RE<sub>2</sub>O<sub>3</sub> (Pusstinen 1971). The minerals in glimmerite are phlogopite, apatite and carbonates. They have been analyzed for their REE potential by Hornig-Kjarsgaard (1998). Samples of total rock have revealed REE contents between 499 and 1,629 ppm. Apatite has relatively high REE contents varying between 2,986 and 3,820 ppm. A recent study carried out by Decrée et al. (2020) revealed the content of rare earths contained in the apatite of this alkaline complex. Thus, the apatite present in the glimmerite shows contents between 3,195 and 6,665 ppm REE, whereas the apatite contained in the fenite contains between 663 and 4,567 ppm REE. It appears that the rare earth contents in glimmerite or fenite are proportional to the P<sub>2</sub>O<sub>5</sub> content since apatite encloses the greater part of the rare earths. By considering reserves of 200 Mt @ 4 wt. % P<sub>2</sub>O<sub>5</sub>, and average contents between 576 ppm REEs (all rocks combined) and 697 ppm REEs (in the glimmerite-carbonatite series), Decrée et al. (2020) estimated that it would be possible to extract between 133,000 and 161,000 tons REO. It must be remembered that in 2012, an exploration permit was obtained for the Siilinjärvi complex (Tasman Metals Ltd. 2012). This REE exploration project covers 450 ha and lies close to the phosphate (apatite) mine of Siilinjärvi (by the Yara company), 30 km north of Kuopio. This site mainly produces fertilizer and phosphoric acid and remains the sole producer of phosphate ore in western Europe (800,000 ton/year of phosphates).

#### 1.5.1.2.9. Carbonatites at Kortejärvi and Laivajoki (Finland)

In central-northern Finland, the carbonatite massifs of Kortejärvi and Laivajoki intrude basic volcanic rocks dating back to the lower Paleoproterozoic along a crustal-scale fault and form a substantial part of Finland's REE potential (Sarapää et al. 2013). The Kortejärvi carbonatite is an intrusive massif approximately 2 km long and 60 m thick, while the Laivajoki massif measures 4 km in length and 20 m thick (Nykänen et al. 1997). The two intrusions are formed above all calcite carbonatite and dolomite, even though the intrusion at Laivajoki also contains silico-carbonatite. Moreover, glimmerite and olivine-magnetite rocks are also visible in the Kortejärvi intrusion. Within the Kortejärvi carbonatite, a study has been carried out on cores from older drillings and has revealed the abundant presence of apatite with monazite and allanite (Al-Ani et al. 2011). For the Laivajoki carbonatite, some samples analyzed have shown high calcite, dolomite, phlogopite, magnetite and apatite contents. The main REE-bearing minerals in the two massifs are allanite and monazite. Unfortunately, the REE contents in the Laivajoki (210–1,644 ppm) and Kortejärvi massifs (443–892 ppm) are relatively low. Further studies are needed to better define the REE potential of the Kortejärvi and Laivajoki carbonatites.

#### 1.5.1.2.10. The REE-Zr nepheline syenite of Norra Kärr (Sweden)

The nepheline syenite of Norra Kärr was discovered in 1906 by Törnebohm in central southern Sweden, 300 km from Stockholm and 15 km to the NNE of Gränna, near the eastern bank of lake Vättern. The intrusive complex is elongated N–S and is nearly 1.3 km long and 460 m wide, covering a surface of approximately 380,000 m<sup>2</sup> (Figure 1.19). This complex intrudes into the gneiss and granites of the Paleoproterozoic ( $1,791 \pm 8$  Ma; Johnsen and Grice 1999), belonging to the Småland-Värmland granitoids of the “Växjö” type, which form part of the Trans-Scandinavian igneous belt (1.85–1.65 Ga; Högdahl et al. 2004). The granite of Växjö is a red biotite granite, generally of coarse and isotropic grain, although a cataclastic fabric oriented N–S is visible along the lake Vättern (Adamsson 1944). Contacts between the Norra Kärr nepheline syenite and the surrounding Växjö granite dip approximately 45° toward the west. Until recently, the age of the Norra Kärr intrusion was wrongly established at approximately  $1,545 \pm 61$  Ma by Rb–Sr (Blaxland 1977; Welin 1980). Indeed, more recent dating using the U/Pb method on zircon revealed the metasomatic alteration of the surrounding rocks (finitization) and hence the magmatic activity linked to the intrusion dating back to  $1,489 \pm 8$  Ma (Christensson 2013; Sjöqvist et al. 2013). The emplacement of the Norra Kärr complex is still under discussion, although it already seems that this intrusion is considered to be a metamorphosed agpaitic complex (Schilling et al. 2011; Sjöqvist et al. 2013 and references therein).

The Norra Kärr complex seems to be concentrically zoned and is formed of four main lithologies: “grenaite”, “kaxtorpите”, “pulaskite” and “lakarpite” (Figure 1.19). Grenaite is a gray–green rock, partially recrystallized and fine-grained with alkaline feldspars, nepheline, aegirine, eudialyte and catapleiite. The central part of the massif shows pegmatite zones and schlieren surrounding a recrystallized to migmatized unit of grenaite. There are pulaskite (alkaline rock of medium to thick grain) outcrops to the west of the massif, and they are formed of albite, microcline, aegirine, sodium amphibole, biotite and nepheline as minor phases. The additional minerals are rosenbuschite, apatite, titanite and fluorine (Sjöqvist et al. 2013; Gates et al. for Tasman Metals Ltd. 2012, 2013). Outcropping mainly in the central part of the intrusion, Kaxtorpите generally consists of black alkaline rocks that are coarse-grained and have low Zr contents. Its constitutive minerals are microcline, which is present within a matrix formed of dark alkaline amphibole, aegirine, eckermannite, pectolite and nepheline. Finally, lakarpite is a medium-grained rock rich in albite-arfvedsonite-nepheline with small amounts of microcline and rosenbuschite and titanite, apatite and fluorine as minor phases.

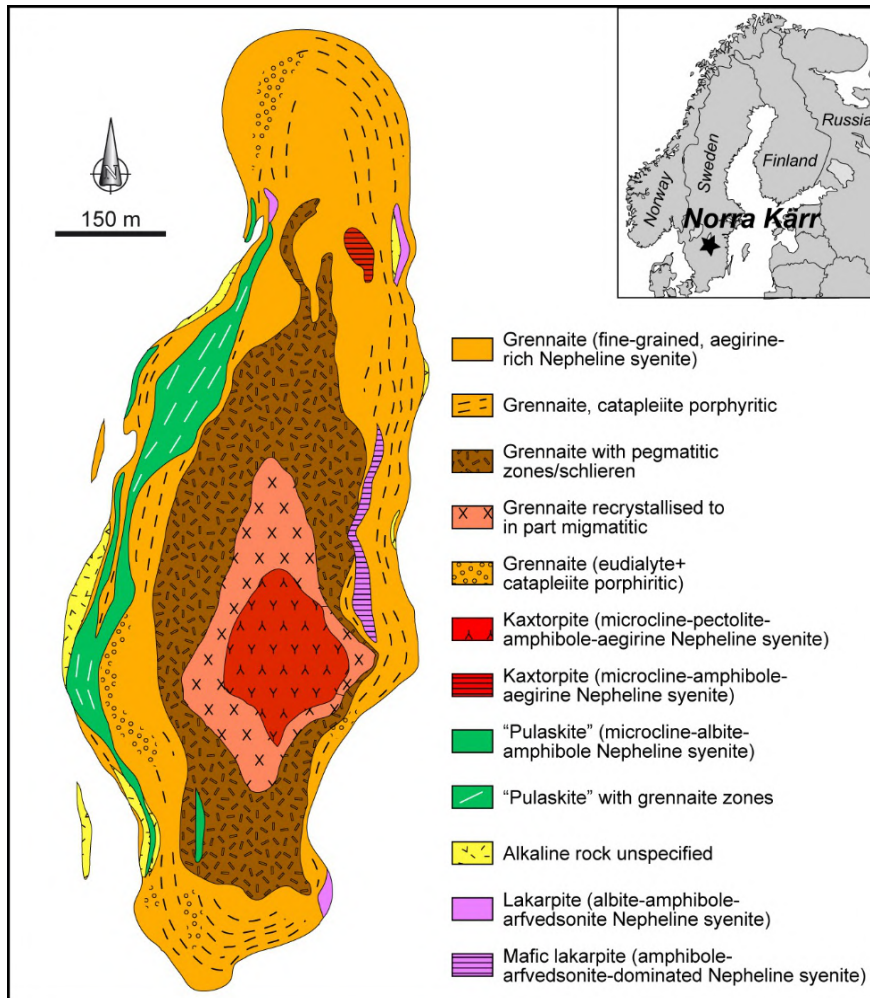


**Figure 1.19.** REE-Zr nepheline syenite at Norra Kärr, Sweden (Gates et al. 2013)

Chemical analyses have been carried out on each of these lithologies and are presented in Gates et al. (2013). Thus, grennaite contains between 0.14 and 0.67% REO, with maximum levels in the pegmatitic facies. Pulaskite contains between 0.09 and 0.24% REO. Kaxtorpite shows values of 0.20% REO. Finally, lakarpite includes between 0.42 and 0.54% REO. Whole-rock analyses are also presented in the study by Sjöqvist et al. (2013) for each of the lithologies of the Norra Kärr complex. Thus, grennaite with catapleiite has levels of 0.28% REO+Y<sub>2</sub>O<sub>3</sub>, while the

grenaite associated with the pegmatites and the deformed grenaite (recrystallized texture) have levels of 1.19 and 0.47% REO+Y<sub>2</sub>O<sub>3</sub>, respectively. The levels of kaxtorpite and lakarpite are 0.08% and 0.62% TREO+Y<sub>2</sub>O<sub>3</sub>, respectively.

Previous mineralogical studies have allowed the reporting of REE-bearing minerals such as eudialyte, rinkite-mosandrite, britholite-(Y), lessingite, apatite and tritomite-(Ce), as well as a rosenbuschite REE-bearing assembly. In a recent mineralogical study on the eudialyte group from Norra Kärr, Sjöqvist et al. (2013) distinguished three distinct groups:

- classic pink eudialyte enriched in Fe and low in REEs in the lakarpite;
- eudialyte rich in HREEs and Fe-Mn in grenaite associated with the pegmatites;
- eudialyte rich in Mn and LREE in the “migmatitic” grenaite.

Chemical analyses carried out by Tasman Metals on eudialyte concentrates show values ranging from 3.91 to 4.63% REO, with high contents of eudialyte collected in pegmatitic grenaite (Gates et al. 2013). In 2011, an initial estimate of resources for the REE-Zr deposit at Norra Kärr was published according to standard NI43-101. With a cutoff grade of 0.4% REO, the Norra Kärr deposit contains 60.5 Mt @ 0.54% REO and 1.72% ZrO<sub>2</sub>. In 2012 and 2013, the resources indicated were 41.6 Mt @ 0.57% REO, corresponding to 237,120 t REO, and the resources inferred from 16.5 Mt @ 0.64% TREO, corresponding to 105,600 t REO (Gates et al. 2013). In July 2013, a preliminary economic study estimated production capacity at 6,800 ton/year for a lifespan for the mine of 40 years, although the deposit was still exploited underground.

#### 1.5.1.2.11. Phosphorite at Pålång (Sweden)

The phosphorite at Pålång is an occurrence situated 50 km to the northwest of Luleå. The surrounding rocks are formed of metasediments and volcanic rocks dating back to the Paleoproterozoic (2.1–2.3 Ga), which belong to the Karelia supergroup (Notholt et al. 1989; Frietsch and Perdahl 1995): micaschists with quartzite, phyllite and limestone-dolomite interbeds. The limestone and dolomite contain levels of apatite, or even fragments of apatite associated with a breccia formed during regional metamorphism. The phosphate rocks are situated in two steeply dipping areas at levels of 1 m thickness showing contents of 10% P<sub>2</sub>O<sub>5</sub>. The Pålång deposit has an average content of 2% P<sub>2</sub>O<sub>5</sub> and 0.03% U for 6 Mt of ore and a thickness estimated at 100 m (Gustafsson 1979). Frietsch and Perdahl (1995) analyzed the REE content in apatite and showed a low splitting (La/Yb)<sub>cn</sub> = 4) and REE levels 50–400 times higher than chondritic values (i.e. ~730 ppm REE). It should be noted that 100 km to the north of the Pålång zone, a similar deposit is

present in Mustamaa (Finland), where phosphorite and dolomite outcrop in basic volcanic rocks, the phyllites and schists of the Karelia supergroup.

#### 1.5.1.2.12. REE-Pb carbonatite at Korsnäs-Svartören (Finland)

The Korsnäs deposit is a historic REE-Pb mine situated in central-western Finland, 350 km north of Helsinki and only 25 km southwest of the port of Vaasa on the Baltic Sea. The Korsnäs mine was exploited by the Outokumpu Oy company, above and below ground from 1959 to 1972. The Korsnäs deposit was identified in 1950 through the discovery of erratic blocks rich in lead sulfides. Afterward, the ore was intersected by a substantial drilling campaign carried out by GTK in 1955 (see the references in Sarapää et al. (2013)). The deposit was formed of a network of carbonatite dykes, the most important of which is the one at Svartönen, which is home to the main mineralized body. This dyke, the establishment of which has been dated back to 1,830 Ma using the U/Pb on titanite method (Papunen 1986), measures 5–30 m in width for 1.5 km in length and continues at nearly 350 m underground. The network of dykes intrudes migmatitic gneisses that date back to 1.9 Ga and belong to the south-ostrobothnian schist belt (Lehtonen et al. 2005). The deposit is situated in an intensely deformed zone and oriented N–S with a 40–60° dip toward the east. Immediately next to the mineralized body, a chlorite alteration zone is weakly expressed in the surrounding rocks. The deposit appears as a heterogeneous body with mineralizations in the pegmatites and carbonatites or in the form of a scapolite-diopside-barite skarn in the surrounding rocks.

The main REE-bearing minerals are apatite, monazite and allanite, although the site is also known for its many other exotic REE minerals. More precisely, monazite is found in the altered zones and presents in the form of small crystals or in diffuse inclusions in apatite (Isokangas 1975). The apatite has REE contents of more than 6%, with a slight excess of HREEs compared to monazite and allanite (Papunen and Lindsjö 1972). On the basis of a sample – certainly fragmented – of REE minerals, the total level of these elements is mainly represented by Ce, La and Nd for 80–90% (Papunen 1986). Moreover, more than 50 different minerals have been identified in the deposit, including rare phases such as carbonates and phosphates, and famous harmotome crystals (hydrated barium silicate) and apophyllite crystals within the small vacuoles (Isokangas 1975). Historically, the Korsnäs mine provided a total of 0.87 Mt of ore with 3.6% Pb and 0.83% REE between 1959 and 1972 (Himmi 1975; Tasman Metals Ltd. 2010c). Past production is evaluated at a total of 45,000 tons of Pb and 36,000 tons of La between 1961 and 1972 (Himmi 1975). Other figures have been published and give an average ore grade of 3.57% Pb and 0.91% RE<sub>2</sub>O<sub>3</sub> (Papunen and Lindsjö 1972). Since then, the GTK has resumed exploratory work on REEs and discovered erratic blocks formed of Svartören-type rocks at approximately 1 km to the southwest of the Korsnäs mine (Kärkkäinen and Huhta

1993). These blocks seem to come from a source that has still not been discovered and that is similar to the Svartören dyke. Moreover, some samples taken from drill cores in the 1950s have been analyzed again and have revealed REE contents ranging from 0.7 to 2.2% with a fraction rich in LREE. More specifically, the Eu content is high (between 66 and 242 ppm), and the Th content varies between 107 and 604 ppm. Finally, weak negative gravimetric anomalies have been measured to the south of the Korsnäs zone and could be the marker of a potential zone for identifying REE-Pb weathered carbonatite dykes. The Tasman Metals company has acquired the old Korsnäs REE-Pb mine (Tasman Metals Ltd. 2010c).

#### 1.5.1.2.13. The metamorphosed paleoplacer and REE hydrothermal alteration at Olserum (Sweden)

The Olserum occurrence is situated near Gamleby, 220 km southwest of Stockholm. This occurrence was discovered in the 1950s during prospection for uranium and was studied for its REE content in the 1990–2000s. In 2013, an exploration campaign was carried out by the Tasman Metals company (IGE Nordic 2007; Reed 2013; Tasman Metals Ltd. 2013).

The Olserum zone forms part of the Västervik formation, which is a metasedimentary succession formed between 1.88 and 1.85 Ga in the southernmost part of the Svecofennian domain (Kleinhanns et al. 2012). This psammitic to pelitic formation has been intruded by granitoids dating back to 1.85–1.80 Ga and linked to the Småland granite, which belongs to the Trans-Scandinavian igneous belt. HT-BP metamorphism affected the sediments transformed into mica quartzites, gneiss and metapelites. In this metasedimentary sequence, intercalations of black sandy horizons rich in iron oxides (i.e. magnetite) are present in abundance and contain the main REE mineralization. However, metasomatism contemporary with metamorphism is well developed (Andersson et al. 2018b). It is responsible for the hydrothermal alteration of the black sandy horizons and leads to a remobilization of the REE-bearing minerals. The authors consider the Olserum deposit to be a paleoplacer that has been metamorphosed and weathered by the concomitant hydrothermal episode (Reed 2013; Tasman Metals Ltd. 2013).

The most abundant REE-bearing minerals are monazite and xenotime. Moreover, apatite is abundant, albeit with a low REE content. These three REE-bearing phosphates seem to be of metamorphic origin and associated with the hydrothermal episode, although a primary sedimentary (detritic) origin may also be possible (Reed 2013). Monazite and xenotime are present mainly in the form of inclusions in apatite and biotite, suggesting that apatite is the old, main REE-bearing mineral,

which was then leached during metamorphism. The highest REE contents are associated with the layers rich in magnetite and the quartzite to biotite-amphibole layers, while the lowest REE contents are associated with the levels of gneiss and quartzites.

In 2007, the IGE Nordic AB company estimated the resources of the Olserum deposit to be 2.8 Mt @ 0.83% REO (0.53% LREOs + 0.30% HREOs) or 23,226 t REO (IGE Nordic 2007). In 2013, an estimate following standard NI43-101 was published by the Tasman Metals company, indicating resources of 4.5 Mt @ 0.6% REO (33.9% HREOs from REO) or 27,260 t REO and inferred resources of 3.3 Mt @ 0.63% REO (33.7% HREOs from REO) or 20,770 t REO (Reed 2013; Tasman Metals Ltd. 2013). The cutoff grade was fixed at 0.4% REO.

#### 1.5.1.2.14. Nb-Zr-REE alkaline complex at Alnö (Sweden)

The alkaline complex at Alnö is situated in the middle of eastern Sweden and outcrops to the north of the isle of Alnö. The main intrusion is formed of alkaline silicate rocks and carbonatites that can be divided into four series (Morogan 1988; Hode Vuorinen and Hålenius 2005): pyroxenite, ijolite (melteigite-ijolite-urtite), nepheline syenite and calcium carbonatite, laid down in this order (Figure 1.20). The magmatic rocks of this complex are surrounded by a fenitized zone 500-600 m broad within the surrounding rocks (Morogan and Woolley 1988). The complex has been dated back to  $553 \pm 6$  Ma using the Rb-Sr method on whole rock (Brueckner and Rex 1980). A more recent and reliable dating using the Ar-Ar method has given an age of  $584 \pm 7$  Ma (Ediacarian; (Meert et al. 2007)). This age is interpreted as that of the crystallization of the alkaline complex (Andersen 1996). The Alnö complex intrudes the Proterozoic basement, mainly the migmatites belonging to the Svecofennian domain.

Additional minerals such as titanite and apatite are present in the ijolite series and incorporate non-negligible contents of Nb, Zr and LREE (Vuorinen and Hålenius 2005). Indeed, the titanite shows significant contents of Nb (0.4-7.3 wt.%  $\text{Nb}_2\text{O}_5$ ) within the melteigite and to a lesser extent in the ijolite with higher contents (6.5 wt.%  $\text{Nb}_2\text{O}_5$ ). Contents of a similar order of magnitude are sometimes measured in the titanite present in the nepheline syenite (up to 7 wt.%  $\text{Nb}_2\text{O}_5$ ). For zirconium, the highest grades are found in the borders of the titanite present in the melteigite and reach more than 2.8 wt.%  $\text{ZrO}_2$ . Finally, LREE contents (i.e.  $\sum \text{La}_2\text{O}_3 + \text{Ce}_2\text{O}_3 + \text{Pr}_2\text{O}_3 + \text{Nd}_2\text{O}_3$ ) are significant in the titanite present in the melteigite and can reach 1 wt.% with maximum values of up to 3.9 wt.%.

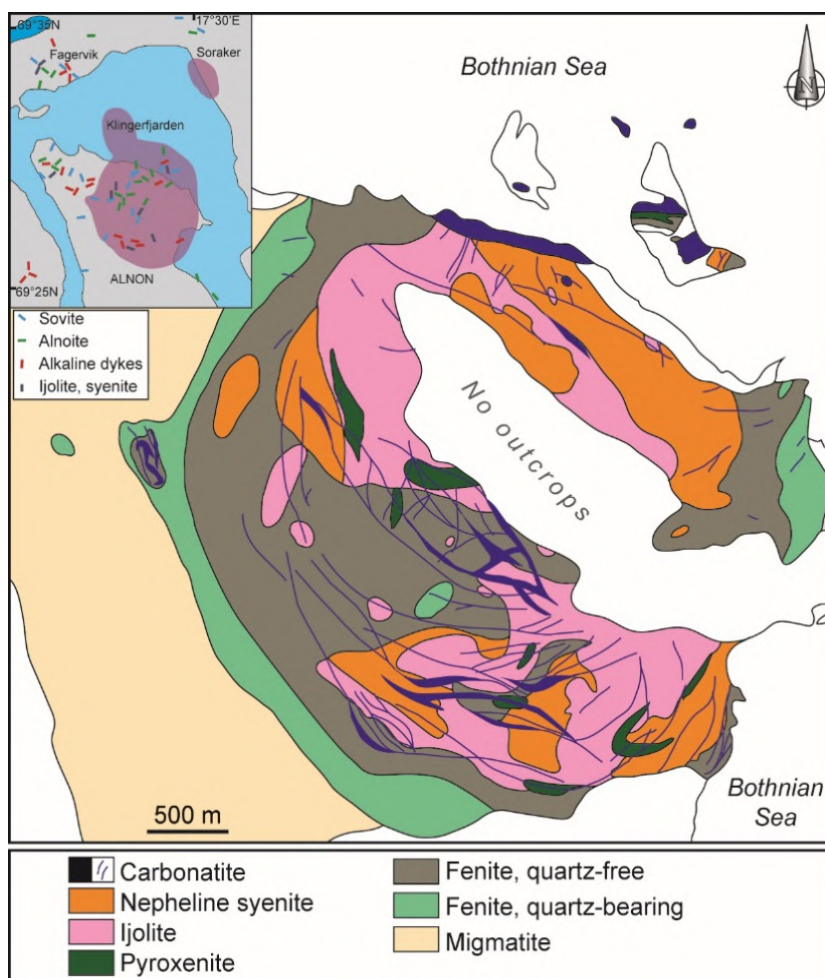


**Figure 1.20.** Nb-Zr-REE alkaline complex in Alnö (Sweden), modified from Vuorinen and Hälenius (2005)

#### 1.5.1.2.15. Bastnäs type Fe-REE-(Cu) skarns (Sweden)

The Fe-REE-(Cu) deposit at Bastnäs is situated in the Svecofennian domain, close to Skinnskatteberg, in the Bergslagen region in the center of southern Sweden (Figure 1.21). This deposit forms part of the mining district of Riddarhyttan and is a historical site for the discovery of REEs, with unpublished descriptions of many REE-bearing minerals (e.g. bastnäsite, cerite, törnebohmit). The Bastnäs deposit was first exploited for iron and copper, and approximately 160 tons of REEs were

extracted between 1860 and 1919 (Carlborg 1923). Geijer (1961) first introduced the notion of a “Bastnäs type” deposit in reference to iron deposits very rich in REEs. These deposits are situated near the districts of Norberg (30 km to the northeast of Bastnäs) and Rödbergsgruvan-Nora (50 km to the southwest of Bastnäs; (Geijer 1961; Holtstam and Andersson 2007, 2013 and references therein). The Bastnäs-type deposits are surrounded by felsic metavolcanic rocks and marbles from the lower Svecofennian (1.91–1.88 Ga), which have undergone significant hydrothermal alteration with metasomatism leading to richness in K, Na and particularly Mg in areas close to the mineralizations (Geijer 1923; Trägårdh 1991; Hallberg 2003). Afterwards, these rocks were metamorphosed in the amphibolite facies and intruded by at least two generations of plutonic rocks (i.e. 1.90–1.86 Ga and 1.81–1.75 Ga) (Lindh and Persson 1990; Andersson and Öhlander 2004).

Thus, Bastnäs-type deposits are characterized by skarn-type hydrothermal mineralization and a complex assemblage of iron oxides, calcic and magnesian silicates, REE silicates, REE fluorocarbonates, sulfides and Cu, Mo, Bi, Co sulfo-salts and Au-Ag minor alloys (Holtstam 2004; Sahlström et al. 2019). The deposits can be divided into two subtypes depending on their composition and the paragenesis of the REE-bearing minerals (Holtstam and Andersson 2007; Andersson et al. 2013):

- the LREE deposits at Bastnäs and Rödbergsgruvan (La, Ce) and rich in Fe;
- the Norberg district deposits, rich in LREE, Y+HREE, Mg, Ca and F.

The main REE-bearing minerals of the first subtype are cerite-(Ce), ferriallanite-(Ce), törnebohmit-(Ce) and bastnäsite-(Ce), while those of the second subtype are fluorobriholite-(Ce), västmanlandite-(Ce), dollaseite-(Ce), gadolinite-(Ce) and gadolinite-(Y). The precipitation of REE silicates in these deposits (i.e. cerite and fluorobriholite) results from the reaction between the relatively acidic fluids carrying the majority of the REEs complexified by ligands (F and Si) with the surrounding dolomitic rocks (Holtstam and Andersson 2007). Bastnäs-type deposits are almost unique, for example, an exoskarn with carbonated protolith of sedimentary origin. Recent datings using the Re–Os method on molybdenite have given crystallization ages for the sulfides associated with REE-bearing minerals between 1.90 and 1.84 Ga (Andersson et al. 2013). In detail, a space-time evolution is observed between the Rödbergsgruvan deposit, which is considered the most ancient in the southwest, and the most recent deposits from the Norberg district in the northeast.

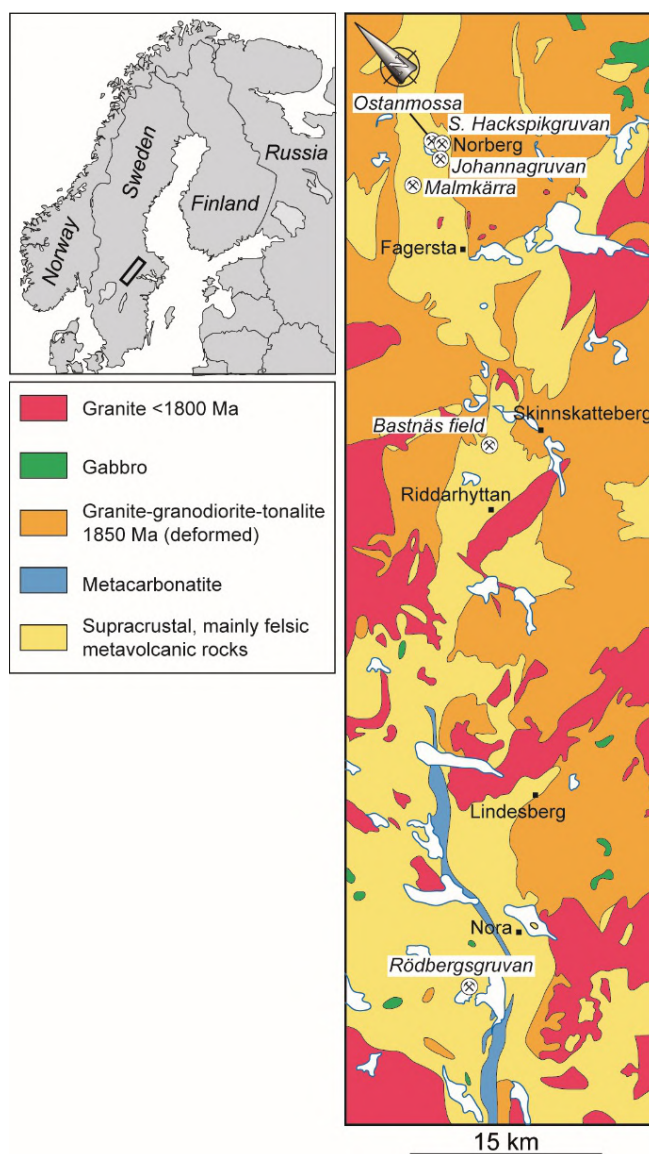


**Figure 1.21.** Bastnäs type Fe-REE-(Cu) skarns, Sweden (Holtstam and Andersson 2007)

In 2010, a joint venture was signed between a Swedish consultancy group and the Tasman Metals company to carry out an exploration campaign for REEs in the

Bastnäs region on a permit of 915 ha (Tasman Metals Ltd. 2010b). A series of samples taken in former mining sites have been analyzed by the Swedish Geological Survey (SGU) using XRF and ICP techniques. Samples have provided variable but high contents comprising between 1.82 and 17.47% REO, with an average of 6.97% REO (Tasman Metals Ltd. 2010b). Moreover, geochemical analyses have revealed U and Th depletion, still unexplained, in gadolinite, fluorobriholite and minerals from the allanite group (Holtstam and Andersson 2007).

### 1.5.1.3. Sveconorwegian domain

#### 1.5.1.3.1. Nb-REE-Fe and carbonatite complex at Fen-Søve (Norway)

The carbonatite complex at Fen-Søve (Figure 1.22) is established within Telemark gneisses dating from the Lower Proterozoic. It is situated near Ulefoss, 120 km to the southwest of Oslo, in Norway (Barth and Ramberg 1966; Mitchell and Brunfelt 1975; Andersen 1986, 1988; Kresten and Morogan 1986). This complex covers a surface of 9 km<sup>2</sup> and has already been exploited for iron between 1657 and 1927 (Fen mines) and for niobium from 1953 to 1965 (Søve mine), with 1 Mt of raw ore @ 0.31–0.57% Nb<sub>2</sub>O<sub>5</sub> (Dahlgren 2005). Moreover, the Fen-Søve complex is known as the type locality for søvite and fenite. The massif is formed mainly of alkaline rocks and carbonatites dating back to the Ediacaran, or approximately 565 Ma (age K/Ar on biotite) (Faul et al. 1959) and 583 ± 15 Ma (age <sup>40</sup>Ar/<sup>39</sup>Ar on biotite) (Meert et al. 1998). The erosion level makes it possible to have a section at approximately 1–3 km depth compared to the complex's initial emplacement (Sæther 1957).

The geological history of this complex can be broken down as follows:

- intrusion of alkaline rocks (melteigite, ijolite, urtite series);
- intrusion of calcic carbonatites (søvite and silico-søvite);
- intrusion of dolomite carbonatites (magmatic rauhaugite I);
- intrusion of alkaline lamprophyres (damkjernite);
- late alteration of the damkjernite, forming metasomatic rauhaugite II (Kresten and Morogan 1986; Andersen 1988; Dietzel et al. 2019 and references therein);
- a fenite aureole surrounds the complex at the level of the western and southern borders.

In 2011, the Danish exploration company 21st North obtained a permit for REEs covering the external carbonatite part of the Fen-Søve complex. Indeed, the eastern parts of the complex are richer in REEs, especially in ankerite-dolomite carbonatite (rauhaugite) and hematite carbonatite (rødberg) (Lie and Østergaard 2011).

However, large parts of the complex are still little known, given the well-developed surficial cover. Before 21st North's recent works, the Geological Survey of Norway (NGU) carried out a detailed study on REE potential between 1967 and 1970, focusing on the northeastern part of the complex. The most promising REE contents are situated in hematite carbonatite (rødberg) with approximately 2.8% REO (8 elements + Y), and in ankerite-dolomite carbonatite (rauhaugite) with 1.51% REO (Lie and Østergaard 2011). Historical mineralogical and geochemical studies in the Fen complex have shown that the abundance of REEs increased in the following order: ijolite-damkjernite < søvite-rauhaugite < rødberg, reflecting the order of differentiation of the magma with the highest REE contents within the last rocks formed (Mitchell and Brunfelt 1975). REEs are mainly carried by monazite, bastnäsite, synchysite and parisite.

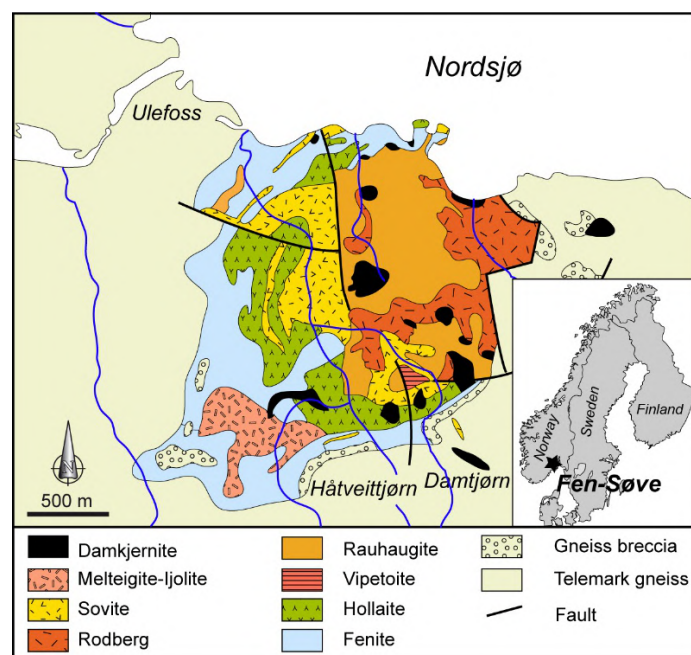


**Figure 1.22.** Nb-REE-Fe and carbonatite complex at Fen-Søve (Norway), modified from Lie and Østergaard (2011)

In 2011, the 21st North company collected 58 samples to measure the REE content and identify the minerals within each type of REE mineralized rock. Ankerite-dolomite carbonatite contains approximately 1.32% REO carried by bastnäsite, synchysite and parisite (in the form of aggregates with grains from 0.1 to

1.0 mm). Hematite carbonatite contains approximately 2.32% REO carried by the finer monazite and complex phases of Nb-Fe-Ti-Y-REE, rich in HREEs. Moreover, apatite concentrates extracted from calcic carbonatites contain 3,752–5,220 ppm REE and 164–288 ppm Y, and those extracted from ankerite-dolomite carbonatites contain 5,143 ppm REE and 199 ppm Y (Hornig-Kjarsgaard 1998; Ihlen et al. 2013). To the south and east of the massif, an envelope has been estimated with inferred resources of 84 Mt @ 1.08% REO (0.8% REO in cutoff grade), but the resources of the entire complex are probably greater (Lie and Østergaard 2014).

#### 1.5.1.3.2. Pegmatitic Ta-Nb-REE fields at Evje-Iveland, Froland and Glamsland (Norway)

To the south of Norway, at the end of the Sveconorwegian orogeny, the NYF-type pegmatite fields outcrop (Figure 1.23): Evje-Iveland, Froland and Glamsland ((Andersen 1926; Bjørlykke 1937; Larsen 2002; Müller et al. 2012, 2018) and references therein). These pegmatites form the south Norwegian pegmatite belt formed over the course of the Sveconorwegian orogeny (1.14–0.90 Ga) on the western margin of the Fennoscandian Shield, when the Bamble “terrane” overlaid the Telemark terrane along the Porsgrunn-Kristiansand fault at approximately 1.09–1.08 Ga (Bingen et al. 2008). However, the datings available for these pegmatites are scarce and often based on obsolete methods (Rb–Sr on simple mineral). Despite this, the pegmatites date back to  $1,060^{+8}_{-6}$  Ma at Froland (age U/Pb on euxenite) (Baadsgaard et al. 1984) and  $910 \pm 14$  Ma at Evje-Iveland (age U/Pb on gadolinite) (Scherer et al. 2001), leading the authors to consider a post-orogenic emplacement. Indeed, later structural studies have shown that the pegmatites were laid down syntectonically, which implies a space-time relation between the deformation and magmatism over the course of the Sveconorwegian orogeny (Hendersen and Ihlen 2004).

Most of the pegmatites are laid down in basic rocks (amphibolite, norite and basic gneisses). The veins rarely exceed 20 m in width in the form of subhorizontal lenses that very often intersect the foliation of the surrounding rocks. In the Froland field, the pegmatites belong, according to the classification by Černý and Ercit (2005), to the HREE abyssal pegmatites and do not seem to be linked to granitic plutons such as that of Herefoss (in the southwest of the zone). The pegmatites contain, in varying proportions, quartz, alkaline feldspar, plagioclase, biotite and a small amount of white mica, and REE minerals and other additional minerals are rare (Ihlen et al. 2001, 2002). Nevertheless, the only pegmatites to present a significant REE mineral content are those at Bjortjørn and Gloserheia in Froland (Müller et al. 2005); this field has approximately 100 pegmatite veins. In the Evje-Iveland field, the pegmatites are classed as REE pegmatites and muscovite and REE pegmatites (Černý and Ercit 2005; Müller et al. 2012). The genetic relationship

between the pegmatites and the granitic pluton of Høvringsvatnet ( $971^{+63}_{-34}$  Ma) (Andersen et al. 2002) is still under debate. These pegmatites contain mainly K-feldspar, plagioclase, quartz, biotite and muscovite, magnetite and garnet as minors, and variable proportions of REE minerals and rare metals (beryl, allanite, monazite, euxenite, aeschinite, gadolinite or columbite). Approximately 350 pegmatites crop out in the Evje-Iveland field, including the Steli pegmatite and some other lithium pegmatites that include REEs (monazite and euxenite). The Slobrekka pegmatite is highly fractionated and rich in Y-REE minerals (gadolinite-(Y), allanite-(Ce), aeschinite-(Y) and euxenite-(Y)).

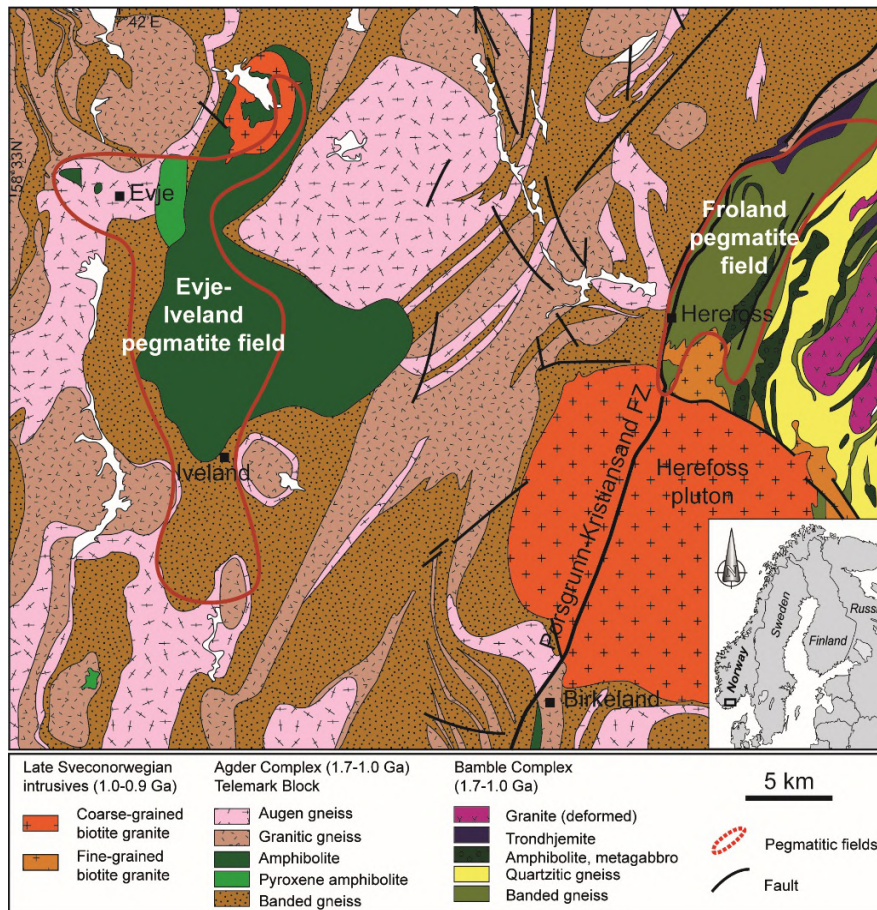


**Figure 1.23.** Ta-Nb-REE pegmatite fields at Evje-Iveland, Froland and Glamsland, Norway (Muller et al. 2012)

## 1.5.2. The rare earths indices of the Caledonides

### 1.5.2.1. Scandinavian Caledonides

#### 1.5.2.1.1. U-REE-P phosphorite at Tåsjö (Sweden)

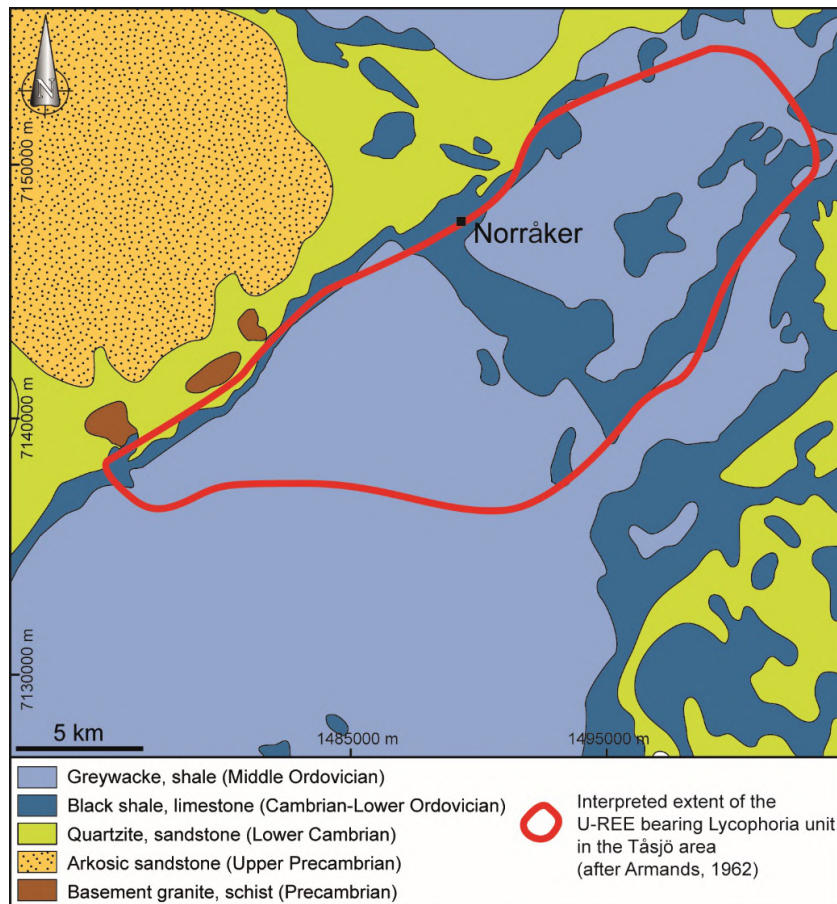


**Figure 1.24.** U-REE-P phosphorite at Tåsjö (Sweden)

The Tåsjö occurrence of U-REE-P is situated in Sweden (Figure 1.24), 200 km north of Ostersund, between the cities of Dorotea and Strömsund (in the counties of Västerbottens and Jämtlands län). This zone was prospected for uranium in 1957 by the Swedish atomic energy company. The Tåsjö occurrence is situated on the Caledonian front in the lower native unit, and mineralization is encased in Lycophoria shales of the Lower Ordovician and aluniferous shales from the

Cambrian-Ordovician (see Browne (2008) and references therein; Sadeghi et al. (2013)). The thickness of the mineralized series reaches 15–20 m in the aluniferous shales and 3–10 m in the Lycophoria shales. Moreover, this zone is greatly deformed by the caledonian tectonic, with overlaps, sheets and folds that led to a thickening of the series (more than 400 m in thickness for the aluniferous shales).

Aluniferous shales are black, foliated pyrite shales, with variable proportions of glauconite and apatite, while Lycophoria shales are formed by siltstone layers and pelitic layers with phosphate nodules. The peculiarity of Tåsjö is the thick phosphate unit (lycophoria shale) with high concentrations of uranium (associated with apatite, which forms 9 to 20% of the rock) and REEs. Estimates show that the uranium content in apatite is 0.16%, while the content of the Lycophoria shale (approximately 75–150 Mt) is 0.03–0.07%  $U_3O_8$ , 0.11–0.24% REE and 3.75–7.5%  $P_2O_5$  (Armands 1964, 1970). Therefore, the total tonnage of this occurrence has been estimated at 47–53 Mt  $U_3O_8$ , 165,000–180,000 tons REE and 5.63 Mt  $P_2O_5$ . The Tåsjö zones continued to be explored for uranium and REEs by the Mawson Resources company (Browne 2008).

#### 1.5.2.1.2. Pyroxenite and P-REE complex at Misværdalen (Norway)

Discovered by Farrow in 1974, the Misværdalen complex contains several intrusions of clinopyroxenite dating from the middle Ordovician to the upper Devonian to the north of Norway, 40 km east of Bodø (Figure 1.25). These pyroxenite bodies occupy approximately 8 km<sup>2</sup> and show richness in apatite. In 2006, the Nordland mineral company and the NGU considered the latter to present mineral potential (Ihlen et al. 2013). Pyroxenite is formed in variable proportions from biotite, alkaline feldspar and apatite at more than 70 vol.%. The  $P_2O_5$  content of the clinopyroxenites is estimated at approximately 2.4 wt.% (see Ihlen et al. (2013) and references therein) with higher values in the coarse-grained pyroxenites (2.5 wt.%  $P_2O_5$  or approximately 6 wt.% apatite). Chemical analyses of the apatite grains extracted from the coarse-grained pyroxenites present REE contents between 1,243 and 11,180 ppm, with averages varying between 4,150 and 6,363 ppm (Ihlen et al. 2013). This great variation in REE levels is a priori linked to the retrograde formation of allanite, which is observed along microfractures within the apatite grains. Moreover, chemical analyses on the apatite concentrates from the fine-grained and coarse-grained pyroxenites show values between 4,276 ppm REE and 3,883–4,075 ppm REE, respectively. Indeed, the relatively high Th content detected in some samples (as high as 100 ppm) does not allow the use of apatite in fertilizers.

### 1.5.2.2. British-Irish Caledonides (United Kingdom)

Several alkaline intrusions crop out to the northeast of the Caledonian belt to the north of the Highlands (Figure 1.26), dated using U/Pb on zircon to the Silurian and Ordovician (Halliday et al. 1987; Thirlwall 1988). The magmatic source seems to have been linked to the limited partial melting of the lithospheric mantle in line with the Caledonian orogeny (Halliday et al. 1987). The rocks are formed of differentiated series ranging from melanocratic syenites to more evolved leucosyenites, with the local presence of ultrabasic rocks such as pyroxenites. The British Geological Survey (BGS) has carried out a study on these alkaline intrusions, especially on their REE potential (Shaw and Gunn 1993; Walters and Lusty 2011; Walters et al. 2012).

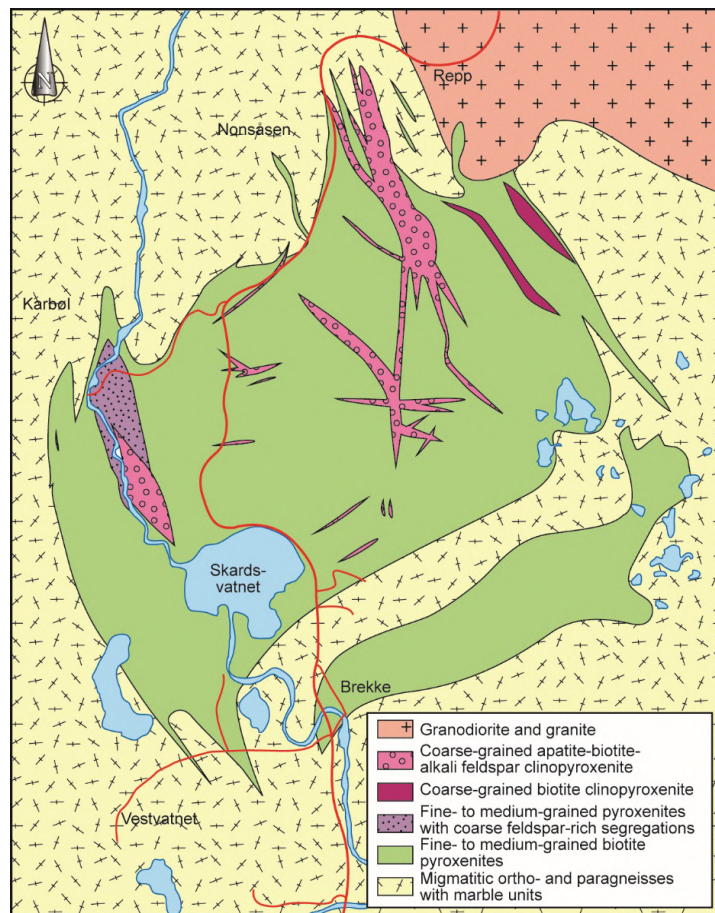


**Figure 1.25.** Pyroxenite and P-REE complex at Misværdalen, Norway (Ilhen et al. 2013)

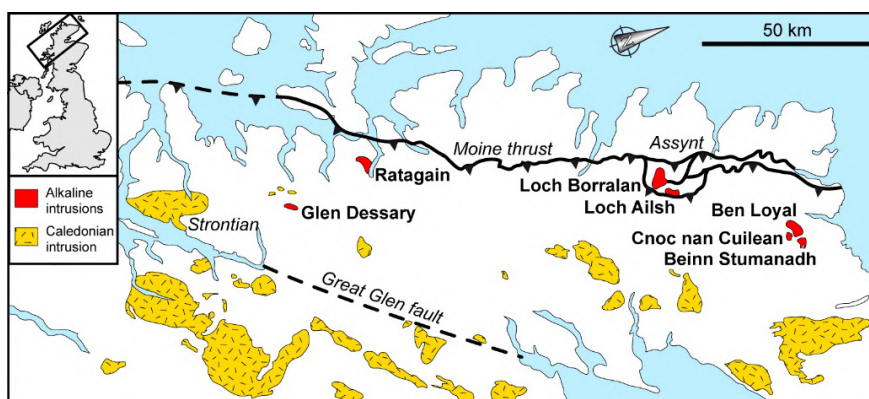


**Figure 1.26.** Caledonian magmatism and associated alkaline intrusions (Halliday et al. 1987)

#### 1.5.2.2.1. Alkaline intrusion at Loch Borralan

The intrusion at Loch Borralan has been dated back to  $426 \pm 9$  and  $430 \pm 4$  Ma using the U/Pb method on zircon. From 1988–1989, geochemical analyses were carried out on samples from 37 drillings performed in apatite-biotite-melanite-phlogopite pyroxenites, with the aim of exploring elements of the platinum group. These 37 drillings had been made 10 years earlier for an exploration of phosphates. Apatite is present in the form of euhedral crystals (of some millimeters). REEs have been detected in apatite thanks to measurements taken using X-ray fluorescence spectrometry. In 1990, an additional 37 drillings in the pyroxenites and syenites revealed REE contents of up to 739 ppm La, 1,764 ppm Ce and 986 ppm Y. Apatite contents reach up to 2% and make this mineral the main REE carrier. Unfortunately, the alkaline intrusion at Loch Borralan is not an economic target for REE exploitation.

#### 1.5.2.2.2. Alkaline intrusion at Loch Ailsh

Following the discovery of levels rich in platinoids in the Loch Borralan intrusion, additional studies were carried out in the Loch Ailsh alkaline intrusion in 1989 and 1990. This alkaline intrusion has been dated back to  $430 \pm 4$  and  $439 \pm 4$  Ma using the U/Pb method on zircon. The average contents of La and Ce are similar to those found in the Loch Borralan intrusion. Nevertheless, the Allt Cathair Bhan zone presents significant enrichment, with maximum concentrations of 3,239 ppm La and 3,956 ppm Ce in syenite and 840 ppm La and 1,456 ppm Ce in pyroxenite. An enrichment in U (maximum 65 ppm) and in Th (maximum 244 ppm) has also been measured. Finally, allanite is another REE-bearing mineral in addition to apatite.

#### 1.5.2.2.3. Alkaline intrusions at Ben Loyal and Cnoc nan Cuilean

In 1990, limited exploration was carried out for REE minerals in the alkaline intrusions of Ben Loyal and Cnoc nan Cuilean (dated back to  $426 \pm 9$  Ma using the U/Pb method on zircon). Two samples of Cnoc nan Cuilean syenite show an enrichment of REEs with a maximum of 5,667 ppm La and 19,785 ppm Ce and an average value of 3,800 ppm REO (Shaw and Gunn 1993; Walters and Lusty 2011; Walters et al. 2012). Many REE minerals have been recognized, and allanite is the main REE mineral. Three generations of allanite have been identified: a late generation in a “crown” around the apatite, a generation of crystals in microveins intersecting the syenite, and a generation of crystals within biotite and magnetite veins (Walters et al. 2012). For all allanite generations together, the average content is 22% REO. Finally, it should be noted that the alkaline intrusion of Ben Loyal presents no major enrichment of REEs among the samples analyzed to date.

### 1.5.3. Rare earth occurrences in the Variscan belt

#### 1.5.3.1. *The domains of western and central Europe (Gondwana-Avalonia-Armorica)*

##### 1.5.3.1.1. The Armorican massif – gray monazite shales from the Ordovician in Brittany (France)

Since the 1960s, the Armorican massif has been known for black shales from the Paleozoic, including nodular gray monazites, to heights of 50–200 g/t (Donnot et al. 1973). The monazite grains (up to 2 mm in diameter, flattened ellipses) are characterized by many mineral inclusions (phyllites, quartz, rutile, graphite, iron oxides), the absence of an inherited core, a notable enrichment of intermediate rare earths (Sm, Eu, Gd) and very low concentrations of Th and U. The core of the grains presents up to 10 wt.%  $\text{Sm}_2\text{O}_3$ , 1.3 wt.%  $\text{Eu}_2\text{O}_3$  and 5 wt.%  $\text{Gd}_2\text{O}_3$ , whereas their rims are rich in LREEs. The crystallization of monazites is authigenic and occurs under conditions of deep diagenesis at the limits of very low-grade metamorphism (Tuduri et al. 2013). The erosion of these gray monazite shales gave rise to the formation of placers similar to those in Iberia, the Belgian Ardenne or the Welsh basin.

##### 1.5.3.1.2. Wales and the southwest of England – nodular gray monazites of the Ordovician-Silurian of the Welsh basin (United Kingdom)

In the United Kingdom, nodular gray monazite occurrences have been listed in the Welsh basin due to pan concentrates collected over the course of the inventory by the BGS mineral exploration programme (Cooper et al. 1983, 1984; Smith et al.

1994) in Wales, Exmoor and southwestern England. The concentrates presented high levels of REE with, notably, more than 5,000 ppm of Ce (Figure 1.27).

These anomalies have been attributed to the presence of nodular gray monazite. The highest Ce contents have been measured in rocks from the Silurian and Ordovician, which are detrital sediments, including black shale layers intercalated in clays, siltstones and sandstones with turbidite facies. The monazite grains are on the millimeter scale (0.05–2 mm), ovoid and have marked zoning between LREE and HREE between the core and the rims. The monazites also present low-grade metamorphic fabrics, similar to the surrounding rocks, and a low Th content (Read et al. 1987). Milodowski and Zalasiewicz (1991) and Evans and Zalasiewicz (1996) proposed that the nodular monazites were formed by the migration of REEs from the clay layers to layers rich in organic matter where grains could crystallize over the course of late diagenesis.

These gray monazite occurrences are not isolated in the Welsh basin and are also found in Brittany (Donnot et al. 1973), the Ardenne massif (Nonnon 1984; Limbourg 1986; Burnotte et al. 1989) and northwestern Spain (Vaquero 1979; Windle and Nesbitt 1993). These nodular monazites, present in sediments from the Lower Paleozoic, have – on a European scale – similar chemical and mineralogical properties (Smith et al. 1994).

In the United Kingdom, an estimate of the economic potential of these occurrences has been carried out by Smith et al. (1994). Although the nodules present low contents of Th and interesting contents of Eu, the surrounding rocks do not contain sufficient monazites to be exploited economically. Moreover, the study recommends studying placers resulting from the erosion of shales from the Ordovician-Silurian more precisely. These are the source of the monazites and so of the REEs.

#### 1.5.3.1.3. The Bohemian massif – NYF Pegmatites from the Třebíč pluton (Czech Republic)

The Třebíč pluton is situated in western Moravia (Czech Republic) and is formed of rocks running from melasyenite to melagranite (durbachite) corresponding to type I granitoids (Foley et al. 1987; Finger et al. 1997). The rocks are generally amphibole, biotite and quartz porphyries. They are locally foliated, especially at the edges. The additional minerals are fluorapatite in abundance, zircon and titanite. Phlogopite is associated with trace minerals such as allanite-(Ce), thorite, thorianite, monazite-(Ce), xenotime-(Y), cheralite and sulfides (Sulovský 2000). The granite has been dated back to  $342 \pm 2$  Ma (Kusiak et al. 2010) using the U/Pb method on zircon.

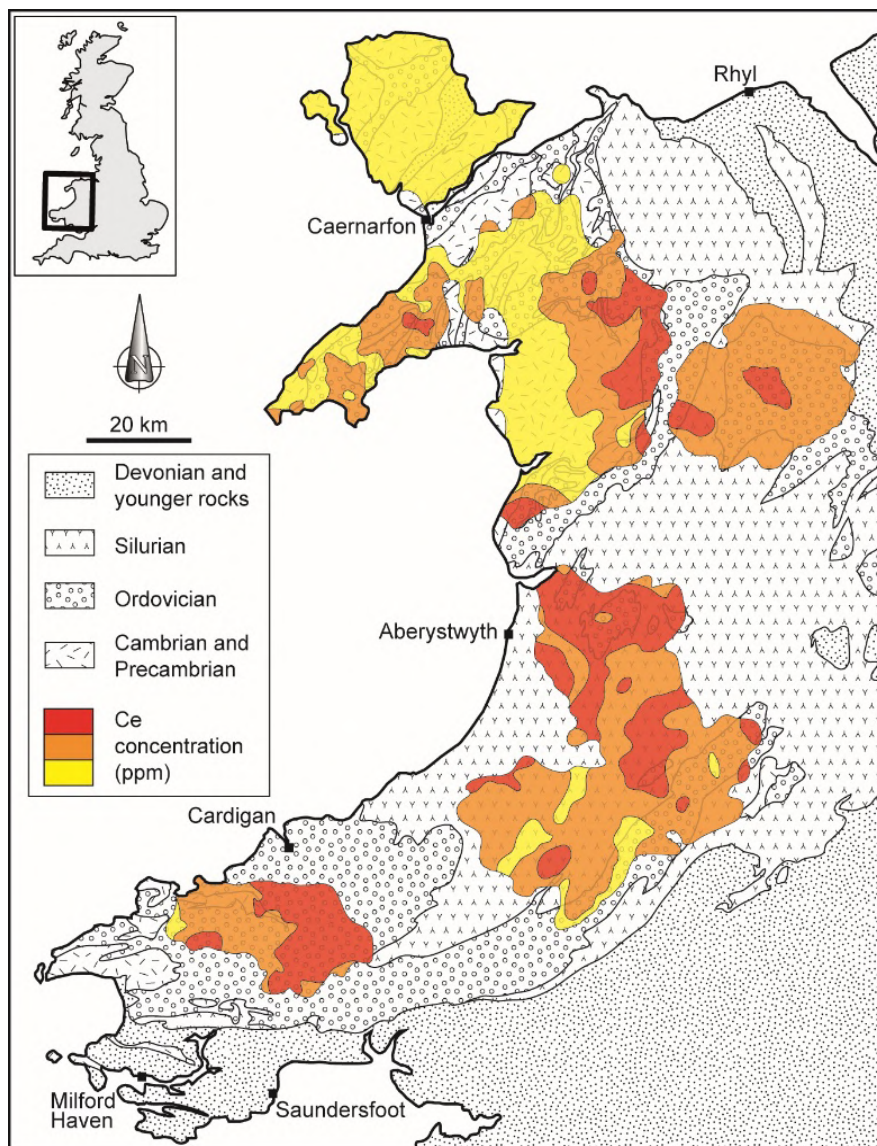


**Figure 1.27.** Welsh basin and Ce anomalies associated with gray monazite occurrences (Smith et al. 1994)

The Třebíč pluton also includes pegmatites distributed over two zones (Škoda et al. 2006; Škoda and Novák 2007): to the south (Třebíč-Vladislav) and the north

(Velké Meziříčí-Bochovice). On the basis of the internal structure, geochemical fractionation and mineralogical composition, two varieties of pegmatites (allanite subtype and euxenite subtype) are distinguished and are of the NYF type (Černý and Ercit 2005; Škoda et al. 2006). The pegmatites are characterized by K-feldspar, phlogopite and the absence of muscovite, titaniferous minerals (titanite, ilmenite) and REE minerals (allanite-(Ce), aeschinite and euxenite) (Škoda et al. 2006; Škoda and Novák 2007). Despite these mineralogical specifics, the Třebíč pluton is not an economic target.

#### 1.5.3.1.4. The Bohemian massif – Ti-Zr-Th-REE paleoplacer from the Ordovician at Brtná (Czech Republic)

On the basis of radioactive sites listed by the Czech uranium industry (Křištiak and Záliš 1994), Goliáš (2001) published a summary of Th occurrences in the Czech Republic. Where REEs are concerned, the Brtná region (in the west of the country, near Dolní Žandov) presents radiometric anomalies associated with sericite quartzite layers 50–80 m thick within the Dyleð micaschists (Saxothuringian).

The Th concentration varies between 126 and 542 ppm. This rock contains zircon, rutile of metamorphic origin, hematite and xenotime. Th is situated within the monazite and the cheralite of metamorphic origin. The Th occurrences, although they underexplored, are interpreted as belonging to a Ti-Zr-Th-REE paleoplacer dating back to the Ordovician and metamorphosed (Goliáš 2001).

#### 1.5.3.1.5. The Ardenne massif – gray monazite shales from the Ordovician in the Ardenne (Belgium)

The first nodular gray monazite occurrences in the Belgian Ardenne were described in shales from the Upper Cambrian (“Revinian”) in the Rocroi massif by Nonnon (1984) from the mineralogical pan bottom study. Other occurrences have been discovered in metasediments from the Upper Devonian (Siegenian) in the syncline at Neuf-château (Limbouurg 1986), shales from the Cambrian-Ordovician in the Stavelot massif (Burnotte et al. 1989) and the Brabant massif (Nonnon 1989) (Figure 1.28). In the Stavelot massif, the gray monazites are present in black shales intercalated into a microconglomerate with phosphate nodules (Burnotte et al. 1989). The monazite grains rarely exceed 700 µm, with an average size of 300 µm. The grains are formed of polycrystalline aggregates, with the exception of a few single crystals or, more rarely, pairs. The chemical and mineralogical characteristics are similar to the gray monazites of the Welsh basin (Smith et al. 1994) and Brittany (Donnot et al. 1973).

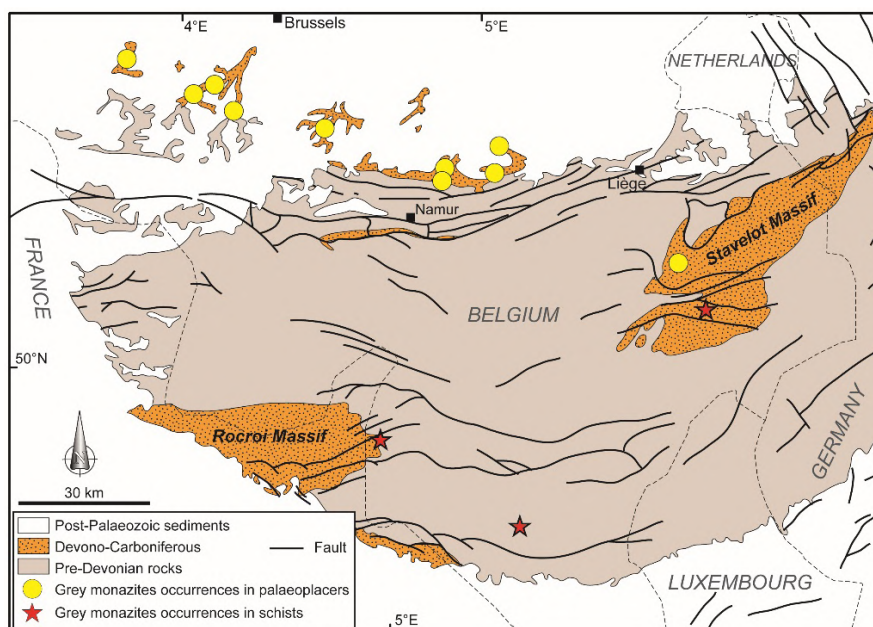


**Figure 1.28.** Gray monazite shales from the Ordovician in the Ardenne, Belgium (Burnotte et al. 1989; Nonnon 1989)

#### 1.5.3.1.6. French Massif Central – the phosphorites of the Cévennes and the Montagne Noire (France)

To the south of the French Massif Central, the Cévennes and the Montagne Noire include dolomites and limestone with phosphate nodules that show high radioactive anomalies (2,000 ppm U and 1,500 ppm Th) (Laval et al. 1990). In the Cévennes, close to Le Vigan, phosphate levels of 2–3 m thickness and limited lateral extension have been sampled with dolomites from the Cambrian to estimate their REE content. The nodules are mainly formed of microcrystalline apatite associated with quartz and white mica geodes. The nodules sampled are rich in U (1,000–2,200 ppm), Th (1,000–1,800 ppm) and REO (1,700–2,500 ppm, with wealth in HREEs). Unfortunately, the low REO content (0.2%) is not sufficient to excite economic interest (Laval et al. 1990). In the Montagne Noire, the phosphate levels are localized in carbonates from the Cambrian on the northern flank of the massif. The phosphate nodules are on the centimeter scale, gray–black and form levels of 20–30 cm thickness broadly parallel to the bedding of the carbonates. The nodules are formed of quartz, microcrystalline apatite and micas (Laval et al. 1990; Clausen and Alvaro 2007). The REO content varies between 300 and 2,100 ppm and is

associated with low U concentrations (10–40 ppm) and Th concentrations (5–20 ppm) (Laval et al. 1990). The negative Ce anomaly led Laval et al. (1990) to consider a marine origin for the phosphate nodules. The phosphate nodules of Montagne Noire no longer present any economic interest for REEs.

#### 1.5.3.1.7. Iberia – rocks with nodular gray monazite (Spain and Portugal)

In Portugal, REEs were prospected for the first time by the IGM (Institute of Geology and Minerals) in the regions of Beira Baixa and to the north of Alentejo. In the region north of Alentejo, gray monazites resulting from the weathering of quartzites from the Silurian-Ordovician were identified on the southwest flank of the Portalegre syncline (IGM 1998; Rosa et al. 2010; Salgueiro et al. 2020). An enrichment of REEs was measured within the quartzites intercalated into the Alegrete schists (Portalegre) at the level of the regions of Vale de Cavalos and Penha Garcia.

In Spain, at Becerreá in Galicia, the Aqueira Formation is considered one of the potential sources of gray monazites that form the region's paleoplacers (Vaquero 1979; Rosenblum and Mosier 1983). This formation is formed of layers of clay, silt and sandstone affected by low-grade regional metamorphism and contact metamorphism (Marcos et al. 1980).

#### 1.5.3.1.8. Iberia – hyperalkaline complex at Galiñeiro (Spain)

The hyperalkaline complex at Galiñeiro is a circular massif of approximately 10 km<sup>2</sup> close to Vigo in northwestern Spain. This complex forms one of the many orthogneisses from the Lower Paleozoic in the Variscan belt (the Armorican massif, Portugal, northwest and southwest Spain). These complexes mainly outcrop in the central part of the orogen and form calc-alkaline, alkaline and sometimes hyperalkaline rocks. The Galiñeiro complex has been dated back to  $484 \pm 5$  Ma (Kusiak et al. 2010) using the U/Pb method on zircon (Montero et al. 2009). It is formed of two lithologies: aegirine-riebeckite gneiss and amphibole-biotite gneiss. Within the massif, veins and small hydrothermally altered clusters contain additional mineral phases rich in Th (thorite, thorite enriched in P), as well as REE-bearing minerals: bastnäsite, REE silicates (allanite, thalenite-yttrialite), REE niobiotantalates (aeschinite, fergusonite-formannite, samarskite, pyrochlore-betafite) and REE phosphates (monazite, xenotime) (Montero et al. 1998; Floor et al. 2007). The magmatic fractioning is initiated from an alkaline basaltic mantle magma, which has resulted in differentiated siliceous and hyperalkaline rocks with residual fluids extremely rich in fluorine and other ligands that have made it possible to complex the REEs. The decrease in fluorine activity with the drop in temperature and the crystallization of fluorine minerals remobilized the complexes created previously, leading to the

formation of minerals rich in REEs. Moreover, the Galiñeiro complex after alteration and erosion would be the source of REE minerals that form the alluvial and coastal placers and the Ría Vigo valley (Marmolejo-Rodríguez et al. 2008).

### 1.5.3.2. *The Oslo Rift (Norway)*

#### 1.5.3.2.1. Pegmatite field at Langesundsfjord-Larvik

The pegmatite field at Langesundsfjord-Larvik is situated to the south of the Oslo rift, at approximately 100 km from Oslo (Larsen et al. 2008). This field forms part of the plutonic complex at Larvik, known for nearly 200 years. A book published by Larsen (2010) retraces the geology, mineralogy and history of the district. The Larvik complex (50 km long and 20 km large) is formed of monzonite and larvikite, and integrates lardalite and foyaite in the Lågendalen-Farris region, as well as the nepheline syenites around Langesundsfjord (Larsen 2010). In the Langesundsfjord region, larvikite intrudes sediments from the Silurian and Carboniferous as well as basalt flows. Larvikite and lardalite have been dated back to  $298.6 \pm 1.4$  Ma and  $292.1 \pm 0.8$  Ma, respectively, using the U/Pb method on zircon and baddeleyite (Dalghren et al. 1996). Moreover, the larvikite and the pegmatites near Larvik and Tveladen were laid down at approximately 290 Ma.

Within the Larvik complex, a great variety of pegmatites have been described according to the mineral textures and parageneses: Stålaker type (coarse-grained alkaline feldspar, dendritic crystals of amphibole and biotite, thin prisms of apatite and zirconolite), Stavern type (prismatic zircon of up to 5–6 cm, alkaline feldspar of 0.3–0.5 m in length), Tveladen type (microcline, nepheline, aegirine, ferro-edenite, magnetite and biotite with many REE minerals), Bratthagen type (feldspar alkaline, nepheline, aegirine prisms and additional minerals such as loparite) and the nepheline syenite type from Langesunfjord (agpaitic pegmatites). The known pegmatite sites in the Larvik complex (quarries, mainly) are Låven, the southern part of Stokkøya, the Arøy isles, Eikaholmen, Skutesundskjærene, Sagåsen, Tvedalen, Jahren, Bratthagen, Ula and Vøra (Larsen 2010; Piilonen et al. 2018 and references therein). The main REE minerals described in the pegmatites are allanite-(Ce), ancylite-(Ce), bastnäsite-(Ce), britholite-(Ce), cerite, chevkinite-(Ce), eudialyte, fergusonite-(Y), gadolinite-(Ce), hingganite, kainosite-(Y), loparite-(Ce), monazite-(Ce), parisite-(Ce), perrierite-(La), thorite, tritonite-(Ce), xenotime-(Y), zirconolite and zirsilite-(Ce).

#### 1.5.3.2.2. Fe-Ti-REE apatite pyroxenite ores at Kodal

The Kodal deposit is situated in the Oslo rift (Permian), 100 km south of Oslo, and belongs to the plutonic complex at Larvik (Bergstøl 1972; Lindberg 1985; Korneliussen et al. 2000; Ihlen et al. 2013) (Figure 1.29).

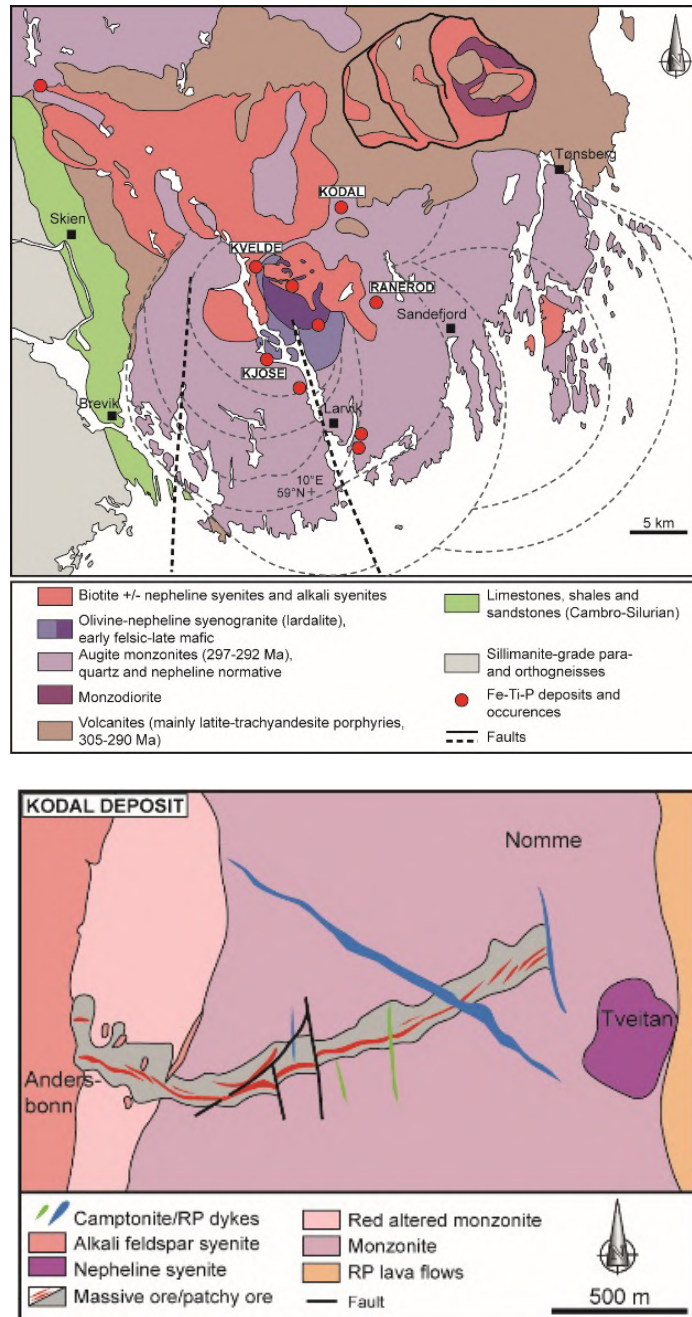


Figure 1.29. Fe-Ti-REE apatite pyroxenite ores at Kodal (Ilhen et al. 2013)

This deposit was explored by Norsk Hydro from 1959 to 1984 for its apatite potential, with ilmenite and magnetite as possible by-products. A recent survey campaign was carried out by Kodal minerals. The deposit is a set of massive pyroxenite lenses within nepheline monzonite. The ores are fine-grained and contain clinopyroxene (20–40% diopside) surrounded by an ilmenite matrix (5–15%), magnetite (25–60% ilmenomagnetite and titanomagnetite) and apatite (15–24% and an average of 17%). Other minerals have been identified: phlogopite (3–10%), magnesiohastingsite hornblende, olivine, feldspar, nepheline, fluorapatite and carbonates (Bergstøl 1972; Lindberg 1985; Andersen and Seiersten 1994). The apatite contains fluid inclusions (H<sub>2</sub>O-CO<sub>2</sub>) and crystals of calcium amphibole, titanite, calcite and REE carbonates (Andersen and Seiersten 1994). According to Lindberg (1985), the reserves are 70 Mt @ 4.9 wt.% P<sub>2</sub>O<sub>5</sub>, considering a transition zone with surrounding rocks. Moreover, the ore massif would represent deep reserves of 35 Mt @ 6.8 wt.% P<sub>2</sub>O<sub>5</sub>. The Kodal apatite presents acceptable contents of Th for use as fertilizer (26–71 ppm and an average of 40 ppm) (Ihlen et al. 2013). The apatite contains approximately 1 wt.% REE (between 7,588 and 10,990 ppm REE), which would represent a by-product of value.

#### 1.5.3.2.3. Zr-Nb-REE alkaline volcanic rocks at Sæteråsen

The Sæteråsen occurrence is southwest of Oslo in the eponymous rift. This Zr-Nb-REE index is formed of two aphyric trachyte flows within a broader volcanic sequence (the Vestfold Plateau). Petrographic and mineralogical studies have shown the presence of minerals bearing Nb, Ce, La and Y within lavas: euxenite, pyrochlore, chevkinite, fergusonite and apatite. A preliminary estimate on the basis of four drillings gives a tonnage of 8 Mt @ 0.245% Nb; 0.35% REE; 2.25% Zr; 0.180% Ce; 0.110% La; 0.075% Y; 0.069% Nd and 0.049% Th (Ihlen 1983; Ryghaug 1983; Ihlen et al. 2013; NGU 2013). It seems possible to find other similar occurrences on the vast Vestfold volcanic plateau.

### 1.5.4. Rare earths indices from the Mesozoic

#### 1.5.4.1. The fluorine district in Pennines (United Kingdom)

To the south of the English-Scottish border, the mining district north of the Pennines occupies two high points, the Alston block to the north and the Askrigg block to the south (see Bouch et al. (2008) for details). This district is reputed for its Mississippi-Valley type (MVT) Pb-Zn-F-Ba-Ag deposits. Its past production is estimated at approximately 4.0 Mt Pb; 0.3 Mt Zn; 2.1 Mt of fluorine and 1.5 Mt of barite (Bouch et al. 2008). This region (Figure 1.30) is formed of volcanic and

sedimentary rocks from the Lower Paleozoic intruded by Caledonian granitoids (Tynehead, Scordale, Corsnay and Weardale plutons) (Kimbell et al. 2010), since the whole is covered by Carboniferous sediments (limestone, sandstone, pelites with coal veins). The mineralizations (lenses and veins) were established at the end of the Permian in three stages:

- dolomitization and ankeritization of the surrounding carbonate rocks;
- the main sulfide mineralization;
- barite mineralization (Cann and Banks 2001; Bouch et al. 2008).

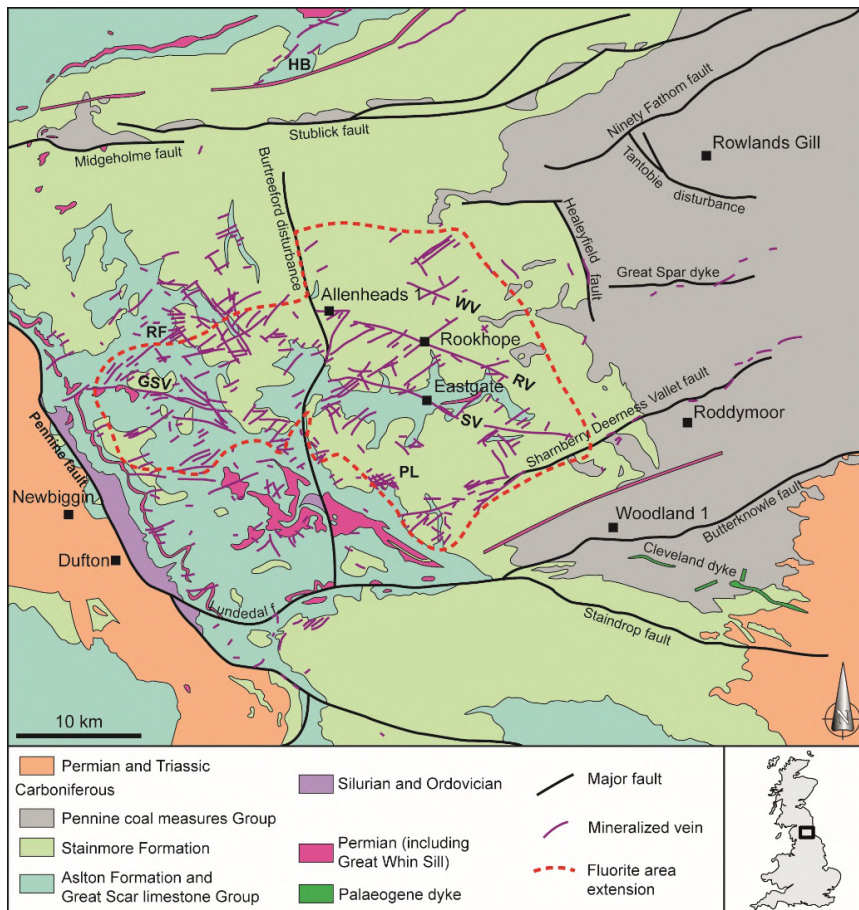


**Figure 1.30.** Fluorine district in the Pennines (United Kingdom). GSV: Great Sulfur Vein; HB: Haydon Bridge mining area; PL: Pike Law; RF: Rotherhope Fell; RV: Rookhope Red Veins; WV: Hunstanworth White Vein (Kimbell et al. 2010)

A quantity of synchysite and other REE-bearing minerals has been identified in these deposits (Shepherd et al. 1982; Ixer et al. 1996; Plant and Jones 1999; Walters 2011). Near the Stanhope and Rookhope deposits, synchysite has been described in quartz and bismuthinite veins in the form of intergrowth between crystals in the bismuthinite (Ixer et al. 1996). To a lesser extent, similar crystals of monazite, xenotime and adular have also been observed. Synchysite has also been observed in the Tynebottom mine at Garrigill. Some studies have shown that fluorine in Pennines is rich in REEs (e.g. > 1,888 ppm Ce + La + Y) (Smith 1974; Shepherd et al. 1982; Plant and Jones 1999; Walters 2011; Kraemer et al. 2019), the origin of which is debated. Indeed, an initial hypothesis recorded the presence of microinclusions of REE minerals in fluorine, while another hypothesis mentions the presence of REEs within the fluorine crystalline network. Kraemer et al. (2019) suggest a Permian (Asselian) age for this F-Pb–Zn-Ba and REE hydrothermalism.

#### 1.5.4.2. *Bauxite and Ni karst of the Mediterranean belt*

Across the whole northern edge of the Mediterranean belt, from Spain to Turkey via the South of France, Hungary, Italy, the Balkans and Greece, numerous bauxite deposits are located on the Alpine carbonate platform (Agard 1975; Bárdossy 1982; Özlü 1983). A large proportion of these deposits are associated with karsts defining a type of deposit according to Bárdossy (1982). It should be noted that some of these karst bauxite deposits present an enrichment in nickel (Maksimović 1987). The weathering profiles developed from the Middle Trias to the Neogene, with the major mineralization episode dating back to the Cretaceous (Bárdossy and Dercourt 1990).

A pioneering study mentioned the presence of secondary authigenic REE-bearing minerals within these deposits, especially at San Giovanni Rotondo, in Italy (Bárdossy and Pantó 1973; Sinisi 2018). The presence of these REE minerals was confirmed by Bárdossy et al. (1976) for the Nagyharsány deposits (Hungary), the deposits in Greece (Marmara, Marmeiko, Mont Parnasos, Panormos, Stenis Arahovis, Nisi, Smerna, Atalandi, Pylos, Nafpactos), Bosnia-Herzegovina (Nazda-Vlasenica), Montenegro (Zagrad, Štitovo), and Kosovo (Grebnik) (Maksimović and Pantó 1996; Kalatha et al. 2017 and references therein) (Figure 1.31). It should be noted that Mondillo et al. (2019) analyzed the REE potential of substantial bauxite deposits in southern France. Average REE concentrations in French bauxites are approximately 700 ppm (Mondillo et al. 2019). REEs, such as Ni, Co, Mn and Zn, are mobile during the bauxitization process, and the base of a weathering profile is generally rich in these elements (Maksimović 1976; Maksimović and Roaldset 1976). From a clayey material initially rich in REEs within karst cavities, bauxitization leads to the formation of authigenic REE minerals where there is contact between the bauxite and the carbonate hanging wall of the surrounding rock. Moreover, ultrabasic rocks may also be weathered in some places, leading to

enrichment in nickel at the clayey levels within the weathering profile. In this region, it is thus possible to observe a transition between the bauxite karst deposits and those with nickel with the unusual association of REE and Ni minerals (takovite, brindleyite, nepouite). This unusual mineralogy is doubtlessly linked to the multitude of rocks leached over the course of bauxitization. The main deposits illustrating this transition are Marmara, Nisi and Marmeiko (Greece), and Grebnik in Kosovo.

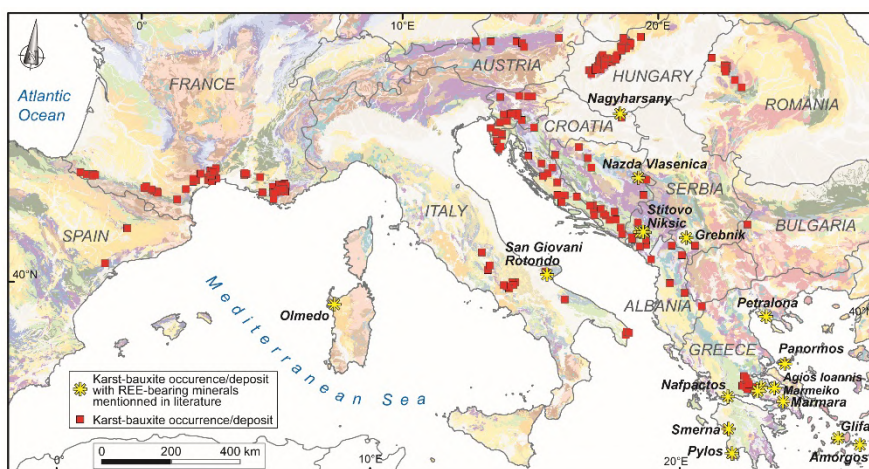


**Figure 1.31.** Bauxite and Ni karsts of the Mediterranean belt (Promine and EURARE bases). References for bauxite deposits and REE minerals (Bárdossy and Pantó 1973; Maksimović and Pantó 1991, 1996; Jones et al. 1996)

REE minerals are only present in deposits where intense leaching occurs in situ. In the Mediterranean belt, the majority of authigenic REE minerals were formed during the Cretaceous period. The most abundant minerals are hydroxylbastnäsite, followed by synchysite-(Nd), bastnäsite-(Ce) and bastnäsite-(Nd). To a lesser extent, the following are also found: monazite-(Nd), monazite-(La), goyazite-Nd, florencite and crandallite (Maksimović and Pantó 1996; Gamaletsos et al. 2017, 2019). The maximum REE levels are situated at the bottom of the profile, as in Montenegro (6.6 wt.% Nd + La + Pr). However, the basal part of the karstic nickel deposit at Aghios Ioannis (Greece) has only 180 ppm REEs. In fact, weathering profiles developed on basic rocks are naturally poor in REEs since the initial rocks were also poor in REEs. The Ni deposit at Marmeiko (Greece) is an exception. This shows richness in REEs with authigenic REE minerals from two initial rocks (an ultrabasic Cr-Ni rock and siliceous rock rich in REEs). In contact with the surrounding limestone, which acts as a geochemical barrier, the REE content reaches nearly

1,140 ppm at Nazda-Vlasenica (Bosnia-Herzegovina), 1,153 ppm at Marmeiko (Greece), 1,320 ppm at Štitovo (Montenegro), 1,450 ppm at Grebnik (Kosovo), 1,582 ppm at Marmara (Greece), and 4,576 ppm at the base of the Nisi deposit (Greece) (Maksimović and Pantó 1996). The REE content also depends on the intensity of the leaching from the rocks by the meteoric waters circulating in the karstic network.

#### ***1.5.4.3. Authigenic black clays and gray marls from the Southeast basin (France)***

The Southeast basin (France) includes thick sedimentary series of gray marls, black clays, limestones and detritic interlayers (more than 9 km thickness) deposited during the Mesozoic (Debrand-Passard et al. 1984; Lemoine 1984). This basin was then affected at the end of the Cretaceous and Cenozoic by the Pyrenean and Alpine orogenies, leading to its uplift, erosion and folding (Roure et al. 1992). During the Jurassic, especially during the Callovian-Oxfordian, thick layers (several hundreds of meters) of black clays with carbonated interbeds filled the basin and are locally called “black earths”. In 1990, a study was carried out on these rocks’ REE level and level of organic matter (Laval and Dromart 1990). It appears that these black clays have a low REE content (158 ppm REO), which seems disconnected from the organic matter content. Conversely, the gray marls dating back to the Cretaceous (the Albian especially) contain phosphate nodules rich in REEs and present an average content of 2,924 ppm REO. Finally, the study revealed that the LREEs are contained in the marls, whereas the HREEs are concentrated in the phosphate nodules.

### ***1.5.5. Rare earth occurrences from the Cenozoic and Quaternary***

#### ***1.5.5.1. Paleoplacers (from the Neogene to the Quaternary)***

##### ***1.5.5.1.1. Gray monazite paleoplacers of the Armorican massif (France)***

Since the 1960s, the Armorican massif has been known for its monazite paleoplacers (Figure 1.32), including gray monazite placers resulting from the erosion of black shales from the Paleozoic (Donnot et al. 1973). Two old mining projects have made it possible to estimate the resources for two occurrences: the Ti-Zr-REE-Th paleoplacer at Bailleul (3.5 Mt @ 0.45% REO) (Lemarchand 1970) and the gray monazite placer at La Monnerie (0.08 Mt @ 0.08% REO) (Cornet and Sapinart 1967).

The gray monazite is present in the form of small ellipsoidal lenses, the lengths of which measure 0.1–0.8 mm along the main axis. Nodules are often formed by polycrystalline aggregates. The monazites present the following REE contents:

23.5%  $Ce_2O_3$ ; 8.4%  $La_2O_3$ ; 3.1%  $Pr_2O_3$ ; 13.4%  $Nd_2O_3$ ; 2.9%  $Sm_2O_3$ ; 2.2%  $Gd_2O_3$ ; 0.7%  $Y_2O_3$ ; and 0.5%  $Eu_2O_3$  (Donnot et al. 1973). The monazites have similar properties to those of the Welsh basin, the Belgian Ardenne or Iberia (Burnotte et al. 1989; Ferrero et al. 1989; Smith et al. 1994).

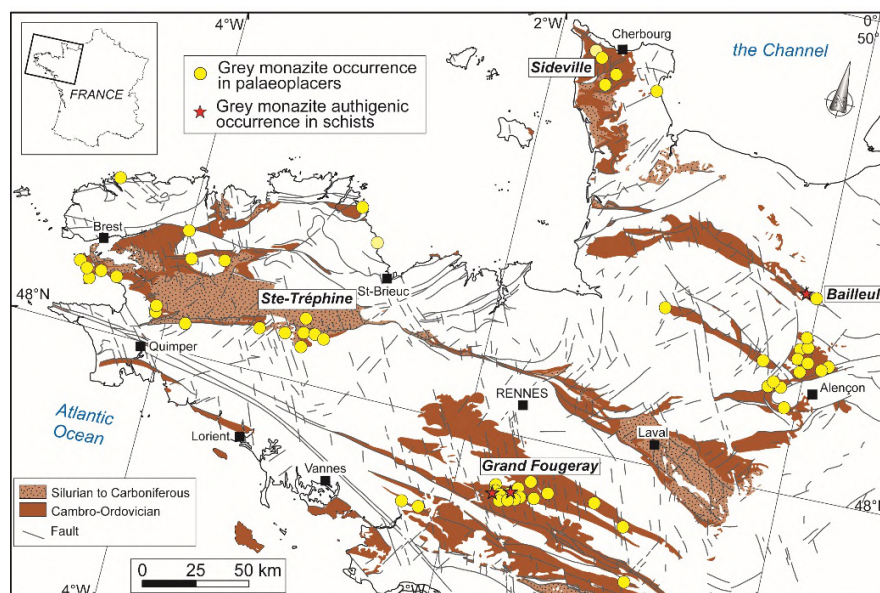


**Figure 1.32.** Gray monazite paleoplacers and black shales in the Armorican massif (France) (Donnot et al. 1973)

#### 1.5.5.1.2. Zr-REE paleoplacers of the Ardenne massif (Belgium)

The Belgian Ardenne massif includes several gray monazite paleoplacers, especially in the Rocroi massif, the Neufchâteau syncline, and the Stavelot and Brabant massifs (Nonnon 1984; Limbourg 1986; Burnotte et al. 1989). The source of the monazites has been identified as being the Upper Cambrian schists (“Revinian”) of the Rocroi massif, the metasediments of the Lower Devonian (“Siegenian”) of the Neufchâteau syncline, and the rocks from the Cambrian-Ordovician of the Stavelot and Brabant massifs. The monazite grains (polycrystalline aggregates) measure as much as 700  $\mu m$  for an average of 300  $\mu m$ . The chemical and mineralogical characteristics of the monazites are similar to those of the Welsh basin (Smith et al. 1994), Brittany (Donnot et al. 1973) and Iberia (Ferrero et al. (1989) and references therein). The monazites contain on average 14.7%  $La_2O_3$ , 32.4%  $Ce_2O_3$ , 14.6%  $Nd_2O_3$ , 0.4%  $Eu_2O_3$ , 1.3%  $Gd_2O_3$  and 77.0 ppm  $Yb_2O_3$  (Burnotte et al. 1989).

#### 1.5.5.1.3. The gray monazite placers of Spain

In Galicia, Calderón (1910) was the first to identify the presence of monazite in alluvial and coastal placers. Later, Pardillo and Soriano (1929) mentioned these placers with monazite concentrations of up to 1.25% around Vigo. Monazite placers are also described at the Insuela beach and in the Ría de Arosa valley by Parga Pondal (1935), with concentrations that can reach as high as 30%.

Both gray and yellow monazites exist. The gray monazites are similar to those described in Brittany (Donnot et al. 1973) and contain between 0.3 and 1.0% Eu. The yellow monazites are rich in LREEs and are mainly present in the coastal placers (along the coast north of Ría Arose and Ría Vigo) and the placers developed on granitic terrains (Ferrero et al. (1989) and references therein). The gray monazite placers developed thanks to the alluvial network with sediments of the Middle Ordovician from the Agüeira and Pizarras de Luarca formations (Ferrero et al. 1989).

Placers generally date back to the Cenozoic and Quaternary and contain xenotime, as well as Ti-Zr-Sn-(W)-Nb-Ta minerals (ilmenite, zircon, rutile, columbo-tantalite, wolframite and scheelite). Recent analyses have shown interesting concentrations of Y (0.3–23.1 ppm, an average of  $14.5 \pm 3.5$  ppm) with the Ría Vigo sediments (Marmolejo-Rodríguez et al. 2008; Prego et al. 2009). The origin of the yttrium would be linked to the Galiñeiro complex. To the north of Galicia, Prego et al. (2012) measured the REE content within alluvium from the Ortigueira, Barqueiro and Viveiro valleys, as well as in the Mera, Sor and Landro estuaries. The highest REE contents are found in sediments from the heart of the valleys (233 ppm), while most of the alluvium has between 11 and 70 ppm REEs.

#### 1.5.5.1.4. The gray monazite placers of Portugal

In the center-east of Portugal, near Bisa, Santo António das Areias and Marvão, black sands from pan concentrates were collected by the Geological and Mining Institute (IGM) in 2005-2007 to identify the REE-bearing minerals in the placers (Inverno et al. 2007). Rosa et al. (2010) have shown that these sands contain xenotime in the form of round grains of approximately 250  $\mu\text{m}$  (between 100 and 375  $\mu\text{m}$ ) and nodular monazite, as well as the following minerals: ilmenite, cassiterite, scheelite and wolframite. The xenotime shows concentrations of 39.7%  $\text{Y}_2\text{O}_3$ , 3.5%  $\text{Gd}_2\text{O}_3$ , 51%  $\text{Dy}_2\text{O}_3$ , 4.3%  $\text{UO}_2$  and 0.31%  $\text{ThO}_2$ . The direct association of xenotime, monazite, tourmaline, rutile and zircon shows that the source should be linked to the granitic rocks of the Nisa and Penamacor massifs. However, it should also be noted that the

Ordovician quartzites near Salvador, Penha Garcia, Monfortinho and Portalegre are rich in nodular gray monazite and in REEs (Inverno et al. 1998; Salgueiro et al. 2020).

#### 1.5.5.1.5. Ti-Zr-Th-REE-Nb placer at Lužnice (Czech Republic)

On the basis of the radioactive sites listed by the Czech uranium industry (Křištiak and Záliš 1994), Goliáš (2001) published a summary of the Th occurrences in the Czech Republic. Where REEs are concerned, the alluvium of the river Lužnice (in the south of the country, near Austria) presents gamma spectrometric anomalies linked to the contrast between sediments, resulting from the erosion of granitoids from the moldanubian and Cretaceous rocks from the bedrock of the river (Goliáš 2001). The main anomaly is a recent alluvial silty horizon described by Maòour et al. (1992). The thickness has been measured to be between 0.8 and 1.1 m, and the Th and U contents reach 47 ppm and 12 ppm, respectively. A zircon-ilmenite concentrate with nearly 9 wt.% monazite and 0.36 wt.% Th has been obtained. Th and U contents have been measured in zircon (0.022 wt.% Th and 0.046 wt.% U) and monazite (5.8 wt.% Th and 0.29 wt.% U). Brabantite forms the most radioactive grains. The recent placers of the river Lužnice show a Ti-Zr-REE-Th-Nb mineral association that could be exploited as a by-product of the exploitation of feldspathic gravels (Maòour et al. 1992).

#### 1.5.5.1.6. The paleoplacers of the Welsh basin (United Kingdom)

In the United Kingdom, nodular gray monazite paleoplacers have been reported in the Welsh basin (draining the shales from the Ordovician-Silurian), thanks to pan concentrates collected over the course of the mineral inventory by the BGS (Cooper et al. 1983, 1984; Smith et al. 1994) in Wales, Exmoor and southwestern England. The study by Smith et al. (1994) on the potential of these paleoplacers concluded that there was no economic benefit, even though more in-depth studies would be desirable.

#### 1.5.5.1.7. The paleoplacers and gray monazite placers of the Arize massif (France)

The Arize massif, in the French Pyrenees, 80 km south of Toulouse, revealed the presence of alluvial deposits containing gray monazites (Lacomme et al. 1993). In the Pyrenees, the gray monazite was discovered for the first time to the north of the belt within the alluvial deposits of the Pliocene-Quaternary associated with cassiterite, scheelite and gold (Lacomme and Fontan 1971). It seems that this alluvium resulted from the erosion of, among others, metasediments from the Ordovician and Silurian that contain gray monazites. Moreover, the gray monazite alluvial occurrences of the Arize are almost exclusively found near the Ordovician sandstones and metapelites (Lacomme et al. 1993). Unfortunately, the torrential

character of the water courses limits the accumulation of these monazite alluviums, excluding any economic benefit. The monazites measure between 80 and 500  $\mu\text{m}$ . Analyses carried out on the Ordovician gray rocks give concentrations between 65 and 67% REO, and an average level of 0.5–1.0%  $\text{ThO}_2$ .

#### 1.5.5.2. *The Alpine and Pyrenean orogenies*

##### 1.5.5.2.1. Carbonatite and lamprophyre complex at Delitzsch (Germany)

In eastern Germany, the carbonatite and lamprophyre complex at Delitzsch lies under a cover of sediments from the Cenozoic, approximately 100 m thick (Seifert et al. (2000) and references therein). This complex was discovered during uranium prospecting from 1960 to 1970. It is formed of dykes and diatremes established during the Campanian (75–71 Ma) (Krüger et al. 2013) within Upper Paleozoic volcano-sedimentary rocks. REEs are known in carbonatites in the form of apatite, pyrochlore and bastnäsite. Within the Storkwitz diatreme, the carbonatites have been explored from surveys, and the Deutsche-Rohstoff company published an estimate of resources in 2013, compatible with the JORC code. The total resources are estimated at 4.4 Mt @ 0.45% REO (part indicated, part inferred), which is 20,100 tons of REEs.

##### 1.5.5.2.2. REE-Sc and lazulite-quartz Alpine veins (Austria)

There are many Alpine veins in the belt (Luckscheiter and Morteani 1980; Mullis 1996; Wagner et al. 2010; Rauchenstein-Martinek et al. 2014). These veins measure some meters in length for some tens of centimeters in width and are associated with shear zones at the brittle–ductile boundary. The Alpine veins are present in the form of veins alone or in an echelon formation and contain euhedral crystals of quartz and other minerals that depend on the surrounding lithology (adularia, albite, muscovite and quartz in the granitoids; calcite, ankerite, rutile and quartz in the carbonates; albite, chlorite, epidote, actinolite, titanite and quartz in the basic rocks). In southeastern Austria (47.5°N–15.6°E near Mürzzuschlag), the Pretul site in the Styria region is known for its Alpine lazulite-quartz veins that contain REE minerals and Sc (apatite, florencite-(Ce), goyazite, xenotime-(Y), monazite-(Ce), and pretulite; Cornelius 1931; Berl 1996; Bernhard et al. 1998). These occurrences present no economic benefit for REEs.

##### 1.5.5.2.3. Talc deposit at Trimouns-Luzenac (France)

In the French Pyrenees, the Trimouns-Luzenac quarry is the largest talc exploitation in the world, with more than 400,000 tons/year (Fortuné 1971; Fortuné et al. 1980; Moine et al. 1989; de Parseval et al. 1993). The deposit is situated on the eastern flank of the Saint-Barthélémy massif, 100 km south of Toulouse, at

an altitude of 1,700 m. The talc and chlorite are formed by the hydrothermal alteration of Paleozoic dolomites, micaschists and pegmatites along a shear zone (Fortuné et al. 1980; Moine et al. 1989; de Parseval 1992). Thanks to exploitation, centimeter-scale geodes within dolomites containing REE minerals have been identified. The minerals reported are allanite, bastnäsite, parisite, synchysite, gadolinite, monazite, trimoussite-(Y), hellandite-(Y), imoriite-(Y), hingganite-(Y), aeschynite-(Y), gatelite-(Ce), dissakisite-(Ce) and xenotime (Moëlo et al. 1974; Piret et al. 1990; Grew et al. 1991; Favreau 1994; de Parseval et al. 1997; Bonazzi et al. 2003). The formation of geodes seems to be linked to metasomatism along the shear zone (300–350°C/0.2–0.3 GPa). The monazite and xenotime of these geodes have moreover allowed the deposit to be dated back to between 112 and 97 Ma using the U/Pb method (Schärer et al. 1999).

#### 1.5.5.3. *The British part of the Cenozoic North Atlantic igneous province*

Some REE mineral occurrences are described in the granitic massifs from the Cenozoic British igneous province (Exley 1980; Harding et al. 1982; Hyslop et al. 1999; Green et al. 2005; Green and McCallum 2005) (Figure 1.33). This magmatic province is situated in the northwest of the British Isles and forms essential evidence of magmatic activity linked to the North Atlantic in the Paleocene and Lower Eocene (Emeleus and Gyopari (1992) and references therein). The main intrusions are the plutons of the Isle of Skye, Saint-Kilda, Arran and the Mourne Mountains.

##### 1.5.5.3.1. Granitic intrusion on the Isle of Skye

The Isle of Skye (northwestern Scotland) is formed of four granitic complexes dating back to between 55 and 59 Ma (Harker 1904; Brown 1963; Thorpe et al. 1977): Cuilin, Strath na Creiteach, Western Red Hills (57.0–58.5 Ma using the U/Pb method on zircon) (Hamilton et al. 1999) and Eastern Hills (55.7–55.9 Ma using the U/Pb method on zircon) (Hamilton et al. 1999). These complexes integrate hyperaluminous, metaluminous and hyperalkaline granites. Allanite and sphene are the main additional minerals and are particularly rich in REEs (between 25 and 45% RE<sub>2</sub>O<sub>3</sub>) (Exley 1980). Moreover, secondary allanite has been identified. It formed over the course of a late hydrothermal episode and during the stages of meteoric alteration. Finally, miarolitic cavities have been identified as containing REE minerals (Green and McCallum 2005): gadolinite and kainosite.

##### 1.5.5.3.2. The Arran granitic pluton

The Arran granitic pluton is situated on the eponymous island to the southwest of Scotland and has been dated back to  $60.3 \pm 1.0$  Ma using the U/Pb method on zircon (Dickin et al. 1981) and to  $58.5 \pm 0.8$  Ma by  $^{40}\text{Ar}/^{39}\text{Ar}$  (Mussett et al. 1987). To the north of the pluton, REE minerals have been mentioned: fergusonite, gadolinite and

allanite (Hyslop et al. 1999). The miarolitic cavities also include fergusonite and gadolinite crystals associated with albite and orthoclase.

#### 1.5.5.3.3. Saint-Kilda granitic complex

The granitic complex at Saint-Kilda is situated on an island to the extreme northwest of the Hebrides in Scotland. It is formed of the granites of the Conachair plutons ( $55 \pm 1$  Ma, using the Rb/Sr method) (Harding et al. 1984), Glen Bay and h-Heagen and gabbroids. The granites contain quartz, alkaline feldspar, sodium plagioclase, chlorite and amphibole (Cockburn 1935; Harding et al. 1966). Three REE minerals have been identified by order of abundance: chevkinite, allanite and zirkelite (Harding et al. 1982). They represent less than 1% of the rock, and chevkinite contains more than 41% of all the REEs.

#### 1.5.5.3.4. The granitic pluton of the Mourne Mountains

The Mourne Mountains are situated in Northern Ireland and are formed of a granitic pluton that has been dated back to between 53.3 and 55.0 Ma using the  $^{40}\text{Ar}/^{39}\text{Ar}$  method (Thompson et al. 1987). These rocks contain REE minerals, gadolinite and honey-colored monazite within the miarolitic cavities (Hyslop et al. 1999; Green et al. 2005).

#### 1.5.5.4. *The European Cenozoic Rift System – the Kaiserstuhl Nb-Ta-REE alkaline volcanic complex (Germany)*

The Kaisertuhl massif is situated in the center-south of the Rhine Graben, to the southwest of Germany, 15 km from Fribourg. It is a Miocene alkaline volcanic complex (15-18 Ma) that is  $16 \times 12$  km (Van Wambeke et al. 1964; Wimmenauer 1974; Keller 1981; Schleicher et al. 1990; Weisenberger et al. 2014). The predominantly volcanic to subvolcanic rocks have compositions of tephrite and phonolite, while the carbonatites were formed toward the end of the emplacement. The main types of volcanic rock are as follows:

- lava flows (tephrite);
- pyroclastic rocks (tephrite, phonolite and carbonatite) (Keller 1981);
- a porphyric dyke with essexite, phonolite and carbonatite;
- fine-grained subvolcanic intrusions of essexite, phonolite and carbonatite;
- volcanic breccias (Figure 1.34).

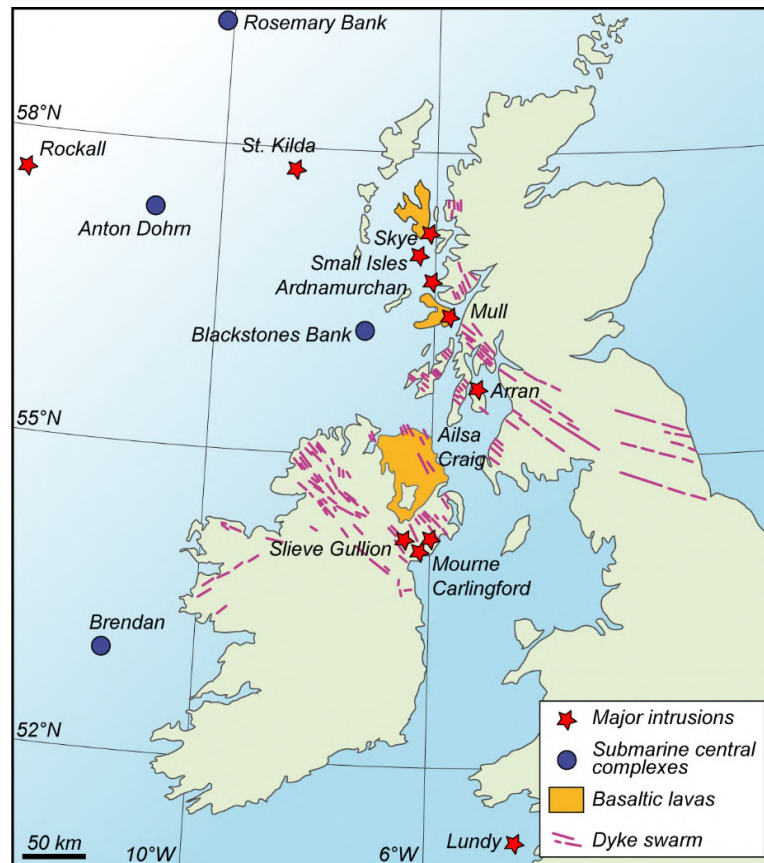


**Figure 1.33.** British part of the North Atlantic Cenozoic igneous province

Carbonatites are present at the core of the complex in the form of an intrusion of approximately  $1 \text{ km}^2$ . This mainly involves coarse-grained *søvite* mainly formed of calcite, then apatite and magnetite, with the following additional minerals: pyrochlore, Nb perovskite (dysanalite), bastnäsite and monazite (Van Wambeke et al. 1964; Keller 1981). A second type of carbonatite is presented in the form of hundreds of small, fine-grained veins and a width varying between 1 cm and 1 m. Calcite forms 90–95% of its volume, followed by magnetite and apatite. The additional phases are pyroxene, melanite and micas. Pyrochlore and Nb-perovskite are rarer. The veins are concentrated at the core of the massif and are the most recent rocks. Thus, the Kaisertuhl carbonatites are for the most part calcitic, and the ankerite-dolomite carbonatites seem restricted to late veins associated with a few *søvite* intrusions (Wimmenauer 1963).

Some REE minerals have been described in the complex's carbonatites. The pyrochlore contains REEs, koppite (Brandenberger 1931), and chemical analyses published by Van Wambeke et al. (1964) show variation between 4.3 and 6.4%  $\text{RE}_2\text{O}_3$ , with Ce being dominant. The pyrochlore is rich in LREE (up to 19% REO) and always radioactive, with up to 11%  $\text{U}_3\text{O}_8$  and 6.5%  $\text{ThO}_2$  (Kirchheimer 1957; Walter et al. 2018). Van Wambeke et al. (1964) distinguished two types of calcite in carbonatites. The first type, associated with sövite, contains variable REE levels between 0.09 and 0.15%  $\text{RE}_2\text{O}_3$ . The second type, associated with late carbonatite veins, shows a higher REE content, with an average of 0.22%  $\text{RE}_2\text{O}_3$ . Moreover, fluorapatite has been described and presents appreciable REE contents. Finally, bastnäsite and monazite are only present in the carbonatites. Thus, the late carbonatites may contain between 1 and 4% REEs.

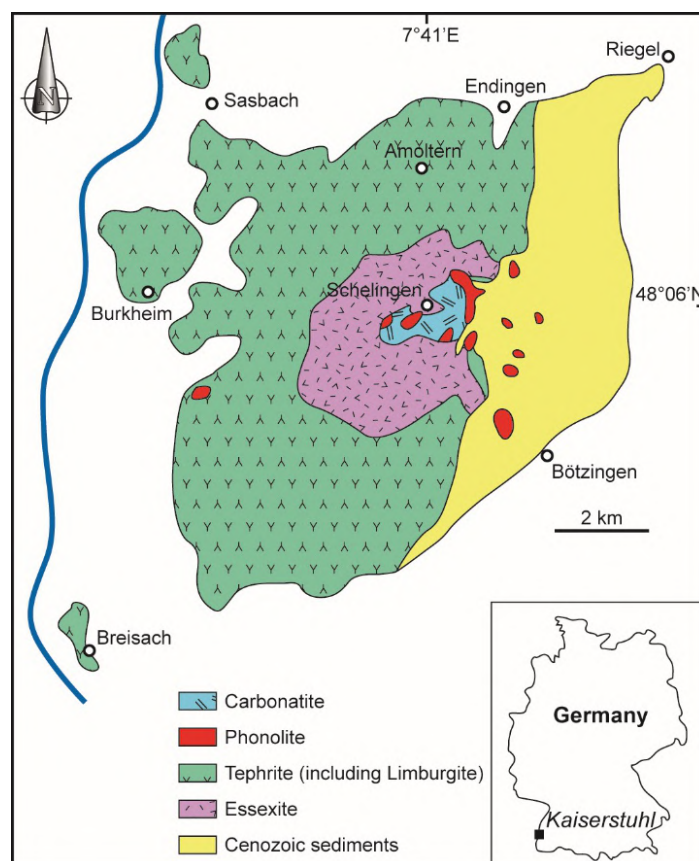


**Figure 1.34.** Kaiserstuhl Nb-Ta-REE alkaline volcanic complex, Germany (Weisenberger et al. 2014)

#### 1.5.5.5. *Coastal placers*

The different REE occurrences of the Quaternary are heavy mineral placers mainly integrating monazite, zircon and ilmenite.

##### 1.5.5.5.1. The coastal placers of Chalkidiki and Kavala (Greece)

In northeastern Greece and north of the Aegean Sea, geochemical studies have been carried out along the coast for 240 km between the Chalkidiki and Kavala Peninsulas, revealing the presence of REEs in the coastal sediments (Perissoratis et al. 1988; Pergamalis et al. 2001a, 2001b; Melfos and Voudouris 2012). Indeed, geochemical anomalies have been revealed in placers, such as that of Nea Peramos, with levels of up to 8,000 ppm REE (including 93.5% LREE with mainly Ce, La, Nd and Pr). The main carrier is allanite. Recent studies mention the magmatic massifs of the Pangaion Mountains near Kavala as the primary source of REEs. Indeed, analyses carried out on these mountains show concentrations of 6,171 ppm La, 10,883 ppm Ce, 1,062 ppm Pr, 3,249 ppm Nd, 334 ppm Sm and 214 ppm Eu.

##### 1.5.5.5.2. The coastal placer at Hanstholm (Denmark)

The placer at Hanstholm is situated in northern Denmark in the province of North Jutland. This heavy mineral placer contains ilmenite, rutile, zircon and monazite sands (Hedrick and Templeton 1991), and has been the subject of exploration by the Morstal Minerals company (Orris and Grauch 2002).

##### 1.5.5.5.3. The coastal placer at Cuxhaven (Germany)

The placer at Cuxhaven is situated on the North Sea coast, 100 km west of Hamburg, and contains heavy mineral sands. The resources are estimated at 10 Mt of heavy minerals, including ilmenite, rutile, zircon and monazite (Hedrick 1985).

##### 1.5.5.5.4. Radioactive anomaly on Espiguette beach (France)

In the South of France, near Grau-du-Roi, the beach at Pointe de l'Espiguette presents radioactive anomalies, with average values between 600 and 850 c/s and a maximum of 1,050 c/s (Vazquez-Lopez and Jézéquel 2002). This anomaly extends over 1,500 m in length and 10–50 m in width, and is situated above the intertidal zone. The heavy mineral sands contain crandallite (the florencite type) and zircon, which are probably responsible for the radioactive anomaly.

## 1.6. The rare earths deposits of Greenland

In response to increasing demand for mineral resources, Greenland is today generating international interest in the discovery of new deposits (Stensgaard et al. 2016). Greenland benefits, in particular, from varied geological settings favorable to the presence of REE deposits attractive to exploration companies (GEUS 2010; Sørensen and Kalvig 2011; Steenfelt 2012; Stendal 2014; Goodenough et al. 2016; EURARE 2017; Andersson et al. 2018a). The main REE occurrences in Greenland are situated in carbonatites, alkaline intrusions, pegmatites and paleoplacers (Figure 1.35).

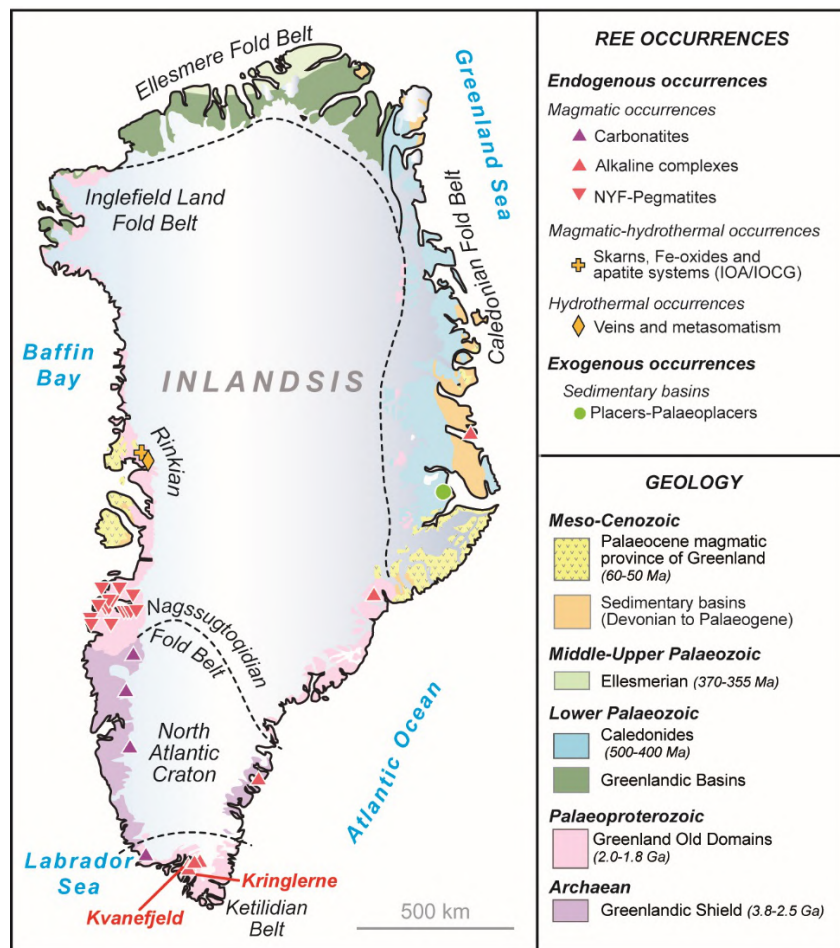


**Figure 1.35.** REE occurrences in Greenland (Stensgaard et al. 2010; Charles et al. 2013; Tuduri et al. 2020)

### **1.6.1. The alkaline provinces of the Archean (2,750–2,700 Ma)**

The alkaline rocks of the Archean are rare globally and only outcrop in the Baltic shield (e.g. Keivy), the Canadian shield, Australia (Yilgarn), Greenland (e.g. Skjoldungen) and South Africa (Fitton and Upton 1987; Blichert-Toft et al. 1995; Zozulya et al. 2007). These geological features form REE potential, such as the Siilinjärvi carbonatite (Finland) or the Sakharjok alkaline complex (Russia). In Greenland, two regions have Archean alkaline rocks:

- the Tupertalik carbonatite in the west;
- the Skjoldungen alkaline province in the southeast, with the Singertåt carbonatite and the Timmiarmiut alkaline complex (Larsen et al. 1983; Fitton and Upton 1987; Nielsen and Rosing 1990; Blichert-Toft et al. 1995; Steensgaard et al. 2010; Berger et al. 2014).

#### **1.6.1.1. Sr-Zr-REE carbonatite at Tupertalik (western Greenland)**

In western Greenland, the Tupertalik carbonatite massif (65.50°N–51.85°W) extends over 500 × 200 m and is situated only 11 km north of the Upper Jurassic carbonatite at Qaqqarsuk, near the Sønder Isortoq fjord (Larsen et al. 1983). The carbonatite is present in the form of a blade, with a thickness of 10 m within orthogneiss, having undergone metamorphism in the granulite facies during the Archean, without undergoing a major retrograde stage afterwards. The high concentrations of Sr, Zr and REE are comparable to those of other carbonatites. Archean carbonatite dykes with a similar geochemical signature have been discovered at Fiskeneset, 310 km south of Tupertalik (Bollingberg et al. 1976). The Tupertalik carbonatite has been dated back to 2,620 ± 80 Ma and 2,691 ± 80 Ma using the K/Ar method on phlogopite (Larsen et al. 1983). This age has been re-evaluated and established at 3,007 ± 2 Ma using the U/Pb method on baddeleyite (Bizzarro et al. 2002). Further studies are needed to better estimate the real REE potential of the older, land carbonatite massif.

#### **1.6.1.2. Alkaline province from the Neoproterozoic at Skjoldungen (southeast Greenland)**

In southeastern Greenland, the alkaline province of Skjoldungen (63°N–43°W) extends along a NW–SE axis over a width of 30 km, with a variety of late to post-tectonic alkaline intrusions established between 2,700 and 2,665 Ma (Rosing et al. 1992; Blichert-Toft et al. 1995). The alkaline rocks intrude a craton formed of migmatitic orthogneiss and supracrustal rocks (e.g. amphibolite, metapelite), all affected by metamorphism in the granulite facies (2,750–2,740 Ma) during the Skjoldungen orogeny (Kolb et al. 2013; Berger et al. 2014).

#### 1.6.1.2.1. Singertât Sr-REE carbonatite

The Singertât carbonatite-ijolite complex (63.23°N–42°W) intrudes fenitized gneisses south of the Skjoldungen province, near the Kattertooq fjord (Nielsen and Rosing 1990; Blichert-Toft et al. 1995). The core of the massif is formed by bedded sills of coarse-grained melteigite, ijolite and urtite containing aegirine-augite and/or alkaline amphibole, nepheline and biotite in variable proportions. The additional phases are magnetite, apatite, sphene, alkaline feldspar, calcite and zircon. The cancrinite (feldspathoid) often presents as a reaction rim between calcite and nepheline. Dykes and veins (<1 m) of nepheline syenite and carbonatite intersect the massif. The nepheline syenite dykes are dominated by perthite with variable levels of nepheline, aegirine-augite and/or alkaline amphibole, biotite, apatite, calcite and Fe-Ti oxides. The carbonatite dykes are formed of apatite-biotite sövite. The peripheral alteration (fenite) zone reaches approximately 2 km in width. The Singertât carbonatite dates back to  $2,664 \pm 3$  Ma (U/Pb age on zircon) (Blichert-Toft et al. 1995) and is rich in Sr (5,260 ppm) and REE (2,400 ppm with 1,122 ppm Ce, 464 ppm La, 524 ppm Nd). Further studies are needed to estimate the REE potential of this massif.

#### 1.6.1.2.2. Timmiarmiut Sr-REE alkaline complex

Approximately 100 km south of the Singertât carbonatite, the Timmiarmiut alkaline complex (62.37°N–42.28°W) includes alkaline carbonate rocks rich in Sr (2,000 ppm) and REE (2,300 ppm REE with 1,100 ppm Ce and 120 ppm Y) (Steensgaard et al. 2010). This zone remains largely underexplored, although it presents good REE potential.

### 1.6.2. *Paleoproterozoic deposits at Karrat (NIAQ and UMIA)*

In central-west Greenland, in the Rinkian fold-thrust belt, the Karrat project (71.67°N–52.77°W) includes two potential deposits (Figure 1.36): Niaqornakassak (NIAQ) and Umiammakku Nunnaa (UMIA), discovered by Avannaa Resources in 2007–2009 (Avannaa Resources 2010; Sørensen and Kalvig 2011; Stendal 2014). The sites are located on two peninsulas 7 km apart, and the two deposits are grouped under the name “Karrat”. Exploratory works are focused on NIAQ, where the geometry of the mineralized body has been defined by eight drilling campaigns (1,320 m in total). It is a layered horizon of metacarbonates parallel to the regional foliation (30° toward the south) of the surrounding rock (amphibolite from the Karrat group dated back to the Paleoproterozoic) (Garde 1978; Henderson and Pulvertaft 1987; Kalsbeek et al. 1998; Mott et al. 2013).

The mineralized body is at least 1.5 km long, while the extent of its extremities is not known. Its thickness varies between 10.3 and 32.5 m for depths between 56 and 168 m above sea level. The main REE minerals are as follows: bastnäsite (39%), allanite (26%), monazite (22%), monazite-(Th) (4%), fergusonite-(Y) and fluorides-Y (4%), and chevkinite and diversilite (Fe-Ti-Ba-REE silicates) (4%). Avannaa Resources proposes a tonnage and grades: 26.3 Mt @ 0.996% REO+Y<sub>2</sub>O<sub>3</sub> and 0.13% HREO+Y<sub>2</sub>O<sub>3</sub> in an optimistic scenario and 19.5 Mt @ 1.02% REO+Y<sub>2</sub>O<sub>3</sub> and 0.13% HREO+Y<sub>2</sub>O<sub>3</sub> in a more limited scenario. The average Th content varies between 400 and 500 ppm (huttonite), and uranium seems to be absent from the deposit NIAQ (< 5 ppm). We should note the low contents of Be, Zr, Sc or Ta, with Nb contents varying between 300 and 500 ppm. The origin of the REEs would be linked to the metasomatic fluids affiliated to a ferrocarbonatite (Mott et al. 2013). Indeed, the mineralized body is not considered a carbonatite, given its SiO<sub>2</sub> content of 15–25% (< 5% for a carbonatite) and CaO content of 18–20% (> 30% in a carbonatite).

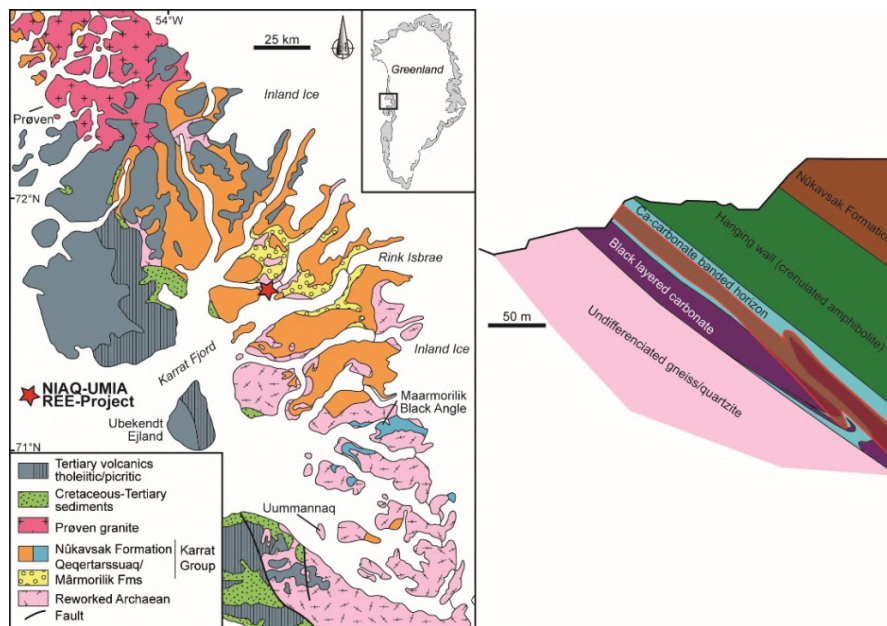


**Figure 1.36.** Deposits from the Paleoproterozoic at Karraat (NIAQ and UMIA) (Avannaa Resources 2010)

Although exploration is limited at the UMIA site, two drillings (420 m in total) and 347 samples have provided an estimate of the REE content, reaching up to

1.98% REO+Y. The real thickness and global geometry are still not defined due to a lack of sufficient exploratory work.

### **1.6.3. Pegmatites from the late Paleoproterozoic (1,800–1,785 Ma)**

To the southwest of Greenland, to the north of the Nassugtoqidian orogeny, three pegmatite fields are present within the Archean base. Two pegmatite fields (Nassuttutata tasia and Nordre Isortoq) are situated in the regions of Nassuttooq and Nordre Strømfjord, respectively (Secher 1976, 1980). These are white biotite and plagioclase pegmatites, concordant with the foliation of the surrounding rock (Archean gneisses affected by metamorphism in the granulite and amphibolite facies and supracrustal rocks from the Paleoproterozoic) (Secher 1980; GEUS 2014) and dating back to approximately 1,800 Ma. The width of the pegmatite bodies varies from 5 to 10 m, with lengths of 50–200 m. The main REE mineral is monazite in the form of orange euhedral crystals of 0.5–5 mm. The monazite contains Nd (5–7%) and 1–2% La, 2.5–4.0% Ce, 500 ppm Y, and 5–10% Th (GEUS 2014).

The third pegmatite field is situated in the Attu region, where the pegmatites intrude the Archean gneisses and amphibolites. The pegmatites, dated back to  $1\,785 \pm 5$  Ma, are concordant or discordant and present in the form of veins up to 5 m in width over lengths of several hundred meters. The main REE mineral is allanite (crystals of up to 5 cm), accompanied by sphene, apatite, magnetite (centimetric aggregates with allanite) and iron sulfides in a gangue where K-feldspar, quartz and biotite are associated. Moreover, a pyrite and magnetite alteration zone is observed at the contact between the pegmatites and the surrounding amphibolite, over nearly a meter in thickness. No exploration campaign has been carried out until now in these three pegmatite fields.

### **1.6.4. Gardar Mesoproterozoic alkaline province**

The province of Gardar (Figure 1.37) is a rift zone formed at the end of the Mesoproterozoic south of Greenland (Upton and Emeleus 1987; Upton et al. 2003; Upton 2013). Associated with sediments, many plutonic rocks were laid down between 1,280 and 1,120 Ma. These alkaline intrusions are formed of syenites, nepheline syenites, quartz syenites and granites associated with a swarm of giant basic veins. They form the main REE and U potential in Greenland. The intrusion at Ilímaussaq ( $1,160 \pm 5$  Ma; Krumrei et al. 2006) includes the two world-class deposits at Kringlerne and Kvanefjeld, and the Igaliko intrusion includes the Motzfeldt Sø deposit.

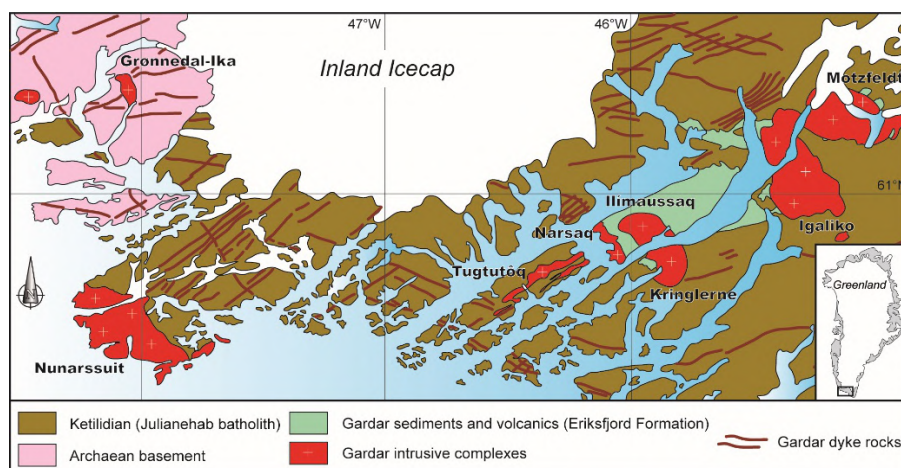


**Figure 1.37.** Alkaline province from the Mesoproterozoic at Gardar

#### 1.6.4.1. Kvanefjeld U-REE-Zn-F deposit

To the south of Greenland, the U-REE-Zn deposit at Kvanefjeld (Figure 1.38) is situated a few kilometers from Narsaq and occupies the northeastern part of the Ilímaussaq intrusion (Ferguson 1964; Larsen and Sørensen 1987; Sørensen et al. 2011). This alkaline complex consists of four successive intrusions:

- an augite syenite in the form of a discontinuous band on the edge of the intrusion;
- a hyperalkaline quartz syenite and an alkaline granite at the top of the complex and in the form of enclaves in the third intrusion;
- a layered series hyperalkaline nepheline syenite (agpaite);
- cumulates of kakortokite, aegirine lujavrite and arfvedsonite lujavrite (Sørensen 1969; Bohse et al. 1971; Nielsen and Steinfeldt 1979; Sørensen et al. 2011 and references therein).

These rocks (especially sodalite foyaite, naujaite, kakortokite and lujavrite) are interpreted as resulting from highly fractionated phonolitic magma rich in iron and incompatible elements (Zr, Hf, Nb, REE, U). The Ilímaussaq complex ( $1,160 \pm 5$  Ma; Krumrei et al. 2006) is an igneous body, unique with regard to its extreme enrichment of many rare elements in more than 200 minerals.

The world-class deposit at Kvanefjeld occupies a plateau of  $2.1 \times 0.9$  km and forms part of the 4.5 km lujavrite belt in the Ilímaussaq complex. The northern and western edges of the plateau correspond to the northern and western borders of the alkaline complex. To the northeast, the lujavrite level at Kvanefjeld is continuous as far as the Steenstrup fjord. On the western part, the lujavrite of the plateau forms the base of the augite syenite and the naujaite. Finally, the eastern part is formed of medium- to coarse-grained lujavrite (“M-C lujavrite”), fine-grained lujavrite and then naujaite. In the 1950s, the Ilímaussaq complex was widely prospected for uranium, then for REEs, as well as Zr, Be, Nb and Ta. For political and socioeconomic reasons, no development took place. The recent back and forth on legislative relaxation on mineral exploration in Greenland, especially for uranium and oil, is not conducive to foreign investors.

The Kvanefjeld deposit is being explored by the Greenland Minerals company for U, REE, F and Zn. It appears that U, Th and REEs are concentrated in the upper parts – that is, the most recent parts – of the complex. Thus, hyperagpaitic lujavrite and agpaitic nepheline syenite are the main ores. The upper units of the lujavrite are very rich in REEs, U and Zn, with REE contents of over 1.5% and 400 ppm  $U_3O_8$ . At depth, these concentrations decrease. The mineralized areas may exceed 250 m in width within dome-shape structures. The mineralized lujavrite mainly outcrops in the northern half of the Ilímaussaq complex. Kvanefjeld is the main deposit, and satellite deposits have recently been discovered at Sørensen (formerly zone 2) and in zone 3 (GME 2014). The main REE-U-Zn minerals are steenstrupine, britholite, monazite, vitusite, xenotime and various Na-Zr silicates, such as eudialyte and lovozerite. In 2015, an estimate of NI43-101 or JORC compatible resources showed a total resource of 673 Mt @ 1.09% REO and 248 ppm  $U_3O_8$  (7.34 Mt REO including 0.27 Mt HREO). The indicated resources represent 308 Mt (3.42 Mt REO including 0.13 Mt HREO) and the inferred resources are 222 Mt (2.22 Mt REO including 0.08 Mt HREO), with a cutoff grade of 150 ppm  $U_3O_8$ . The total project (Kvanefjeld, Sørensen and zone 3) represents 1,010 Mt @ 11,000 ppm REO, including 9,700 ppm LREO, 399 ppm HREO and 266 ppm  $U_3O_8$  (11.14 Mt REO, including 0.40 Mt HREO). Moreover, tests for extraction using froth flotation and open air leaching are conclusive (GME 2012). In 2014, 30 tons of ore was used for the pilot plant in the EURARE project (GME 2014; EURARE 2017).

#### 1.6.4.2. *Kringlerne Ta-Nb-REE-Zr deposit*

The world-class polymetallic deposit (Ta-Nb-REE-Zr, hence the name Tanbreez) at Kringlerne is situated in southern Greenland, 15 km southeast of the Kvanefjeld deposit to the south of the Ilímaussaq intrusion (Bohse et al. 1971; Bohse and Andersen 1981; Sørensen 2001; GEUS 2014). This deposit (Figure 1.38) is situated at the base of the alkaline complex in the lower levels of layered agpaitic nepheline

syenite cumulates called kakortokite. Kringlerne is situated in the Kangerluarsuk region, and the kakortokite cumulates are formed of 29 regular layers over a total thickness of 200 m. These layers are a repetition of banding of black syenite (dominated by arfvedsonite), red syenite (dominated by eudialyte) and white syenite (dominated by feldspar). Each banding measures between 1 and 20 m in width. The origin of this banding is still being debated and results from minerals being sorted by density when the magma solidified, as well as from rhythmical deposition within the magmatic chamber (Sørensen 2001). The Kangerluarsuk zone covers a surface of  $2 \times 3$  km, 400 m above sea level. Kakortokite has been studied for decades, especially for the following elements: Zr, Y, Ta, Nb and REEs. The Kringlerne deposit is being explored by the Tanbreez company.

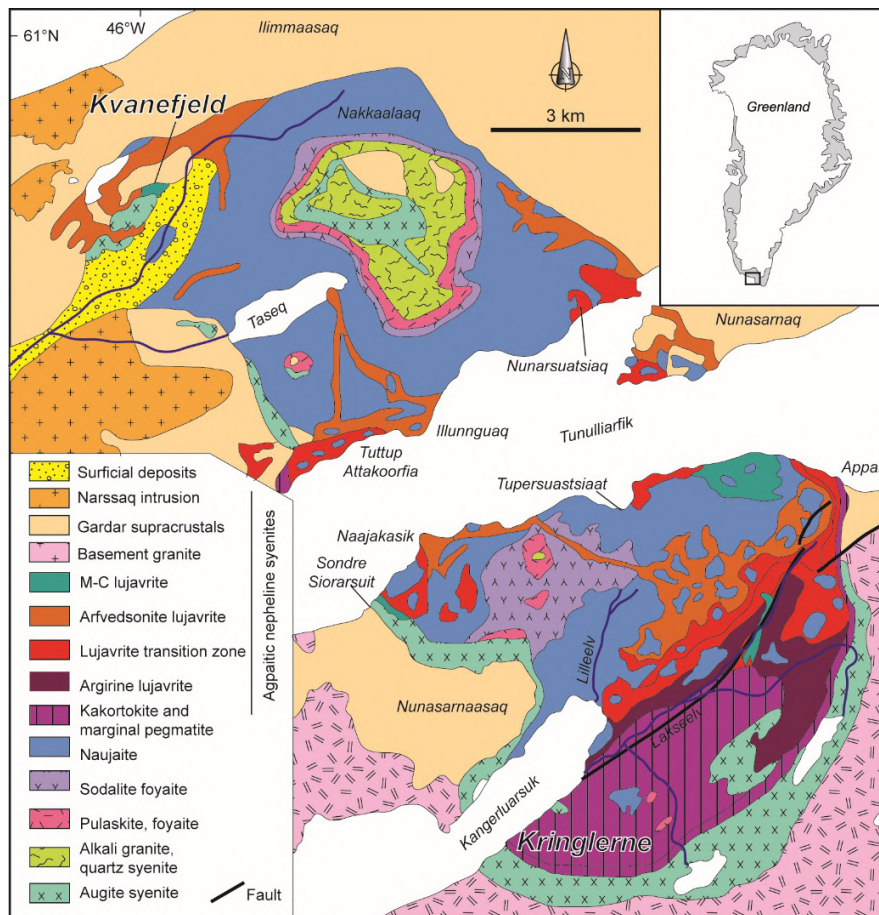


**Figure 1.38.** Ilimaussaq complex including the Kvanefjeld and Kringlerne deposits

Eudialyte is the main mineral of economic interest and carries Zr, Nb and REE (Ferguson 1964; Andersen et al. 1988; Johnsen et al. 2001; Sørensen and Kalvig 2011; GEUS 2014). The three types of cumulate layers have been analyzed for Zr content by Bohse et al. (1971): black kakortokite (1.1%), red kakortokite (3.8%) and white kakortokite (1.3%). The eudialyte contains 12 wt.% ZrO<sub>2</sub>, 2 wt.% RE<sub>2</sub>O<sub>3</sub> and 1% wt.% Nb<sub>2</sub>O<sub>5</sub>, on average (Borst et al. 2016). Moreover, the eudialyte shows low contents of Th and U (similar to contents in the surrounding rock). The eudialyte can be extracted easily from the surrounding materials using magnetic separation, and extraction of the REEs requires acid treatment (Tanbreez 2014). Indeed, recent studies have shown that eudialyte is often replaced by complex assemblages of secondary minerals resulting from the late magmatic interaction of fluids rich in Na and F. This alteration fractionates the major elements within these secondary minerals with separation of the Zr-, Nb- and REE-bearing phases, which complexifies the ore and its processing. Tanbreez published an estimate of the inferred (JORC compatible) resources of more than 4,300 Mt of eudialyte ore, with an average of 1.8% ZrO<sub>2</sub>, 0.2% Nb<sub>2</sub>O<sub>5</sub>, 0.5% LREOs and 0.15% HREOs (which is 27.95 Mt REO), which makes Kringlerne the most substantial REE deposit on the planet (Tanbreez 2014).

#### 1.6.4.3. *Motzfeldt Sø Nb-Ta-U-Zr-REE deposit*

Within the alkaline province at Gardar, alkaline complexes have been established inside and outside the Gardar rift. In addition to the Nunarssuit and Paatusoq complexes, the Igaliko complex is the most substantial in the province, formed of four intrusions (Motzfeldt, Qôroq Nord, Qôroq Sud, Idglerfigssalik) and some smaller intrusive bodies, dated between 1,280 and 1,140 Ma (Emeleus and Upton 1976; Upton and Emeleus 1987; Upton et al. 2003; Bartels 2013). The Motzfeldt intrusion (Figure 1.39) is situated to the northeast of the Igaliko complex and covers a surface of 20 × 15 km (McCreath et al. 2012). It is a pluton of multiple syenite intrusions intersecting the batholite of the Julianehåb, which dates back to the Proterozoic age, and the Gardar metasediments, which date back to between 1,280 and 1,220 Ma (Emeleus and Harry 1970; Tukiainen et al. 1984; Upton et al. 2003; Schoenenberger and Markl 2008).

Motzfeldt Sø is the oldest intrusion and is formed of whole and altered nepheline syenite and a border of arfvedsonite syenite. A complex network of hyperalkaline microsyenite sills and pegmatites associated with a hydrothermal alteration allowed the emplacement of Th-U-Nb-Ta-Zr-REE mineralization at the top of the intrusion (Thomassen 1988; Tukiainen 1988). The main ore is formed of pyrochlore (Nb, Ta, U, REE), thorite (Th), zircon (Zr) and bastnäsite (REE, Th) (Tukiainen 1986). The pyrochlore contains 1.3–8.3% Ta. The first estimate of resources by GEUS dates back to the 1980s and gives a mineralized volume of more than 500 Mt @

0.14% Nb, 120 ppm Ta, 60 ppm U and 90 ppm Th (Thomassen 1988; Tukiainen 1988; GEUS 2014). The estimated resources are less than 30 Mt, with a cutoff grade of 250 ppm Ta. Where Nb resources are concerned, the figures give 130 Mt @ 0.4–1.0% Nb<sub>2</sub>O<sub>5</sub>. In 2010, an exploration permit was obtained by Ram Resources to study the prospects of Aries, Merino, Rams Head and Romney. The Aries site has inferred resources of 340 Mt @ 120 ppm Ta<sub>2</sub>O<sub>5</sub>, 1,850 ppm Nb<sub>2</sub>O<sub>5</sub>, 4,600 ppm ZrO<sub>2</sub> and 2,600 ppm REO (Ram Resources Ltd. 2012); in other words, 1.56 Mt ZrO<sub>2</sub>, 0.884 Mt REO, 0.629 Mt Nb<sub>2</sub>O<sub>5</sub> and 41,000 t Ta<sub>2</sub>O<sub>5</sub>.

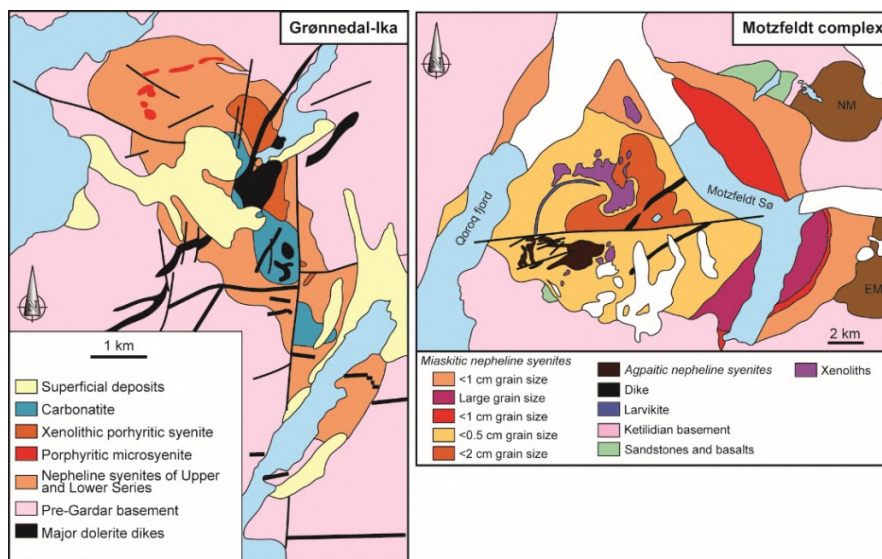


**Figure 1.39.** Alkaline complexes at Motzfeldt and Grønnedal-Ika

#### 1.6.4.4. Grønnedal-Ika alkaline complex

In southern Greenland, the Grønnedal-Ika complex (8 × 3 km) is a nepheline layered syenite intrusion intersecting enclaves of porphyritic syenite and a carbonatite intrusion (Callisen 1943; Emeleus 1964; Pearce et al. 1997; Halama et al. 2005). This complex (Figure 1.39) has been dated back to 1,299 ± 17 Ma using the Rb–Sr method (Blaxland et al. 1978). The core is formed of a calcite-siderite-magnetite carbonatite. The Grønnedal-Ika complex seems favorable to REE potential (Sørensen and Kalvig 2011).

#### 1.6.4.5. *Qassiarsuk alkaline complex*

In southern Greenland, the alkaline complex at Qassiarsuk (1.2 Ga) is situated to the north of the Precambrian Gardar rift, oriented E–W (Stewart 1970; Andersen 1997). This complex, intercalated in the sandstone, includes a series of alkaline silicate tuffs and a carbonatite (discontinuous horizons of tuffs and sills). The massif extends from Qassiarsuk to the Eriksfjord fjord to the east, and to Tasiusaq Creek to the west. The carbonatite varies from calcitic carbonatite to ankerite-dolomite ferrocyanatite. This carbonatite is one of the best targets for REE potential in the Gardar province (Sørensen and Kalvig 2011).

#### **1.6.5. Carbonatites from the Neoproterozoic to the Mesozoic (southwestern Greenland)**

The southwest of Greenland includes a post-Archean alkaline province, including networks of dykes and sills, as well as alkaline complexes established over nearly a billion years (Larsen et al. 1983; Secher et al. 2009). Three distinct magmatic episodes can be described according to their datings: Mesoproterozoic (1,284–1,209 Ma), Neoproterozoic (604–555 Ma) and Jurassic (165–155 Ma). Three carbonatite massifs are studied in particular for their REE and Nb: the Sarfartoq carbonatite (Ediacarian), the Qaqarssuk carbonatites (or Qeqertaasaq) and Tikiusaaq from the upper Jurassic (GEUS 2014; Stendal 2014).

##### 1.6.5.1. *Sarfartoq Ediacaran Nb-REE carbonatite*

In southwestern Greenland, the Sarfartoq carbonatite (66.482°N–51.229°W) is situated approximately 60 km southwest of Kangerlussuaq airport (Figure 1.40). This complex was established at the boundary between the Archean craton to the south and the Paleoproterozoic Nagssugtoqidian orogenic belt to the north (Secher 1986). Carbonatite dates back to 564 Ma (age Rb/Sr on phlogopite) (Secher et al. 2009) and was discovered by GEUS in 1976 using airborne geophysical surveys and field work (Secher 1976, 1986; Secher and Larsen 1980). The massif covers 90 km<sup>2</sup> and the carbonatite occupies 10 km<sup>2</sup>. The surrounding rock is represented by Archean orthogneisses reworked during the Paleoproterozoic. The Sarfartoq complex is a steeply dipping conical body, whose concentric layered core is formed of ferrocyanatite rich in apatite and magnetite (with ankerite rauhaugite dominant). The carbonatite can be divided into a central zone (>50% carbonatite, ~1 km<sup>2</sup>) and an external zone (<50% carbonatite, 1–3 km, ~9 km<sup>2</sup>). The central part is surrounded by concentric bands and carbonatite dykes (beforsite, ferrodolomite dominant), with intercalations of fenitized panels of surrounding rock (light gray aegirine fenite). Hydrothermal processes have allowed the formation of Nb minerals (pyrochlore) and REEs in the dykes and deformed zones 50–200 m in width,

surrounding the core of the massif, with the latter sometimes marked by Th and U anomalies (Bedini 2009). The main minerals in the complex are dolomite, ankerite, apatite, phlogopite, richterite, arfvedsonite and magnetite, and some additional phases include pyrochlore, zircon and Nb-rutile (Secher and Larsen 1980).

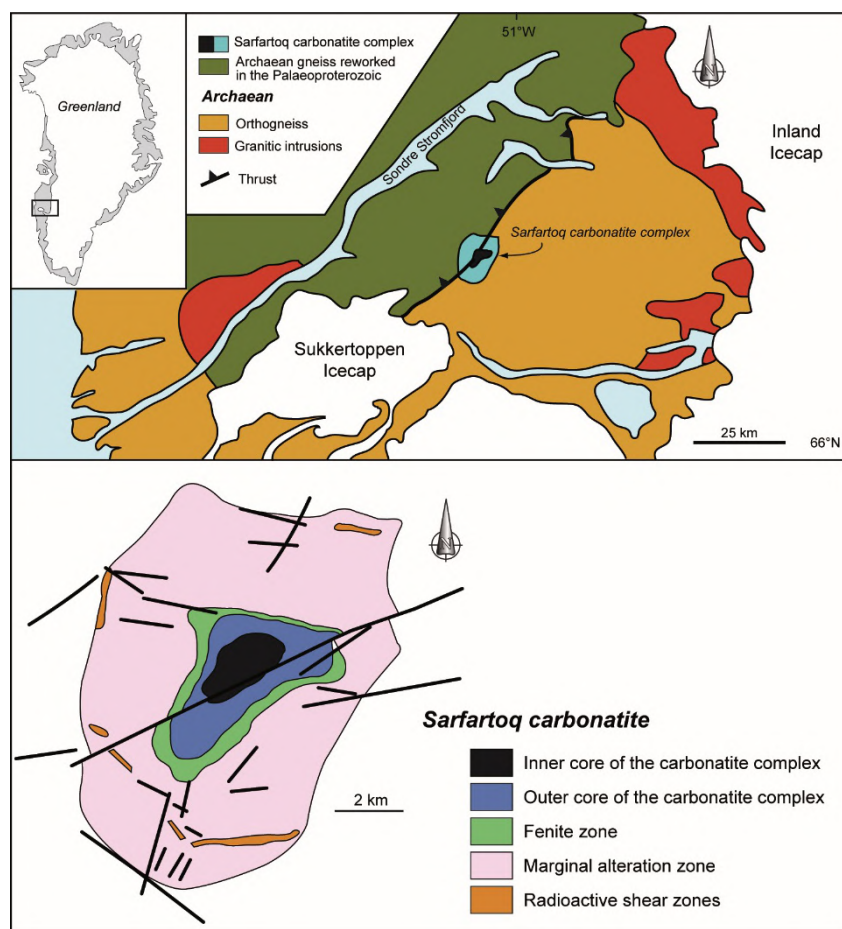


**Figure 1.40.** Sarfartoq carbonatite (Secher et al. 2009)

The carbonatite complex at Sarfartoq has been prospected for diamonds, as well as the following elements: P, Nb, Ta and REE (Sørensen and Kalvig 2010; Druecker and Simpson 2012; GEUS 2014). Since 2003, Hudson Resources has obtained two permits on 783 km<sup>2</sup> to explore Nb (2008) and REEs (2009). The estimate of (JORC compatible) resources gives measured resources of 23,478 t @ 5.95% Nb

(8.51% Nb<sub>2</sub>O<sub>5</sub>) with a cutoff grade of 3% Nb, and inferred resources of 64,301 t @ 3.89% Nb (5.56% Nb<sub>2</sub>O<sub>5</sub>) with a cutoff grade of 1% Nb (New Millennium Resources in 2002). For the REEs, Hudson Resources mentions that they are associated with ferrocarnatite, fenite, hematite alterations and iron carbonates that coincide with the Th anomalies (Druecker and Simpson, 2012). The main REE-bearing minerals are bastnäsite-(Ce), synchysite-(Ce), synchysite-(Nd) and monazite-(Ce). In 2012, Hudson Resources published an estimate of (NI43-101 compatible) resources for the Sarfartoq project with indicated resources of 5.88 Mt @ 1.77% REO and inferred resources of 2.46 Mt @ 159% REO, based on a cutoff grade of 1% and underground exploitation (Druecker and Simpson 2012). Nd and Pr represent 25–54% of all REEs. A recovery rate of 6% has been announced, but it has not yet been subjected to metallurgical tests.

#### 1.6.5.2. Qaqarssuk/Qeqertaasaq Upper Jurassic Nb-REE-P

The Qaqarssuk or Qeqertaasaq carbonatite (65.383°N–51.667°W) is situated in the southwest of Greenland, approximately 135 km northeast of Nuuk, and was discovered in 1969 (Vuotovesi 1974). The carbonatite intrudes Archean gneisses and dates back to 165.0 ± 0.9 Ma (Rb–Sr age on phlogopite) (Secher et al. 2009). The massif covers 15 km<sup>2</sup> and is formed of several concentric carbonatite dykes surrounded by a fenitized zone in the surrounding rock (Larsen et al. 1983; Kunzendorf and Secher 1987; Knudsen 1989; Knudsen and Buchardt 1991). The first stage is represented by dolomite carbonatite and olivine søvite dykes, while the late stage is represented by dykes of fine-grained dolomite carbonatite, ferrocarnatite, søvite, silico-søvite and REE carbonatite. The Qaqarssuk carbonatite has been widely explored for its Nb, REE and P potential since the 1970s by Kryolit Selskabet Oresund (Gothenborg and Pederson 1976; Nielsen 1976). The Nb mineralizations are pyrochlore cumulates in the søvite and pyrochlore precipitations associated with fenite in the surrounding rock, near the carbonatite dykes. The pyrochlore shows contents of more than 15 wt.% Nb<sub>2</sub>O<sub>5</sub> and up to 20 wt.% Ta<sub>2</sub>O<sub>5</sub>. Apatite, present in the silico-søvite, shows content between 3.5 and 6.0 wt.% P<sub>2</sub>O<sub>5</sub>.

Knudsen (1991) shows that carbonatite dykes are rich in REEs. Since 2010, Nuna Minerals has explored the massif by taking surface and trench samples, mapping the facies, and undertaking a drilling campaign totaling 1,590 m (Størensen and Kalvig 2011; Stendal 2014). The REE mineralizations are restricted to the center of the complex in the dykes (1–4.5 m in width and some hundreds of meters in length). The average content, according to surface samples taken over a zone of 1.5 km<sup>2</sup>, is 2.4% REO. The best intersection by drilling amounts to 4.5% REO over nearly 4.7 m. Ancyrite is the main REE-bearing in the dykes in the form of well-developed crystals (0.1–0.3 mm) associated with other phases, such as burbankite

$(\text{Na,Ca})_3(\text{Sr,Ba,REE})_3(\text{CO}_3)_5$ , huanghoite ( $\text{BaREE}(\text{CO}_3)_2\text{F}$ ) and qaqarssukite ( $\text{BaREE}(\text{CO}_3)_2\text{F}$ ) (Grice et al. 2006). LREEs dominate, and the concentrations of some elements are 50% Ce, 27% La, 16% Nd, 5% Pr and 2% other REEs.

#### 1.6.5.3. *Tikiusaaq Upper Jurassic P-REE carbonatite*

In southwestern Greenland, the Tikiusaaq carbonatite ( $64^\circ\text{N}$ – $46.75^\circ\text{W}$ ) is situated 100 km south of Nuuk. This complex was discovered by GEUS in 2005 thanks to an integrated framework/stream sediment geochemistry/aeromagnetism (Steenfelt et al. 2006). The massif seems to cover a surface of  $100 \text{ km}^2$  and intrudes the strongly deformed and metamorphosed Archean basement, which is formed of granite, orthogneiss, amphibolite and anorthosite. The core of the massif ( $3.3 \times 2 \text{ km}$ ) is formed of vertical and closely spaced blades and carbonatite (up to a few meters in thickness) of two types: early white calcitic carbonatite (calcite and planes with green mica, magnetite and apatite) and late gray dolomite carbonatite (ferrous dolomite and ankerite) (Nuna Minerals 2010). A fenitized zone is visible around the carbonatite core. Within the surrounding rock, numerous carbonatite veins (from 1 mm to 20 cm) are described. The Tikiusaaq carbonatite dates back to  $158 \pm 2 \text{ Ma}$  (age U/Pb on zircon; Frei et al. 2006; Steenfelt et al. 2006), which is equivalent to the Qaqarssuk carbonatite (165 Ma).

The Tikiusaaq complex has been explored by Nuna Minerals for REEs and diamonds (Nuna Minerals 2010). The exploration campaign focused on the core of the massif, with 78 carbonatite samples that have confirmed the REE concentration within the late ankerite carbonatite, while phosphates are present in the calcitic carbonatite. The contents amount to 9.6% REO (an average of 0.6% REO, dominated by LREEs) and up to 8.5%  $\text{P}_2\text{O}_5$  (an average of 1.6%  $\text{P}_2\text{O}_5$ ). The REE minerals are ancylite, churchite and parasite. The REE composition is broken down as follows: Ce (47%), La (33%), Nd (12%), Pr (4%) and other REEs (4%). The level of U is low. Nuna Minerals estimates that the mineralized body is 750 m in length and 100 m in width and extends to at least 500 m in depth. The important anomaly in Th indicates a substantial REE deposit, the potential resource of which is estimated to be more than 200,000 t @ 1–5% REO (Stendal 2014), even if further exploratory studies are needed.

#### 1.6.6. *Milne Land Jurassic–Cretaceous REE-Ti-Zr paleoplacer*

In eastern Greenland, the island of Milne Land includes a Jurassic–Cretaceous paleoplacer with heavy mineral sands ( $70.685^\circ\text{N}$ – $25.920^\circ\text{W}$ ) (Sørensen and Kalvig 2011; Stempera 2012; GEUS 2014; Stendal 2014). These zircon and monazite sands have been detected through Th anomalies identified by airborne radiometry and a

sampling campaign carried out by Nordisk Mineselskab and Research Establishment RISØ in 1968. Marine sandstones have been dated from the middle Jurassic to the lower Cretaceous and form part of the Charcot Bugt Formation (Birkelund et al. 1978, 1984; Birkelund and Callomon 1985; Larsen et al. 2003). The paleoplacer is situated at the base of this sedimentary formation, and the main anomaly is located at Bays Fjelde (“Hill 800” site), measuring 500 m in diameter and 40–50 m in width. The heavy mineral sands present as irregular lenses of 10–40 cm in thickness within an arkosic sandstone unit and breccia of approximately 20 m in width (Harpøth et al. 1986). The heavy minerals are as follows: monazite, xenotime, rutile, zircon, garnet and ilmenite with potential in REEs, Ti, Zr and Th. The detrital level of 20 m contains 5 Mt @ 1.0–3.8% Zr and 0.5–1.9% REO (Harpøth et al. 1986).

In 1990, metallurgical tests carried out by Coffs Harbour Rutile concluded that the economic extraction of monazite, zircon and garnet was possible. An estimate of resources for the “Hill 800” site gives 3.7 Mt @ 1.1% zircon, 0.5% monazite, 2.6% anatase, 3.1% garnet and 0.03% xenotime (Sørensen and Kalvig 2011). Monazite is the mineral containing REEs (90% LREE and 10% HREE). Since 2010, the CGRG (Czech Geological Research Group) has explored the Milne Land paleoplacer. In 2011, the CGRG collected 105 samples and made radiometric measurements, demonstrating three Zr-REE-Ti anomalies with levels of 2.0 wt.% ZrO<sub>2</sub>, 2.5 wt.% REO and 35 wt.% TiO<sub>2</sub> (Stembera 2012).

### **1.6.7. Alkaline complexes from the Paleogene (central and eastern Greenland)**

At the start of the Paleogene, central-eastern Greenland was marked by the opening of the North Atlantic, leading to the separation of Greenland from Europe. Magmatic rocks from this period outcrop between the latitudes 68°N and 75°N (Brooks and Nielsen 1982; Nielsen 1987; Saunders et al. 1997; Nielsen 2002). This magmatic event is characterized by vast basalt plateaus and alkaline intrusions established between 62 and 25 Ma (Tegner et al. 1998, 2008; Brooks et al. 2004). REE occurrences have been described at Kap Simpson, Kap Parral and others associated with the Gardiner complex (Stembera 2012; GEUS 2014; Stensgaard et al. 2016; EURARE 2017).

#### **1.6.7.1. Kap Simpson (Bjørnedal-Trail) Nb-REE alkaline complex**

Kap Simpson is situated on the central-eastern coast of Greenland and is one of the most important alkaline intrusions from the Paleogene (Nielsen 1987). This complex includes an alkaline syenite to the northwest and a system of concentric syenite dykes within a volcano-sedimentary unit to the northeast (Harpøth et al.

1986). The southeastern part is a caldeira called the “Dreibuchten Zone” (Schaub 1942; Harpøth et al. 1986). The Kap Simpson complex has been explored by Nordisk Mineselskab and AMAX (Martens and Seemann 1973; Schassberger and Spieth 1978; Geyti 1979; Schassberger and Newall 1980; Damtoft and Grahl-Madsen 1982). Intense hydrothermal alteration has been described across the whole massif, especially in the Dreibuchten zone, with silicification, pyritization and clay enrichment. Harpøth et al. (1986) mention a potential in Mo, fluorine and base metals. Moreover, the samples collected in 1969 by Nordmine have revealed high REE levels.

Further work has allowed the discovery of quartz veins and Nb-REE, 15 cm broad and 30 m long, within Jurassic sediments close to the contact with the Bjørnedal-Traill syenite (72.341°N–22.766°W) (Martens and Seemann 1973; Harpøth et al. 1986). The samples contained up to 3.2% Nb, 3.0% REE and 0.3% Y. The main REE-bearing minerals are euxenite, monazite, bastnäsite, samarskite and fergusonite. More recently, the CGRG (Czech Geological Research Group) explored the Bjørnedal-Traill site for Zr, Nb, Ta, REE and Mo potential (Stembera 2012). In 2011, samples were collected and showed levels up to 2.5 wt.% Zr, 0.3 wt.% Nb and 1.5 wt.% REE.

#### 1.6.7.2. *Kap Parral alkaline complex*

Kap Karral is situated just to the north of Kap Simpson, on the central-eastern coast of Greenland. This cap is formed of an alkaline syenite intrusion similar to that at Kap Simpson (Nielsen 2002). It remains unexplored, although it may form Nb and REE potential.

#### 1.6.7.3. *Gardiner ultramafic alkaline complex*

At the core of the Kangerlussuaq fjord in the center-east of Greenland, the Gardiner massif (68.618°N–33.151°W) is an ultrabasic alkaline complex that dates back to  $50.3 \pm 1.4$  Ma, forming a REE occurrence (Woodley 1987; Campbell et al. 1997; Orris and Grauch 2002). The intrusion is formed of an ultrabasic suite and a system of late concentric melilitolite, syenite and carbonatite dykes (Frisch and Keusen 1977; Nielsen 1979, 1980, 1994; Johnsen et al. 1985). The REE-bearing minerals are perovskite (and loparite in the syenite) and apatite associated with other additional phases, such as titanite and magnetite. Perovskite concentrates more REEs than apatite, even though these two minerals are rich in LREEs (Campbell et al. 1997).

Perovskite is present in dunite, melilitolite and the associated rocks, and may form a modal proportion of nearly 20% in some cases where it is mentioned. Frisch and Keusen (1977) carried out a chemical analysis using a microprobe along a

perovskite grain profile, showing that the perovskite is a calcium titanate with minor substitutions of Na, Nb and LREE, and contents of approximately 7 wt.% RE<sub>2</sub>O<sub>3</sub>. Analyses carried out by Campbell et al. (1997) on some grains of perovskite (melilitolite dike) and loparite (syenite) have given contents of 4.11% REO and 35.5% REO, respectively.

### **1.7. The origin of the rare earth deposits in Europe and Greenland**

The conclusion of this summary is unarguable: Europe includes many occurrences of REEs associated with varied geological environments. The geological processes at the origin of these occurrences can thus be observed at all stages of the geological cycle, from the high temperature and high pressure conditions encountered in the mantle (up to 1,200°C and 1.5 GPa) to more surficial environments that are sensitive to the climate.

These very different processes may be of magmatic, metamorphic, hydrothermal or diagenetic origin, or may quite simply have origins associated with the regolith. Thus, the primary deposits are essentially associated with igneous alkaline rocks and carbonatites, whereas the secondary deposits, especially placers or bauxite, generally have a source in the fertile terrain of the European subsoil. One point is essentially to understand the main mechanisms at the origin of REE enrichment in endogenous environments as in exogenous ones, as well as the geological cycle of REEs in the continental crust (Figure 1.41).

#### **1.7.1. Partial melting and crystal fractionation**

The hyperalkaline carbonatites and magmas (including kimberlites) are enigmatic witnesses of the deep carbon cycle linking diamonds in the Earth's crust to the volcanic emission of CO<sub>2</sub> and other gases (Green and Wallace 1988; Nelson et al. 1988; Hammouda and Keshav 2015; Foley and Fischer 2017). These two types of magma are often linked and are generally encountered in hotspot- or rift-type environments, as observed in extended intracontinental domains (Woolley and Kjarsgaard 2008; Goodenough et al. 2016). They are uncommon (approximately 5% of volcanism in volume), and their compositions and physical-chemical properties are part of the spectrum of conventional silicate magmas. They are particularly rich in volatile constituents (CO<sub>2</sub>, H<sub>2</sub>O, halogens and sulfides in order of abundance) and poor in silica (Le Bas 1981; Le Maitre 2005).

Another peculiarity of these magmas is the wide range of differentiation temperatures, ranging from more than 1,300°C to less than 500°C (Weidendorfer

et al. 2017). The cold temperatures correspond to the only carbonatites currently emitted by the Doiño Lengai volcano in Tanzania (Keller and Krafft 1990). It was in the course of this particular magmatic differentiation that gigantic geochemical anomalies developed to the point of forming deposits of REEs and other rare metals. The formation of these deposits remains an exception, however. In fact, out of nearly 500 carbonatites listed globally, only five are exploited today for their exceptional tonnage and REE content (Verplanck et al. 2016). The reason behind such evolutions is debated. A deeper investigation on the formation modes and differentiation modes of these highly specific magmas is key.

Carbonatites are mostly formed by magmatic immiscibility: two liquids, one a silicate and the other a carbonate, coexist in equilibrium without mixing chemically, similar to oil and water (Kjarsgaard and Hamilton 1989; Kjarsgaard et al. 1995; Weidendorfer et al. 2017). Over the course of this immiscibility, the REEs are shared very variably between the two liquids, a process that remains poorly understood. Using experiments at high temperature and high pressure, recent works (Nabyl et al. 2020) modeled the behavior of REEs during the formation of immiscible carbonatites. Nabyl et al. (2020) demonstrate that REEs follow calcium and can be overconcentrated in carbonatites coexisting with fairly viscous phonolite-type liquids. On the other hand, although carbonatites do not form at the stage known as phonolitic, they focus on no or few REEs. The latter therefore remain in the silicate liquid, and given their incompatible behavior, the fractionated crystallization processes will be concentrated in highly differentiated magmas, such as those in hyperalkaline complexes.

Magmatic mechanisms are thus able to concentrate REEs highly in the carbonatites at levels comparable to the large, world-class deposits. It is very possible, however, that the final stages of the magmatism of carbonatites, in other words, degassing at the transition between magmatic and hydrothermal processes, are the root of the still poorly understood remobilization of REEs. Indeed, enrichments in REEs in carbonatites are often described as resulting from late magmatic and hydrothermal processes (Bühn et al. 2002; Nadeau et al. 2016). At this stage, hot aqueous fluids rich in halogens, phosphorus and sulfides are surely able to redistribute REEs from carbonatites. Today, decoding all these magmatic and hydrothermal processes remains the key to understanding the formation of these geochemical anomalies and suggesting “proxies”, that is, easy-to-use mineralogical indicators, which are nevertheless able to record and rebuild the magmatic and hydrothermal stages leading to the formation of a rare metal deposit.

### 1.7.2. Chlorinity of hydrothermal systems

The behavior of REEs in solution can be considered a scientific paradox. Since the 19th century and the first attempts at solvent extraction from rare ores such as *yttria* (i.e. gadolinite), cerite or even samarskite, it has been known that REEs are soluble in aqueous solutions (Mosander 1843; Marignac 1880). Until the second half of the 20th century, these REEs have been considered immobile by geologists (Menzies et al. 1979; Michard and Albarède 1986), even though the latter, contained in monazite or bastnäsite, were processed and separated by solvation in industrial applications.

Moreover, it seems that REEs can be mobile in hydrothermal fluids (Juteau et al. 1979; Wood 1990a, 1990b; Lottermoser 1992) and that the latter can mobilize REEs during the leaching of rocks and minerals to then concentrate them in many instances. These processes are at the origin of economic deposits in many contexts. They may involve the following:

- exsolved fluid phases of magmatic liquids such as Strange Lake in Canada (Gysi et al. 2016) or Lofdal in Namibia (Bodeving et al. 2017);

- but also, although rarer, fluids resulting from non-magmatic processes such as in the Browns Range dome in northwestern Australia (Nazari-Dehkordi et al. 2018) and the Maw Zone in Athabasca in Canada (Rabiei et al. 2017).

The growing role of REEs in energy transition involves the development of innovative technologies to extract these elements from so-called unconventional minerals (e.g. eudialyte, steenstrupine, gadolinite and allanite). This also reminds us of the understanding that is needed about the chemical mechanisms responsible for the transport of REEs in solution, their fractionation and concentration in the natural processes that lead to the genesis of unconventional economic concentrations of hydrothermal affiliation.

At the atomic scale, lanthanides are characterized by the gradual filling of the electron sublayer 4f, deeply buried and protected by the external layers  $5s^25p^6$ . This peculiarity makes them relatively insensitive to their chemical environment, hence their supposedly immobile behavior. Mainly present in trivalent state, Pearson's rule (1963) predicts their behavior in acid solutions, which allows them preferential interaction with hard inorganic ligands. The most stable are  $F^- > OH^- > Cl^-$  when monovalent complexing agents are considered and  $CO_3^{2-} > SO_4^{2-} > P_2O_5^{2-}$  for divalent ones. Recent work (Migdisov 2009, 2004, 2019) has made it possible to evaluate the main factors governing the transport and deposit of REEs in hydrothermal fluids. In particular, it has revealed the major role of  $Cl^-$ , as well as  $F^-$  in their complexation in solution and their deposition. Experiments including thermodynamic models suggest that the main ligands responsible for the transport of REEs in hydrothermal

conditions are chloride and sulfate. On the other hand, the presence of fluoride considerably reduces the solubility of REEs in these hydrothermal solutions, contrary to all expectations. Indeed, the presence of  $F^-$  could facilitate the trapping of REEs and contribute to the effective precipitation of REE minerals.

The most effective precipitation mechanism would therefore involve neutralizing an acidic fluorinated fluid rich in REEs using carbonated formations of sedimentary or magmatic origin, which would, for example, trigger precipitation by saturation of REE fluorocarbonates such as bastnäsite. The addition of phosphate complexes would, however, contribute to the precipitation of monazite and/or xenotime. REEs transported in the form of sulfate complexes would be destabilized by the addition of barium and the precipitation of insoluble barite. These results nonetheless remain preliminary insofar as too little research has focused on the speciation in solution of carbonated complexes such as REE-hydrolyzed complexes.

### **1.7.3. Exogenous rare earth cycle**

Exogenous REE deposits form in conditions called surface conditions, and result from interactions between rocks, biosphere and atmosphere. The rocks, like their constituent minerals, undergo chemical and physical transformations in contact with surface agents such as air, wind, water, ice and the living world. It makes sense to distinguish two types of exogenous deposits:

- those associated with regolith;
- more distal ones located in sedimentary basins.

In the environment of the regolith, reactions of hydrolysis, oxidation, hydration, or decarbonation trigger a chemical alteration of the rocks and minerals, in addition to physical phenomena (Freyssinet et al. 2005). It must be specified that the solubility of REEs in solution is moreover strongly dependent on the temperature (Wood 1990a, 1990b); they can be considered very poorly soluble, or indeed immobile, in ambient conditions. The time factor will also be preponderant in the genesis of exogenous REE deposits in aqueous conditions. Thus, enrichment in insoluble elements (Fe, Al, REE) is residual and strongly dependent – partially or wholly – on the leaching of soluble elements in very aggressive climates (Mg, Ca). The hydrodynamism of underground waters will allow the recombination of insoluble elements in neoformed minerals, mainly clays, hydrophosphates or carbonates.

In the ionic clay-type deposits often associated with the weathering of granites, REEs are adsorbed to the surface of halloysite/kaolinite-type neoformed clays

(Roaldset 1973; Chi and Tian 2008; Borst et al. 2020). The adsorption of REEs to the surface of clays is favored under pH neutral conditions (Coppin et al. 2002), such as those encountered in deposits at the interface between saprolite and laterite (Li et al. 2020). The character of ionic clay-type deposits, rich in LREEs or HREEs, can be explained by:

- effects linked to relief (i.e. topographic gradients) (Li et al. 2020);
- the morphology and stability of crystalline surfaces (Coppin et al. 2002);
- variations in the solubility of REEs in surface waters when these elements are complexified by inorganic anions (e.g.  $\text{CO}_3^{2-}$ ,  $\text{F}^-$ ), simple organic anions, or colloidal organo-mineral fractions (Tuduri et al. 2011; Rillard et al. 2019);
- adsorption/resorption phenomena at the surface of minerals (Pourret and Davranche 2013; Liu et al. 2017; Li et al. 2020). These numerous, very small deposits (several tens of thousands of tonnes) are widely exploited in China despite their (very) low contents between 0.03 and 0.35% REO (Chi and Tian 2008; Li et al. 2020).

Thus, in a laterite setting, the weathering of rocks initially rich in REEs (e.g. carbonatite, granite) will be able to produce secondary REE deposits that are even more fertile (Borst et al. 2020). In bauxitization settings, REEs are thus alternatively adsorbed and then desorbed in line with the progression of weathering toward the bottom. The neutralization of surface waters by carbonated formations can lead to the neoformation of hydroxylated bastnäsite in addition to REEs adsorbed to the surface of the clays (Mongelly 1997).

Finally, let us specify that recent research has shown that the processing of karst bauxites using the Bayer process makes it possible to concentrate REEs in waste produced from the manufacture of alumina: red mud (Deady et al. 2016).

Not all the minerals that form rocks, including those carrying REEs, present the same stability in relation to surface agents. Over the course of physical weathering, rocks fragment, disintegrate and the most resistant, insoluble minerals are taken up and leached by the wind and water. Placer-type deposits thus formed in sedimentary environments. These are accumulations of heavy minerals in sands and gravels separated by gravitational processes during their transportation by water and/or wind. With time and subsidence, diagenetic processes consolidated these placers, transforming them into paleoplacers. In fact, the placers are generally recent, of Cenozoic or Quaternary age, although some older ones date back to the Precambrian. The main REE minerals encountered are monazite, xenotime, fergusonite, euxenite and allanite (Donnot et al. 1973; Morteani 1991).

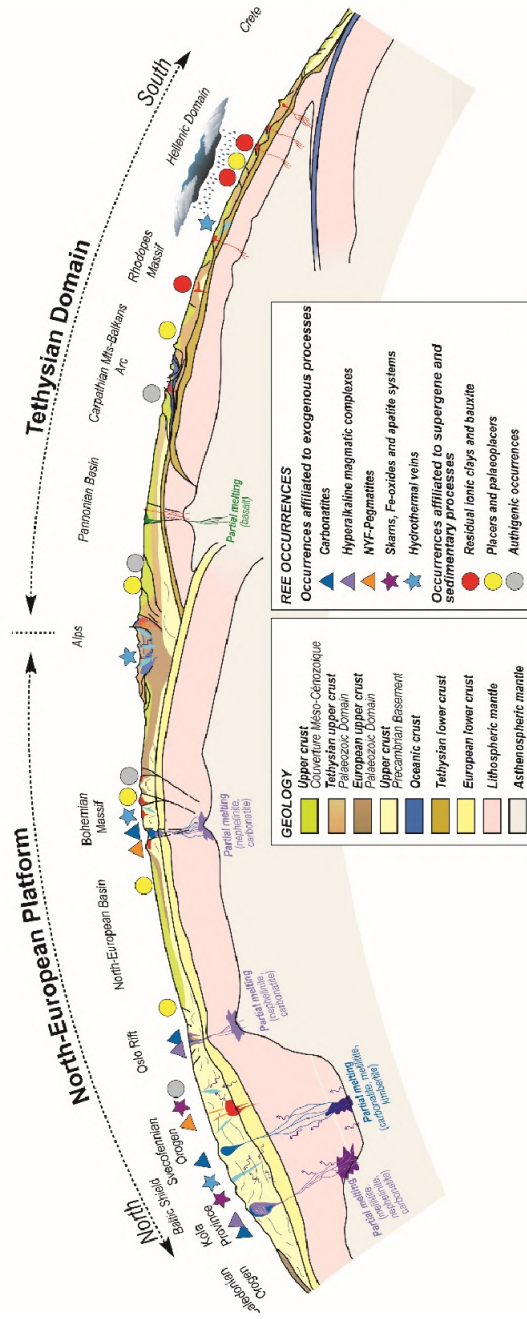


Figure 1.41. Synthetic geodynamic section of Europe with the main types of REE deposits

In a more distal fashion, the oceans are often considered to be in a stable chemical state, thus displaying an elementary balance maintained by input and output rates (Elderfield et al. 1990). However, the total loss of REEs – the quantity of REEs washed onto coastal plateaus and into the oceans – is underestimated (Rasmussen et al. 1998; Lacan and Jeandel 2005).

Recent work has demonstrated the major roles of the coarse colloidal organic fraction on the transport of REEs, such as that of the salinity gradient on their speciation in estuaries (Freslon et al. 2014; Rousseau et al. 2015). REEs are thus gradually eliminated through coagulation of this colloidal fraction, which therefore sediments the bottom of continental plateaus. Pourret and Tuduri (2017) suggest that the diagenesis of some silico-clastic rocks enriched in both organic matter and REEs can lead, under rising temperatures, to the formation of authigenic deposits of gray monazites characterized by a bell spectrum (i.e. enriched in average REEs). Another accumulation process, this time of microorganisms and algae, but in a marine environment, can also produce concentrations of phosphates called phosphorites under the action of diagenesis. These rocks, which are particularly rich in apatite, can in some settings include REEs, as well as uranium. High REE concentrations have also been indicated in manganese nodules, iron and manganese crusts (Kato et al. 2011; Bau et al. 2014; Josso et al. 2017), which are being studied for their economic potential.

### **1.8. Strengths and weaknesses of rare earths deposits in Europe and Greenland**

Although Europe was the first region in the world where REEs were exploited (at Bastnäs-Bergslagen, Sweden), no REE mine is currently active on the Old Continent (except that of Lovozero in Russia). The political desire for better knowledge of the potential of mineral resources in Europe and Greenland strengthened toward the end of the 2000s. Awareness of China's hegemony in the mining of many commodities resulted in the European initiative on raw materials in 2008. The European Union (EU) now wished to secure its supplies in accordance with a list of strategic commodities (i.e. Critical Raw Materials, CRM) published in 2011, in which REEs feature prominently (HREEs and LREEs) in the last list published in 2020 (Blengini et al. 2020). Moreover, the EU imports 95% of the REEs it uses from China (Gislev and Grohol 2018). Some member states are also taking their own initiatives:

- France with COMES (Committee for Strategic Metals);
- Denmark with MiMa (Center for Minerals and Materials);

- the Netherlands with a government program on the circular economy.

The EU is also co-financing networks and expert platforms on mineral resources with:

- ERA-MIN (Network on the Industrial Handling of Raw Materials for European Industries);
- ERECON (European Rare Earths Competency Network);
- EIP (European Innovation Partnership);
- ETP (European Technology Platform on Sustainable Mineral Resources);
- AdWG (Ad hoc Working Group);
- SCRREEN (Solutions for Critical Raw Materials – A European Experts Network);
- research projects and databases with EURARE (Development of a sustainable exploitation scheme for Europe's Rare Earth ore deposits), Mine-rals4EU or Promine.

All these initiatives have made it possible in the past few years to improve knowledge of the REE potential of Europe and Greenland (Ahonen et al. 2015; Goodenough et al. 2016; Machacek and Kalvig 2016; Balomenos et al. 2017; Gislev and Grohol 2018; Lauri et al. 2018).

Europe and Greenland have undeniable REE potential, and the few deposits already studied and enjoying a NI43-101 or JORC compatible resource estimate (Norra Kärr, Kvanefjeld, Kringlerne, Motzfeldt, Olserum, Sarfartoq, Fen and Delitzsch-Storkwitz) demonstrate that the Old Continent has no reason to envy other parts of the globe and could indeed be self-sufficient (Figure 1.42).

Indeed, it is important to note that in the current state of knowledge of global REE reserves, Europe represents merely less than 1% of these estimated reserves (Figure 1.43). These estimates rely on data from deposits and use, and on worldwide feasibility studies for different types of deposits. In 2015, depending on higher or lower estimates, global reserves formed between 137 and 375 Mt REO, and China had an important place here. Where Greenland is concerned, this territory, affiliated to Denmark, includes between 8 and 11% of global REE reserves estimated in 2015 (Figure 1.43).

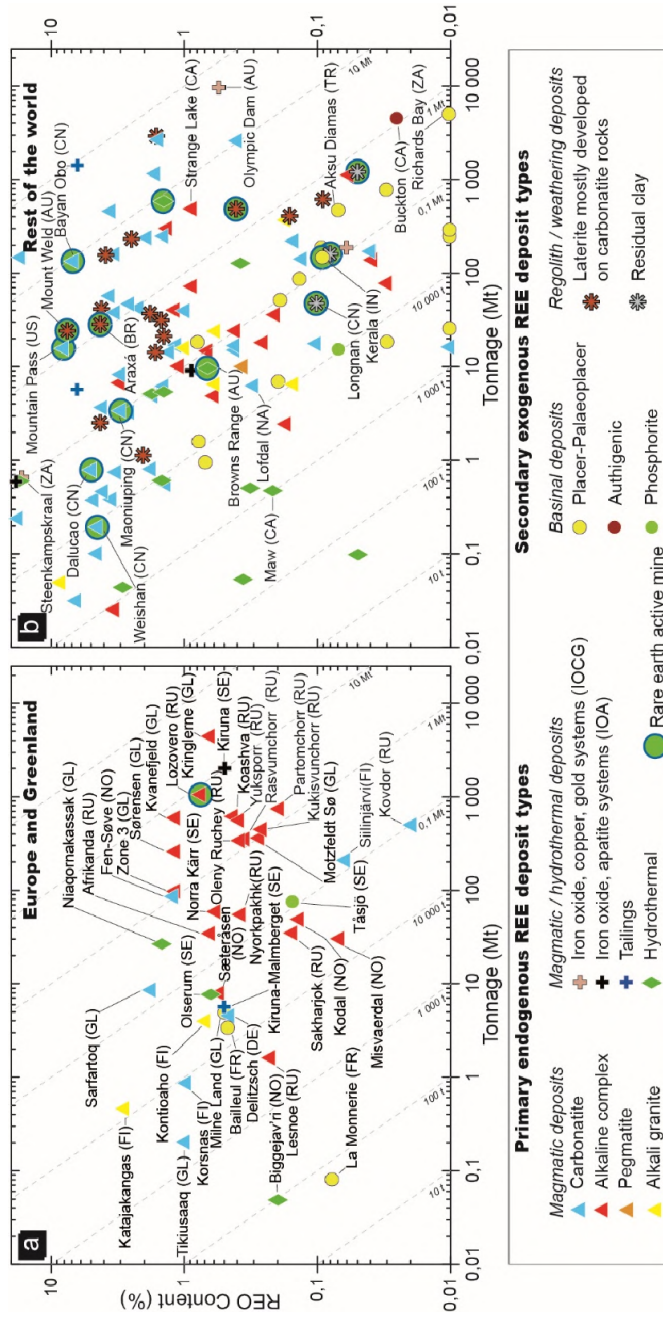


**Figure 1.42.** Grade/tonnage relationship for the different types of localized rare earth deposits

COMMENT ON FIGURE 1.42.– (a) *In Europe and Greenland and (b) in the rest of the world.* Abbreviations: AU (Australia), BR (Brazil), CA (Canada), CN (China), DE (Germany), FI (Finland), FR (France), GL (Greenland), GR (Greece), IN (India), KE (Kenya), NA (Namibia), NO (Norway), RU (Russia), SE (Sweden), TR (Turkey), US (United States), ZA (South Africa). Data for Europe, Greenland (for this study, see the table of deposits in Appendix 1) and the rest of the world are presented (Weng et al. 2015; Zhou et al. 2017 and references therein).

The geodynamic settings in which REE deposits were emplaced are numerous, but only some settings make it possible to concentrate REEs in economically beneficial quantities (Figures 1.41 and 1.42). Thus, the main REE resources are associated with alkaline complexes and with carbonatites that were formed in the setting of intracontinental rifting (Chakhmouradian 2012b; Wall 2014; Goodenough et al. 2016). This rule also applies to Europe and Greenland (Gardar in Greenland, the Svecofennian in Scandinavia).

Other occurrences of REEs have also been highlighted, such as heavy mineral placers (Greece, France, Germany, Spain) or the laterite bauxite deposits of the Mediterranean belt (Charles et al. 2013; Goodenough et al. 2016; EURARE 2017; Mondillo et al. 2019).

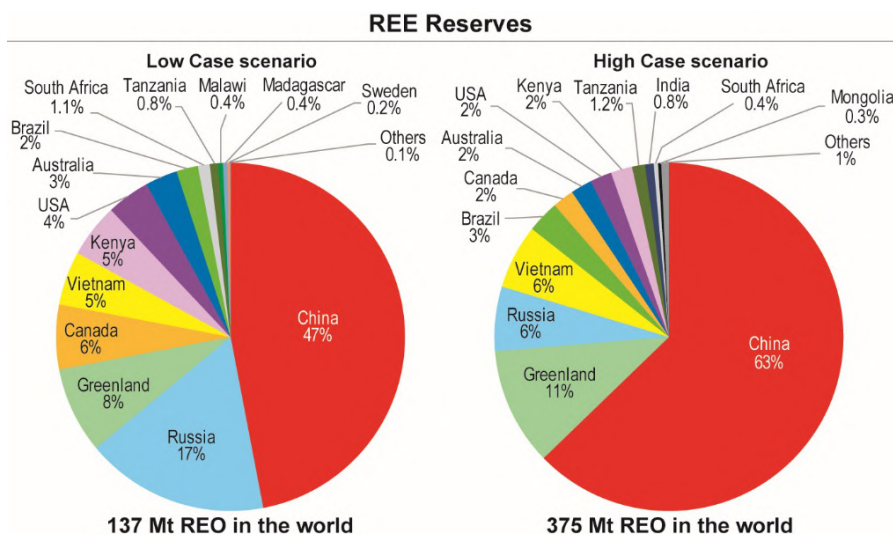


**Figure 1.43.** Global REE reserves estimated in 2015 (Bru et al. 2015)

Moreover, the many other REE occurrences show that further exploration could increase Europe's and Greenland's known potential. Beyond primary deposits, REEs can also be the subject of by-products resulting from the re-processing of mining waste. Although REEs are less abundant than in end-of-life electronic products, the volumes of mining waste are much greater. The best example is that of the Kiruna-Malmberget iron mines, the tailings of which contain 5.6 Mt of apatite with 0.5% REO.

The main question hinges, of course, on the economic viability of REE exploitation in Europe and Greenland. Indeed, there are too few economic studies available on the most promising deposits and on the possibility of comparing them with other deposits in the world via the use of international standards (e.g. NI43-101, JORC). On the other hand, there are few companies that wish to take the risk of investing in exploration, given the fairly unpredictable setting of REEs (global demand, supply, price (Bru et al. 2015)). In addition, the very substantial investment needed to develop innovative techniques with a view to processing different ores depending on the geology of the deposits is a major restriction. The key point is to be able to separate the different REEs, while still respecting a balance between the economic cost and the environmental impact. The environment is indeed very important to European citizens, those who are increasingly consuming REEs in the form of new digital technologies, but also in the form of the "ecological" and energy transition (Machacek and Kalvig 2016; Sebastiaan et al. 2017).

The quality of the deposit remains essential and is guided by its geology. A clever balance has to be found between a tonnage and a grade, between the proportion of HREEs and that of LREEs, between the REE-bearing minerals from which useful commodities can be extracted without investing colossal sums in R&D, or between the other related commodities (e.g. Nb, U, Zr, Ta, P). The geology is also independent of communication routes; although a deposit may present a tonnage and an interesting grade, if it is geographically difficult to access, the economic stakes may drop markedly. This is especially the case for the immense deposits in Greenland, where infrastructure is very often absent: roads, to begin with, electrical installations, housing and bases for miners to live in, a deep-water port for logistics and, if necessary, a processing plant.

A challenge also lies in finding local, qualified manpower without bringing in too many external staff. In Greenland, the hypothesis of the massive influx of Chinese workers is a sensitive subject for this country, which has 56,000 inhabitants and is half the size of the EU. In fact, the development of Kvanefjeld reached an important milestone in 2018 under the impetus of Chinese support and the growing interest of the Middle Empire in Greenland (Andersson et al. 2018a). Shenghe

Resources Holding Co. Ltd. is the main shareholder in the Australian junior, Greenland Minerals, which is developing the project. In January 2019, the formation of a joint venture between Shenghe and China National Nuclear Corp was announced. It was entrusted with the import, export and trading of REOs and  $U_3O_8$ . An agreement was made to take 32 kt/year of concentrate, as well as the chance for Shenghe to become the main shareholder (60% of shares). The last obstacle involved requests for mining permits.

The inhabitants of Greenland and Europe also increasingly consider it important to respect the environment. Like any industrial activity, the mining industry has an impact on the environment. Nevertheless, the application of good practices and the existence of a strict regulatory framework in these regions of the world may allow mines to be exploited while respecting the environment and populations, and in particular, acquiring the SLO Social Licence to Operate and at least the approbation of all stakeholders. Thus, although it appears promising, the Norra Kärr project (Sweden) is still awaiting environmental authorization from the Swedish government. The exploitation of an REE deposit can lead to a substantial impact on the environment and on individuals if certain conditions are not respected: gaseous effluent linked to the use of acids when processing ores, management of tailings, which can impact the hydrosphere and engenders risks of dam failure, management of radioactive elements that can be associated with REEs, the impact of exploitation on the countryside, etc. Although techniques and good practices are known and the legislative framework is already very restrictive in Europe and Greenland, public opinion is becoming increasingly hostile to mining activity. This situation is broadly contradictory, between, on the one hand, the need for a whole continent to ensure its supply of a raw material on which it is very much dependent and, on the other hand, a population that wishes to benefit from a living environment associated with the latest technologies without accepting some downsides. For now, the increasing power of technologies known as green technologies and the policy on the European scale to move toward a carbon-free economy through a Green Pact (EC 2019a, 2019b) do not seem to resolve the situation, which also depends largely on global-scale challenges.

Another sizable challenge is the recycling of REEs on a European scale. Recent figures demonstrate that REEs remain very little recycled: 0% for Dy, Er (and Sc); 1% for La, Ce, Nd, Sm, Gd, Ho, Tm, Yb and Lu; 10% for Pr; 22% for Tb; 38% for Eu and 31% for Y (Gislev and Grohol 2018). Application sectors seem to be a priority for recycling REEs: permanent magnets (Nd, Pr, Dy, Tb, Sm), phosphors (Eu, Tb, Y, Ce, Gd, La), batteries (La, Ce, Nd, Pr), polishing components (Ce) and catalysts (La, Ce, Pr, Nd, Y; Ahonen et al. 2015).

## 1.9. Conclusion

The “vitamins of modern industry” have come a long way since 1794. REEs are already used in numerous domains, both current, cutting edge ones, and those to come, since their substitutability is often synonymous with a loss of performance and increased investment in the face of recycling, which is still limited and costly, while eco-design products are still not widespread. The European Union has defined REEs as critical and strategic metals for its economy. With a view to the independence of its supply, the Old Continent has benefitted from a panorama of its geological potential in REEs through diverse projects, initiatives and expert networks over recent years. The geological potential of the REEs of Europe and Greenland is situated in intracratonic areas associated with old rifting zones, which have given rise to the intrusion of alkaline complexes (Scandinavia, Gardar) (Figures 1.10, 1.35, 1.41 and 1.42). The rare deposits benefitting from an estimate of resources compatible with international standards demonstrate their global size and their capacity to palliate the continent’s need for at least some decades.

Nevertheless, if Europe wishes to increase its independence, a voluntary and assumed investment in R&D remains indispensable to develop ore processing techniques adapted to the REE-bearing minerals specific to the European and Greenland deposits. It is by developing this competency in the extraction and separation of these metals that Europe will be able to secure its supplies and develop a real value chain for REEs. Beyond this technical-economic engagement, Europe and Greenland must also gain the confidence and approbation of stakeholders in the extraction industry and in civil society. The societal, social and environmental challenges are in fact as important, and will be even more so in the future, as the technical-economic challenges. Although the geology is favorable to REEs in Europe and Greenland, this is still not entirely the case with regard to procuring a social license to operate from European citizens.

## 1.10. Acknowledgments

This summary was the result of the ANR-11-ECOT-002 ASTER “*Analyse Systémique des rare earths–Flux et Stocks*” (Systematic Analysis of Rare Earths and Elements – Flows and Stocks) project and a collaboration with the team from the EURARE project since 2014. The authors are keen to thank the BRGM for its support, as well as Dr. Decrée, the editor of this work, for her help in reviewing this chapter.

## 1.11. References

- Abdelnour, S.A., El-Hack, M.E.A., Khafaga, A.F., Noreldin, A.E., Arif, M., Chaudhry, M.T., Losacco, C., Abdeen, A., Abdel-Daim, M.M. (2019). Impacts of rare earth elements on animal health and production: Highlights of cerium and lanthanum. *Sci. Total Environ.*, 672, 1021–1032.
- Adamson, O.J. (1944). The petrology of the Norra Kärr district: An occurrence of alkaline rocks in southern Sweden. *GFF*, 437, 113–255.
- Agard, J. (1975). Évaluation des ressources minérales françaises, les ressources en bauxite de la France. Report, BRGM, Orléans.
- Ager, D.V. (1980). *The Geology of Europe*. McGraw-Hill, Maidenhead.
- Ahonen, H., Arvanitidis, N., Auer, A., Baillet, E., Bellato, N., Binnemans, K., Blengini, G.A., Bonato, D., Brouwer, E., Brower, S. et al. (2015). Strengthening the European rare earths supply-chain. Challenges and policy options. Report, The European Rare Earths Competency Network.
- Äikäs, O. (1990). Torium-ja niobi-lantanidimalmiaiheet Vuolijoen Otanmäessä. Report, Geological Survey of Finland, Espoo.
- Al-Ani, T. and Sarapää, O. (2009). Rare earth elements and their mineral phases in Jammi carbonatite veins and fenites on the south side of Sokli carbonatite complex, NE Finland. Report, Geological Survey of Finland, Espoo.
- Al-Ani, T. and Sarapää, O. (2013). Geochemistry and mineral phases of REE in Jammi carbonatite veins and fenites, southern end of the Sokli complex, NE Finland. *Geochemistry: Exploration, Environment, Analysis*, 13, 217–224.
- Al-Ani, T., Konnunaho, K., Sarapää, O. (2011). Microprobe analysis on REE-minerals of Enontekiö (Palkiskuru and Palovaara) and Kuusamo (Hoinkilehto) hydrothermal mineralizations and Kortejärvi-Laivajoki carbonatites, Northern Finland. Report, Geological Survey of Finland, Espoo.
- Alkane Resources Ltd. (2020). Export finance Australia confirms interest in Dubbo project financing [Online]. Available at: <https://investors.alkane.com.au/site/PDF/c905578e-e9e1-4e05-9daf-0e82adeabbad/EFAConfirmInterestinDubboProjectFinancing>.
- Andersen, O. (1926). *Feltspat I Norges Geologiske Undersøkelse*. Aschehoug, Oslo.
- Andersen, T. (1986). Magmatic fluids in the Fen carbonatite complex, SE Norway: Evidence of mid-crustal fractionation from solid and fluid inclusions in apatite. *Contributions to Mineralogy and Petrology*, 93, 491–503.
- Andersen, T. (1988). Evolution of peralkaline calcite carbonatite magma in the Fen complex, southeast Norway. *Lithos*, 22, 99–112.
- Andersen, T. (1996). Sr, Nd and Pb isotopic data of the Alnö carbonatite complex. Abstract volume. *22nd Nordic Geological Winter Meeting*, Reykjavik.

- Andersen, T. (1997). Age and petrogenesis of the Qassiarsuk carbonatite-alkaline silicate volcanic complex in the Gardar rift, South Greenland. *Mineralogical Magazine*, 61, 499–513.
- Andersen, T. and Seiersten, M. (1994). Deep cumulates in a shallow intrusion: Origin and crystallization history of a pyroxenite (jacupirangite s.l.) body in the Larvik Pluton, Oslo Region, South Norway. *Neues Jb. Miner. Monat.*, 6, 255–274.
- Andersen, S., Bohse, H., Steinfeld, A. (1988). The southern part of the Ilímaussaq complex South Greenland 1:20,000. Report, Geological Survey of Greenland, Copenhagen.
- Andersen, T., Andresen, A., Sylvester, A.G. (2002). Timing of late- to post-tectonic Sveconorwegian granitic magmatism in South Norway. *Norwegian Geological Survey Bulletin*, 440, 5–18.
- Andersson, U.B. and Öhlander, B. (2004). The late Svecofennian magmatism. The Transscandinavian Igneous Belt (TIB) in Sweden. *Geological Survey of Finland, Special Papers*, 37, 102–104.
- Andersson, U.B., Holtstam, D., Broman, C. (2013). Additional data on the age and origin of the Bastnäs-type REE deposits, Sweden. Mineral deposit research for a high-tech world. *Proceedings of the 12th Biennial SGA Meeting 4*, Uppsala.
- Andersson, P., Zeuthen, J.W., Kalvig, P. (2018a). Chinese mining in Greenland: Arctic access or access to minerals? In *Arctic Yearbook 2018*, Heininen, L. and Exner-Pirot, H. (eds). Arctic Portal [Online]. Available at: <https://arcticyearbook.com/arctic-yearbook/2018>.
- Andersson, S.S., Wagner, T., Jonsson, E., Fusswinkel, T., Leijd, M., Berg, J.T. (2018b). Origin of the high-temperature Olserum-Djupedal REE-phosphate mineralization, SE Sweden: A unique contact metamorphic-hydrothermal system. *Ore Geology Reviews*, 101, 740–764.
- Armands, G. (1964). Geologiska undersökningar i Tåsjö-området under 1963 och 1964. Report, AB Atomenergi KOP-102.
- Armands, G. (1970). A uranium-bearing layer from the Lower Ordovician, Sweden. *Geologiska Föreningens i Stockholm Förhandlingar*, 92, 481–490.
- Arzamastsev, A.A., Bea, F., Arzamastseva, L.V., Montero, P. (2005). Proterozoic Gremyakha-Vyrmes polyphase massif, Kola Peninsula: An example of mixing basic and alkaline mantle melts. *Petrology*, 14, 361–389.
- Arzamastsev, A.A., Yakovenchuk, V., Pakhomovsky, Y., Ivanyuk, G. (2008). The Khibina and Lovozero alkaline massifs: Geology and unique mineralization. Field Guide Book, Geological Institute of the Russian Academy of Science, Apatity.
- Asch, K. (2003). The 1:5 million international geological map of Europe and adjacent areas: Development and implementation of a GIS-enabled concept. *Geologisches Jahrbuch*, Hannover.

- Atwood, D.A. (2012). *The Rare Earth Elements: Fundamentals and Applications. Encyclopedia of Inorganic and Bioinorganic Chemistry*. John Wiley & Sons, New York.
- Auboin, J. (1980). Geology of Europe: A synthesis. *Episodes*, 1, 3–8.
- Avannaa Resources Ltd. (2010). Karrat Rare Earth Project, West Greenland [Online]. Available at: [www.avannaa.com](http://www.avannaa.com).
- Baadsgaard, H., Chaplin, C., Griffin, W.L. (1984). Geochronology of the Gloserheia pegmatite, Froland, southern Norway. *Norsk Geol. Tidsskr*, 2, 111–119.
- Balaram, V. (2019). Geoscience frontiers rare earth elements: A review of applications, occurrence, exploration, analysis, recycling, and environmental impact. *Geoscience Frontiers*, 10, 1285–1303.
- Balomenos, E., Davris, P., Deady, E., Yang, J., Panias, D., Friedrich, B., Binnemans, K., Seisenbaeva, G., Dittrich, C., Kalvig, P. et al. (2017). The EURARE project: Development of a sustainable exploitation scheme for Europe's rare earth ore deposits. *Johnson Matthey Technol. Rev.*, 61, 142–153.
- Bao, Z. and Zhao, Z. (2008). Geochemistry of mineralization with exchangeable REY in the weathering crusts of granitic rocks in South China. *Ore Geol. Rev.*, 33, 519–535.
- Bárdossy, G. (1982). *Karst Bauxites. Bauxite Deposits on Carbonate Rocks*. Elsevier, Amsterdam.
- Bárdossy, G. and Dercourt, J. (1990). Les gisements de bauxites téthysiens (Méditerranée, Proche et Moyen-Orient) ; cadre paléogéographique et contrôles génétiques. *Bulletin de la Société Géologique de France*, 7(6), 869–888.
- Bárdossy, G. and Pantó, G. (1973). Trace mineral and element investigation on bauxites by electron probe. *3<sup>e</sup> Congrès ICSOBA*. Comité International pour l'Étude des Bauxites, de l'Alumine et de l'Aluminium, Nice.
- Bárdossy, G., Pantó, G., Várhegyi, G. (1976). Rare metals of Hungarian bauxites and conditions of their utilization. *Travaux ICSOBA*. Comité International pour l'Étude des Bauxites, de l'Alumine et de l'Aluminium.
- Bartels, A. (2013). The Gardar province. In *Geological Excursion to South Greenland. Excursion Book for the 12th Biennial SGA Meeting*, Kolb, J. (ed.). SGU, Uppsala.
- Barth, T.W.W. and Ramberg, I.B. (1966). The Fen circular complex. In *Carbonatites*, Tuttle, O.F. and Gittins, J. (eds). John Wiley and Sons, New York.
- Barton, M.D. and Johnson, D.A. (1996). Evaporitic-source model for igneous-related Fe oxide-(REE-Cu-Au-U) mineralization. *Geology*, 24, 259–262.
- Batieva, I.D. and Bel'kov, I.V. (1984). *The Sakharjok Alkaline Massif, Its Rocks and Minerals*. Kola Branch of the Academy of Sciences of the USSR, Apatity.
- Bau, M., Schmidt, K., Koschinsky, A., Hein, J., Kuhn, T., Usui, A. (2014). Discriminating between different genetic types of marine ferro-manganese crusts and nodules based on rare earth elements and yttrium. *Chemical Geology*, 381, 1–9.

- Bayanova, T.B., Kimarskii, Y.M., Levkovich, N.V. (1997). U-Pb dating of baddeleyite from rocks of the Kovdor massif. *Trans. Russ. Acad. Sci., Earth Sci. Sec.*, 356, 1094.
- Bedini, E. (2009). Mapping lithology of the Sarfartoq carbonatite complex, southern West Greenland, using HyMap imaging spectrometer data. *Remote Sensing of the Environment*, 113, 1209–1219.
- Belolipetskiy, A.P., Britvin, S.N., Voloshin, A.V., Gordienko, V.V., Zozulya, D.R., Kozyreva, L.V., Kulakov, A.N., Mets, O.F., Petrov, S.I., Subbotin, V.V. et al. (1992). *Rare Metals Mineralization of the Kola Metallogenic Province*. Kola Branch of the Academy of Sciences of the USSR, Apatity.
- Berger, A., Kokfeldt, T.F., Kolb, J. (2014). Exhumation rates in the Archean from pressure-time paths: Example from the Skjoldungen Orogen (SE Greenland). *Precambrian Research*, 255(3), 774–490.
- Bergstøl, S. (1972). The jacupirangite at Kodal, Vestfold, Norway. *Mineralium Deposita*, 7, 233–246.
- Berl, R. (1996). Lazulith in Österreich, Teil 1. Bemerkungen zu einigen Lazulithfundgebieten von Niederösterreich und Steiermark. *Der Steirische Mineralog*, 10, 5–14.
- Bernhard, F., Walter, F., Ettinger, K., Taucher, J., Mereiter, K. (1998). Pretulite, ScPO<sub>4</sub>, a new scandium mineral from the Styrian and Lower Austrian lazulite occurrences, Austria. *American Mineralogist*, 83, 625–630.
- Bingen, B., Nordgulen, Ø., Viola, G. (2008). A four phase model for the Sveconorwegian orogeny, SW Scandinavia. *Norwegian Journal of Geology*, 88, 43–72.
- Birkelund, T. and Callomon, J.H. (1985). The Kimmeridgian ammonite faunas of Milne Land, central East Greenland. *Bulletin Grønlands Geologiske Undersøgelse*, 153, 56.
- Birkelund, T., Callomon, J.H., Fürsich, F.T. (1978). The Jurassic of Milne Land, central East Greenland. *Grønlands Geologiske Undersøgelse*, 90, 99–106.
- Birkelund, T., Callomon, J.H., Fürsich, F.T. (1984). The stratigraphy of the Upper Jurassic and Lower Cretaceous sediments of Milne Land, central East Greenland. *Bulletin Grønlands Geologiske Undersøgelse*, 147, 56.
- Bizzarro, M., Simonetti, A., Stevenson, R.K., David, J. (2002). Hf isotope evidence for a hidden mantle reservoir. *Geology*, 30(9), 771–774.
- Bjørlykke, H. (1937). The granite pegmatites of southern Norway. *American Mineralogist*, 22, 241–255.
- Blaxland, A.B. (1977). Agpaitic magmatism at Norra Kärr, Rb-Sr isotopic evidence. *Lithos*, 10, 1–8.
- Blaxland, A.B., van Breemen, O., Emeleus, C.H., Anderson, J.G. (1978). Age and origin of the major syenite centers in the Gardar Province of South Greenland: Rb-Sr studies. *Geological Society of America Bulletin*, 89, 231–244.

- Blengini, G.A., Latunussa, C.E.L., Eynard, U., Torres de Matos, C., Wittmer, D., Georgitzikis, K., Pavel, C., Carrara, S., Mancini, L., Unguru, M. et al. (2020). Study on the EU's list of critical raw materials. Report, European Commission. doi: 10.2873/11619.
- Blichert-Toft, J., Rosing, M.T., Leshner, C.E., Chauvel, C. (1995). Geochemical constraints on the origin of the Late Archean Skjoldungen alkaline igneous province, SE Greenland. *Journal of Petrology*, 36, 515–561.
- Bodeving, S., Williams-Jones, A.E., SwIndian, S. (2017). Carbonate–silicate melt immiscibility, REE mineralising fluids, and the evolution of the Lofdal Intrusive Suite, Namibia. *Lithos*, 268–271, 383–398.
- Bohse, H. and Andersen, S. (1981). Review of the stratigraphic divisions of the kakortokite and lujavrite in southern Ilímaussaq. *Grønlands Geologiske Undersøgelse*, 103, 53–62.
- Bohse, H., Brooks, C.K., Kunzendorf, H. (1971). Field observations on the kakortokites of the Ilímaussaq intrusion, South Greenland, including mapping and analyses by portable X-ray fluorescence equipment for zirconium and niobium. Report, GEUS.
- Bollingberg, H., Hopgood, A.M., Kalsbeek, F. (1976). Some minor and trace elements in Archaean marbles and metamorphosed silico-carbonatites from the Fiskenaeset region. *Grønlands Geologiske Undersøgelse*, 73, 86–90.
- Bonazzi, P., Bindi, L., Parodi, G. (2003). Gatelite-(Ce), a new REE-bearing mineral from Trimouns, French Pyrenees: Crystal structure and polysomatic relationships with epidote and törnebo-hmite-(Ce). *American Mineralogist*, 88, 223–228.
- Borst, A.M., Waight, T., Smit, M., Friis, H., Nielsen, T. (2014). Alteration of eudialyte and implications for the REE, Zr and Nb resources of the layered kakortokites in the Ilímaussaq intrusion, South West Greenland. *1st European Rare Earth Resources Conference*, Milos.
- Borst, A.M., Friis, H., Andersen, T., Nielsen, T., Waight, T., Smit, A. (2016). Zirconosilicates in the kakortokites of the Ilímaussaq complex, South Greenland: Implications for fluid evolution and high-field-strength and rare-earth element mineralization in agpaitic systems. *Mineralogical Magazine*, 80, 5–30.
- Borst, A.M., Smith, M.P., Finch, A.A., Estrade, G., Villanova-de-Benavent, C., Nason, P., Marquis, E., Horsburgh, N.J., Goodenough, K.M., Xu, C. et al. (2020). Adsorption of rare earth elements in regolith-hosted clay deposits. *Nature Communications*, 11(1), 4386.
- Bottke, H. (1981). *Lagerstättenkunde des Eisens – Geochemie, Genese, Typengliederung, wirtschaftl.* Verlag Glückauf, Essen.
- Bouch, J.E., Naden, J., Shepherd, T.J., Young, B., Benham, A.J., Mckervey, J.A., Sloane, H.J. (2008). Stratabound Pb-Zn-Ba-F mineralization in the Alston Block of the North Pennine Ore-field (England) – Origins and emplacement. Report, British Geological Survey.
- Brandenberger, E. (1931). Die Kristallstruktur von Koppit, *Zeitsch. Krist.*, 76, 322–334.

- Brooks, C.K. and Nielsen, T.F.D. (1982). The Phanerozoic development of the Kangerdlugssuaq area, East Greenland. *Meddelelser om Grønland Geoscience*, 9, 31.
- Brown, G.M. (1963). The Skye granites. *Mineralogical Magazine*, 33, 533–562.
- Browne, A. (2008). Report on current resource estimates for Kläppicäcken and Duobblon uranium properties, and review of Tåsjö uranium project, northern Sweden. Report, Mawson Resources.
- Bru, K., Christmann, P., Labbé, J.F., Lefebvre, G. (2015). Panorama mondial 2014 du marché des terres rares. Report, BRGM RP-64330-FR.
- Brueckner, H.K. and Rex, D.C. (1980). K-Ar and Rb-Sr geochronology and Sr isotopic study of the Alnö alkaline complex, northeastern Sweden. *Lithos*, 13, 111–119.
- Bühn, B., Rankin, A.H., Schneider, J., Dulski, P. (2002). The nature of orthomagmatic, carbonatitic fluids precipitating REE, Sr-rich fluorite: Fluid-inclusion evidence from the Okorusu fluorite deposit, Namibia. *Chemical Geology*, 186(1), 75–98.
- Burnotte, E., Pirard, E., Michel, G. (1989). Genesis of grey monazites: Evidence from the Palaeozoic of Belgium. *Economic Geology*, 84, 1417–1429.
- Calderón, S. (1910). *Los Minerales de España*. Eduardo Anas, Madrid.
- Callisen, K. (1943). Igneous rocks of the Ivigtut region, Greenland. Part 1: The nepheline syenites of the Grønnedal-Ika area. *Meddelelser om Grønland*, 131(8), 74.
- Campbell, L.S., Henderson, P., Wall, F., Nielsen, T.F. (1997). Rare earth chemistry of perovskite group minerals from the Gardiner Complex, East Greenland. *Mineralogical Magazine*, 61, 197–212.
- Cann, J.R. and Banks, D.A. (2001). Constraints on the genesis of the mineralization of the Alston Block, Northern Pennine Orefield, northern England. *Proceedings of the Yorkshire Geological Society*, 53, 187–196.
- Carlborg, H. (1923). Ekonomisk-teknisk beskrivning. In *Riddarhytte malmfält i Skinnkattebergs socken i Västmanlands län*. Kungl. Kommerskollegium and Sveriges Geologiska Undersökning. Victor Pettersson, Stockholm.
- Castor, S.B. and Hedrick, J.B. (2006). Rare earth elements. In *Industrial Minerals and Rocks*, Kogel, J.E., Trivedi, N.C., Barker, J.M., Krukowski, S.T. (eds). Society for Mining, Metallurgy and Exploration, Englewood.
- Černý, P. and Ercit, T.S. (2005). The classification of granitic pegmatites revisited. *Canadian Mineralogist*, 43, 2005–2026.
- Chakhmouradian, A.R. and Wall, F. (2012a). Rare earth elements: Minerals, mines, magnets (and more). *Elements*, 8, 333–340.
- Chakhmouradian, A.R. and Zaitsev, A.N. (2012b). Rare earth mineralization in igneous rocks: Sources and processes. *Elements*, 8, 347–353.

- Charles, N., Tuduri, J., Guyonnet, D., Melleton, J., Pourret, O. (2013). Rare earth elements in Europe and Greenland: A geological potential? An overview. *Proceedings of the 12th Biennial SGA Meeting*, Uppsala.
- Chi, R. and Tian, T. (2008). *Weathered Crust Elution-deposited Rare Earth Ores*. Nova Science Publishers Inc., New York.
- Choubert, G. and Faure-Muret, A. (1976). Sheet 9 Europe. Scale 1:10,000,000. With explanatory notes by G. Luetting and F. Delany. Report, Geological Atlas of the World, UNESCO and Commission for the Geological Map of the World.
- Christensson, U. (2013). Characterising the alteration of the contact to the Norra Kärr alkaline complex, southern Sweden. BA Thesis, University of Gothenburg.
- Clausen, S. and Alvaro, J.J. (2007). Lower Cambrian shelled phosphorites from the northern Montagne Noire, France. *Geological Society of London*, 275, 17–28.
- Cliff, R.A., Rickard, D., Blake, K. (1990). Isotope systematics of the Kiruna magnetite ores, Sweden. Part 1: Age of the ore. *Economic Geology*, 85, 1770–1776.
- Cloethingh, S., van Wees, J.D., Ziegler, P.A., Lenkey, L., Beekman, F., Tesauro, M., Förster, A., Norden, B., Kaban, M., Hardebol, N. et al. (2010). Lithosphere tectonics and thermo-mechanical properties: An integrated modeling approach for enhanced geothermal systems exploration in Europe. *Earth-Science Reviews*, 102, 159–206.
- Cockburn, A.M. (1935). The geology of St Kilda. *Trans. Roy. Soc. Edinburgh*, 58, 511–547.
- Cooper, D.C., Bashan, I.R., Smith, T.K. (1983). On the occurrence of an unusual form of monazite in panned stream sediments in Wales. *Geological Journal*, 18, 121–127.
- Cooper, D.C., Rollin, K., Howells, M.F., Morgan, D.J. (1984). Regional geochemical and geophysical surveys in the Berwyn dome and adjacent areas, North Wales. Mineral Reconnaissance Programme Report, British Geological Survey.
- Coppin, F., Berger, G., Bauer, A., Castet, S., Loubet, M. (2002). Sorption of lanthanides on smectite and kaolinite. *Chemical Geology*, 182(1), 57–68.
- Cornelius, H.P. (1931). Neue Lazulithfunde im Mürzthal. *Verhandlungen der Geologischen Bundesanstalt*, 4, 93–94.
- Cornet, A. and Sapinart, J. (1967). Monazite à europium armoricaine. Travaux préliminaires au test d'exploitation envisagé à La Monnerie, sur le ruisseau d'Aron (Ille-et-Vilaine). Report, BRGM, DRMM-67, A-8.
- Dahlgren, S. (2005). Miljøgeologisk undersøkelse av lavradioaktivt slagg fra ferroniobproduksjon ved Norsk bergverk på Søve 1956-1965. Report, Regiongeologen.
- Dahlgren, S., Corfu, F., Heaman, L.M. (1996). U-Pb isotopic time constraints, and Hf and Pb source characteristics of the Larvik plutonic complex, Oslo palaeorift. Geodynamic and geochemical implications for the rift evolution. *Journal of Conference Abstracts*, 1, 120.

- Damtoft, J.S. and Grahl-Madsen, L. (1982). Geological and VLF geophysical mapping of the Bredhorn Ba-Pb prospect and preliminary mapping on SE Traill Ø for porphyry molybdenum mineralisation. Internal NM report 2/81.
- Deady, E.A., Mouchos, E., Goodenough, K., Williamson, B.J., Wall, F. (2016). A review of the potential for rare-earth element resources from European red muds: Examples from Seydişehir, Turkey and Parnassus-Giona, Greece. *Mineralogical Magazine*, 80, 43–61.
- Debrand-Passard, S., Courbouleix, S., Lienhardt, M.J. (1984). Synthèse géologique du sud-est de la France. Report, BRGM.
- Decrée, S., Ihlen, P.M., Schiellerup, H., Hallberg, A., Demetriades, A., Raha, M., Soesoo, A. (2017). Potential of phosphate deposits in Europe. *SGA News*, 41, 1–20.
- Decrée, S., Savolainen, M., Mercadier, J., Debaille, V., Höhne, S., Frimmel, H., Baele, J.M. (2020). Geochemical and spectroscopic investigation of apatite in the Siilinjärvi carbonatite complex: Keys to understanding apatite forming processes and assessing potential for rare earth elements. *Applied Geochemistry*, 123, 104778.
- Dickin, A.P., Mootbath, S., Welke, H.J. (1981). Isotope, trace element and major element geochemistry of tertiary igneous rocks. *Royal Society of Edinburgh Transactions*, 72, 159–170.
- Dietzel, C.A.F., Kristandt, T., Dahlgren, S., Giebel, R.J., Marks, M.A.W., Wenzel, T., Markl, G. (2019). Hydrothermal processes in the Fen alkaline-carbonatite complex, southern Norway. *Ore Geology Reviews*, 111, 102969.
- Donnot, M., Guiges, J., Lulzac, Y., Magnien, A., Parfenoff, A., Picot, P. (1973). Un nouveau type de gisement d'Europium : la monazite grise à europium en nodules dans les schistes paléozoïques de Bretagne. *Mineralium Deposita*, 8, 7–18.
- Druecker, M. and Simpson, R.G. (2012). Technical report on the Sarfartoq project, West Greenland. Hudson Resources Inc.
- Dushyantha, N., Batapola, N., Ilankoon, I., Rohitha, S., Premasiri, R., Abeyasinghe, B., Ratnayake, N., Dissanayake, K. (2020). The story of rare earth elements (REEs): Occurrences, global distribution, genesis, geology, mineralogy and global production. *Ore Geology Reviews*, 122, 103521.
- Eilu, P., Hallberg, A., Bergman, T., Bjerkgård, T., Feoktistov, V., Korsakova, M., Krasotkin, S., Lampio, E., Litvinenko, V., Philippov, N. et al. (2013). Fennoscandian ore deposit database. Annual update [Online]. Available at: <http://en.gtk.fi/informationsservices/databases/fodd/Indiiax.html>.
- Elderfield, H., Upstill-Goddard, R., Sholkovitz, E.R. (1990). The rare earth elements in rivers, estuaries, and coastal seas and their significance to the composition of ocean waters. *Geochimica et Cosmochimica Acta*, 54(4), 971–991.
- Eliseev, N.A. and Fedorov, E.E. (1953). Lovozero pluton and related ore deposits. *Transactions of Laboratory of Precambrian Rocks*, 1, 308.

- Emeleus, C.H. (1964). The Grønnedal-Ika alkaline complex, South Greenland. The structure and geological history of the complex. *Meddelelser om Grønland*, 172, 1–75.
- Emeleus, C.H. and Gyopari, M.C. (1992). *British Tertiary Volcanic Province*. Chapman and Hall, London.
- Emeleus, C.H. and Harry, W.T. (1970). The Igaliko nepheline syenite complex. General description. *Grønlands Geologiske Undersøgelse*, 85, 116.
- Emeleus, C.H. and Upton, B.G.J. (1976). The Gardar period in southern Greenland. In *Geology of Greenland*, Escher, A. and Watt, W.S. (eds). Grønlands Geologiske Undersøgelse, Copenhagen.
- Emsbo, P., McLaughlin, P.I., Breit, G.N., du Bray, E.A., Koenig, A.E. (2015). Rare earth elements in sedimentary phosphate deposits: Solution to the global REE crisis? *Gondwana Research*, 27, 776–785.
- EURARE (2017). Development of a sustainable exploitation scheme for Europe's rare earth ore deposits [Online]. Available at: <http://eurare.brgm-rec.fr/>
- European Commission (2011). Tackling the challenges in commodity and markets and on raw materials. Communication from the Commission to the European Parliament, the European Council, The Council, The European Economic and Social Committee of the Regions, Brussels.
- European Commission (2017). The 2017 list of critical raw materials for the EU. Communication from the Commission to the European Parliament, the European Council, The Council, The European Economic and Social Committee of the Regions, Brussels.
- European Commission (2019a). The European Green Deal. Communication from the Commission to the European Parliament, the European Council, The Council, The European Economic and Social Committee of the Regions, Brussels.
- European Commission (2019b). Masterplan for a competitive transformation of EU energy-intensive industries enabling a climate-neutral, circular economy by 2050. Report, High-Level Group on Energy-Intensive Industries. doi: 10.2873/854920.
- Evans, A.M. (2000). *Ore Geology and Industrial Minerals – An Introduction*. Blackwell Science, Oxford.
- Evans, J. and Zalasiewicz, J. (1996). U/Pb, Pb/Pb and Sm/Nd dating of authigenic monazite: Implications for the diagenetic evolution of the Welsh Basin. *Earth and Planetary Science Letters*, 144(3), 421–433.
- Exley, R.A. (1980). Microprobe studies of REE-rich accessory minerals: Implications for Skye granite petrogenesis and REE mobility in hydrothermal systems. *Earth and Planetary Science Letters*, 48, 97–110.
- Farrow, C. (1974). The geology of the Skjerstad area, Nordland, North Norway. PhD Thesis, University of Bristol.

- Faul, H., Elmore, P.L.D., Brannock, W.W. (1959). Age of the Fen carbonatite (Norway) and its relation to the intrusives of the Oslo region. *Geochim. Cosmochim. Acta*, 17, 153–156.
- Favreau, G. (1994). Trimouns, Ariège, Frankreich: Seltenerden-mineralien aus dem Dolomit. *Lapis*, 12(94), 18–39.
- Fedele, L., Plant, A.J., De Vivo, B., Lima, A. (2008). The REE distribution over Europe: Geogenic and anthropogenic sources. *Geochemistry: Exploration, Environment, Analysis*, 8, 3–18.
- Ferguson, J. (1964). Geology of the Ilímaussaq alkaline intrusion, South Greenland: Description of map and structure. *Meddelelser om Grønland*, 172, 1–82.
- Ferrero, A., Ruíz, J., Vidal, A. (1989). Investigation about rare earths in north-west peninsular. Galicia (España). *Cuaderno Lab. Xeolóxico de Laxe*, 14, 255–270.
- Finger, F., Roberts, M.P., Haunschmid, B., Schermaier, A., Steyrer, H.P. (1997). Variscan granitoids of central Europe: Their typology, potential sources and tectonothermal relations. *Mineral. Petrol.*, 61, 67–96.
- Fitton, J.G. and Upton, B.G. (1987). Alkaline igneous rocks. *Geological Society of London*, 30.
- Floor, P., Corretgé, G., Montero, P. (2007). The Ordovician Galiñeiro peralkaline gneiss complex, Vigo, NW Spain. *Goldschmidt Conference Abstracts*, A286.
- Foley, S.F. and Fischer, T.P. (2017). An essential role for continental rifts and lithosphere in the deep carbon cycle. *Nature Geoscience*, 10(12), 897–902.
- Foley, S.F., Venturelli, G., Green, D.H., Toscani, L. (1987). The ultrapotassic rocks: Characteristics, classification, and constraints for petrogenetic models. *Earth Science Review*, 24, 81–134.
- Fortuné, J.P. (1971). Contribution à l'étude minéralogique et génétique des talcs pyrénéens. PhD Thesis, Université Paul Sabatier, Toulouse.
- Fortuné, J.P., Gavoille, B., Thiébaud, J. (1980). Le gisement de talc de Trimouns près de Luzenac (Ariège). *26th International Geological Conference*, Paris.
- Frei, D., Hollis, J.A., Gerdes, A., Karlsson, C., Vasquez, P., Franz, G., Harlov, D., Johansson, L., Knudsen, C. (2006). Advanced in situ trace element and geochronological microanalysis of geomaterials by laser ablation techniques. *Geological Survey of Denmark and Greenland Bulletin*, 10, 25–28.
- Freslon, N., Bayon, G., Toucanne, S., Bermell, S., Bollinger, C., Chéron, S., Etoubleau, J., Germain, Y., Khripounoff, A., Ponzevera, E. et al. (2014). Rare earth elements and neodymium isotopes in sedimentary organic matter. *Geochimica et Cosmochimica Acta*, 140, 177–198.
- Freyssinet, P., Butt, C.R.M., Morris, R.C., Piantone, P. (2005). Ore-forming processes related to lateritic weathering. In *Economic Geology 100th Anniversary Volume*, Hedenquist, J.W., Thompson, J.F.H., Goldfarb, R.J., Richards, J.P. (eds). Society of Economic Geologists Inc., Littleton.

- Frietsch, R. (1977). The iron ore deposits in Sweden. In *The Iron Ore Deposits of Europe and Adjacent Areas. Explanatory Note to the International Map of Iron Ore Deposits of Europe*, Zitzrnau, A. (ed.). BGR, Hanover.
- Frietsch, R. and Perdahl, J.A. (1995). Rare earth elements in apatite and magnetite in Kiruna-type iron ores and some other iron ore types. *Ore Geology Reviews*, 9, 489–510.
- Frietsch, R., Tuisku, P., Martinsson, O., Perdahl, J.A. (1997). Early Proterozoic Cu-(Au) and Fe ore deposits associated with regional Na-Cl metasomatism in northern Fennoscandia. *Ore Geology Reviews*, 12, 1–34.
- Frisch, W. and Keusen, H. (1977). The Gardiner intrusion, an ultramafic complex at Kangerdlugssuaq, East Greenland. *Grønlands Geologiske Undersøgelse Bulletin*, 122, 62.
- Gamaletsos, P.N., Godelitsas, A., Kasama, T., Church, N.S., Douvalis, A.P., Göttlicher, J., Steininger, R., Boubnov, A., Pontikes, Y., Tzamos, E. et al. (2017). Nano-mineralogy and geochemistry of high-grade diasporic karst-type bauxite from Parnassos-Ghiona mines, Greece. *Ore Geology Reviews*, 84, 228–244.
- Gamaletsos, P.N., Godelitsas, A., Filippidis, A., Pontikes, Y. (2019). The rare earth elements potential of Greek bauxite active mines in the light of a sustainable REE demand. *Journal of Sustainable Metallurgy*, 5(1), 20–47.
- Garde, A.A. (1978). *The Lower Proterozoic Marmorilik Formation, East of Marmorilik, West Greenland. Meddelelser om Grønland 200*. Busck, København.
- Gates, P.E., Horlacher, C.F., Reed, G. (2012). Preliminary economic assessment NI43-101 technical report for the Norra Kärr (REE -Y-Zr) deposit, Gränna, Sweden. Report, Runge Pincock Minarco, prepared for Tasman Metals Ltd., Gränna.
- Gates, P.E., Horlacher, C.F., Reed, G. (2013). Amended and restated preliminary economic assessment NI43-101 technical report for the Norra Kärr (REE-Y-Zr) deposit, Gränna, Sweden. Report, Runge Pincock Minarco, prepared for Tasman Metals Ltd., Gränna.
- Gee, D.G., Fossen, H., Henriksen, N., Higgins, A.K. (2008). From the early Paleozoic platforms of Baltica and Laurentia to the Caledonide orogen of Scandinavia and Greenland. *Episodes*, 31, 44–51.
- Geijer, P. (1931). The iron ores of the Kiruna type. *Sveriges Geol. Unders.*, 367, 1–39.
- Geijer, P. (1961). The geological significance of the cerium mineral occurrences of the Bastnäs-type in central Sweden. *Arkiv Mineral. Geol.*, 3, 99–105.
- Geijer, P. and Ödman, O.H. (1974). The emplacement of Kiruna iron ores and related deposits. *Sver. Geol. Unders.*, 700, 1–48.
- Gerasimovsky, V.I., Volkov, V.P., Kogarko, L.N., Polyakov, A.I., Balashov, U. (1966). *Geochemistry of Lovozero Alkaline Massif. Part 1: Geology and Petrology. Part 2: Geochemistry*. Australian National University Press, Canberra.
- GEUS, Bureau of Minerals and Petroleum (2010). Map of Greenland geology and selected mineral occurrences [Online]. Available at: <http://geus.dk/geuspage-uk.htm>.

- GEUS, Bureau of Minerals and Petroleum (2014). Greenland mineral resources portal [Online]. Available at: <http://geus.dk/geuspage-uk.htm>.
- Geyti, A. (1979). Drilling and mapping in the EGMO concession area. Report, Nordisk Minselskab Prospecting.
- Gislev, M. and Grohol, M. (2018). Report on critical raw materials and the circular economy. Report, Publications Office of the European Union. doi: 10.2873/331561.
- GME (2012). Kvanefjeld concentrator pilot plant campaign complete; results exceed expectations. Report, Company Announcement.
- GME (2014). EURARE project update: Kvanefjeld bulk ore sample selected for demonstration plant operations. Report, Company Announcement.
- Goliáš, V. (2001). Thorium occurrences in the Czech Republic and their mineralogy. In *Uranium Deposits*, Kribek, B. and Zeman, J. (eds). Czech Geological Survey, Brno.
- Goodenough, K.M., Schilling, J., Jonsson, E., Kalvig, P., Charles, N., Tuduri, J., Deady, E.A., Sadeghi, M., Schiellerup, H., Müller, A. et al. (2016). Europe's rare earth element resource potential: An overview of REE metallogenetic provinces and their geodynamic setting. *Ore Geol. Rev.*, 72, 838–856.
- Gothenborg, J. and Pedersen, J.L. (1976). Exploration of the Qaqarssuk carbonatite complex. 1975. Part II. Internal report, Kryolitselskabet Øresund A/S, 1 plate. Geological Survey of Denmark and Greenland.
- Green, D. and McCallum, D. (2005). Kainosite-(Y) from the Strontian Mines, Highland region, Scotland. *UK Journal of Mines and Minerals*, 26, 23–26.
- Green, D. and Wallace, M.E. (1988). Mantle metasomatism by ephemeral carbonatite melts. *Nature*, 336(6198), 459–462.
- Green, D., Bell, R., Moreton, S. (2005). Drusy cavity minerals including the first Irish danalite from Lindsay's Leap, Mourne Mountains. *UK Journal of Mines and Minerals*, 25, 25–30.
- Grew, E.S., Essene, E.J., Peacor, D.R., Su, S.C., Asami, M. (1991). Dissakisite-(Ce), a new member of the epidote group and the Mg analogue of allanite-(Ce), from Antarctica. *American Mineralogist*, 76, 1990–1997.
- Grice, J.D., Gault, R.A., Rowe, R., Johnsen, O. (2006). Qaqarssukite-(Ce), a new barium-cerium fluorocarbonate mineral species from Qaqarssuk, Greenland. *Canadian Mineralogist*, 44, 1137–1146.
- Gupta, C.K. and Krishnamurthy, N. (2005). *Extractive Metallurgy of Rare Earths*. CRC Press, Boca Raton.
- Gustafsson, B. (1979). Uranuppslag inom Norrbotten och Västerbotten. Report, Sveriges Geologiska Undersökning.

- Guyonnet, D., Planchon, M., Rollat, A., Escalon, V., Tuduri, J., Charles, N., Vaxelaire, S., Dubois, D., Fargier, H. (2015). Material flow analysis applied to rare earth elements in Europe. *J. Clean. Prod.*, 107, 215–228.
- Gysi, A.P., Williams-Jones, A.E., Collins, P. (2016). Lithogeochemical vectors for hydrothermal processes in the Strange Lake peralkaline granitic REE-Zr-Nb deposit. *Economic Geology*, 111(5), 1241–1276.
- Halama, R., Venneman, T., Siebel, W., Markl, G. (2005). The Grønnedal-Ika carbonatite-syenite complex, South Greenland: Carbonatite formation by liquid immiscibility. *Journal of Petrology*, 46, 191–217.
- Hallberg, A. (2003). Styles of hydrothermal alteration and accompanying chemical changes in the Sängen formation, Bergslagen, Sweden, and adjacent areas. *Economic Geology Research and Documentation* 2, 2001–2002. *Sver. Geol. Undersök.*, 113, 4–35.
- Halliday, A.N., Aftalion, M., Parsons, I., Dickin, A.P., Johnson, M.R.W. (1987). Syn-orogenic alkaline magmatism and its relation to the Moine thrust zone and the thermal state of the lithosphere in NW Scotland. *Journal of the Geological Society of London*, 144, 611–618.
- Hamilton, M.A., Pearson, D.G., Thompson, R.N., Kelley, S.P., Emeleus, C.H. (1999). Rapid eruption of Skye lavas inferred from precise U/Pb and Ar/Ar dating of the Rum and Cuillin plutonic complexes. *Nature*, 394, 260–263.
- Hammouda, T. and Keshav, S. (2015). Melting in the mantle in the presence of carbon: Review of experiments and discussion on the origin of carbonatites. *Chem. Geol.*, 418, 171–188.
- Harding, R.R. (1966). The major ultrabasic and basic intrusions of St Kilda, Outer Hebrides. *Transactions of the Royal Society of Edinburgh*, 66, 419–444.
- Harding, R.R., Merriman, R.J., Nancarrow, P.H.A. (1982). A note on the occurrence of chevkinite, allanite, and zirkelite on St. Kilda, Scotland. *Mineralogical Magazine*, 46, 445–448.
- Harding, R.R., Merriman, R.J., Nancarrow, P.H.A. (1984). St. Kilda: An illustrated account of the geology. Report, British Geological Survey.
- Harker, A. (1904). *The Tertiary Igneous Rocks of Skye*. Arkose Press, Hawthorne.
- Harlov, D.E., Andersson, U.B., Foerster, H., Nystrom, J.O., Dulski, P., Broman, C. (2002). Apatite-monazite relations in the Kiirunavaara magnetite-apatite ore, northern Sweden. *Chemical Geology*, 191, 47–72.
- Harpøth, O., Pedersen, J.L., Schönwandt, H.K., Thomassen, B. (1986). The mineral occurrences of central East Greenland. *Meddelelser om Grønland Geoscience*, 17, 138.
- Hedrick, J.B. (1985). Rare earth minerals and metals. Minerals yearbook. *Geological Survey*, 1, 791–803.

- Hedrick, J.B. and Templeton, D.A. (1991). Rare-earth minerals and metals. Minerals yearbook. *Geological Survey*, 825–844.
- Hedrick, J.B., Sinha, S.P., Kosynkin, V.D. (1997). Loparite, a rare earth ore (Ce, Na, Sr, Ca) (Ti, Nb, Ta, Fe<sup>3+</sup>)O<sub>3</sub>. *Journal of Alloys and Compounds*, 250, 467–470.
- Henderson, P. (1984). *Rare Earth Element Geochemistry. Developments in Geochemistry 2*. Elsevier, Amsterdam.
- Henderson, I.H.C. and Ihlen, P.M. (2004). Emplacement of polygeneration pegmatites in relation to Sveco-Norwegian contractional tectonics: Examples from southern Norway. *Precambrian Research*, 133, 207–222.
- Henderson, G. and Pulvertaft, T.C.R. (1987). Descriptive text to the geological map of Greenland, 1:100,000, Marmorilik 71 V.2 Syd, Nûgâtsiaq 71 V.2 Nord, Pangnertôq 72 V.2 Syd. GEUS, Copenhagen.
- Henriksen, N., Higgins, A.K., Kalsbeek, F. (2009). Greenland from Archaean to Quaternary. Descriptive text to the 1995 geological map of Greenland, scale 1:2,500,000. *Geological Survey of Denmark and Greenland Bulletin*, 18.
- Himmi, R. (1975). Outokumpu Oy:n Korsnäsän ja Petolahden kaivosten vaiheita. *Vuoriteollisuus-Bergshanteringen*, 33, 35–38.
- Hitzman, M.W., Oreskes, N., Einaudi, M.T. (1992). Geological characteristics and tectonic setting of Paleoproterozoic iron oxide (Cu-U-Au-REE) deposits. *Precambrian Research*, 58, 241–287.
- Hode Vuorinen, J. and Hålenius, U. (2005). Nb-, Zr- and LREE-rich titanite from the Alnö alkaline complex: Crystal chemistry and its importance as a petrogenetic indicator. *Lithos*, 83, 128–142.
- Högdahl, K., Andersson, U.B., Eklund, O. (2004). The Transscandinavian Igneous Belt (TIB) in Sweden: A review of its character and evolution. *Geological Survey of Finland*, 37, 123.
- Holtstam, D. (2004). The Bastnäs-type REE deposits. In *The Bastnäs-type REE-mineralizations in North-western Bergslagen, Sweden – A Summary with Geological Background and Excursion Guide*, Andersson, U.B. (ed.). Sveriges geologiska undersökning, Uppsala.
- Holtstam, D. and Andersson, U.B. (2007). The REE minerals of the Bastnäs-type deposits, south-central Sweden. *The Canadian Mineralogist*, 45, 1073–1114.
- Hornig-Kjarsgaard, I. (1998). Rare earth elements in sövitic carbonatites and their mineral phases. *Journal of Petrology*, 39, 2105–2121.
- Hugg, R. (1985). Katajakangas. Geologinen malmiarvio. Report, Rautaruukki Oy Malminetsintä.
- Hugg, R. and Heiskanen, V. (1986). Otanmäen alueen niobi-lantaniditkimukset, tilanne 31.12.1985 (Lisäys 15.5.1986 L. Pekkarinen). Report, Rautaruukki Oy Malminetsintä.

- Hyslop, E.K., Gillanders, R.J., Hill, P.G., Fakes, R.D. (1999). Rare-earth bearing minerals fergusonite and gadolinite from the Arran granite. *Scottish Journal of Geology*, 35, 65–69.
- IGE Nordic AB (2007). The rare earth deposit of Olserum. Report, Sweden Internal.
- IGM (1998). Mineral potential of Portugal [Online]. Available at: [http://www.lneg.pt/CienciaParaTodos/edicoes\\_online/diversos/potential](http://www.lneg.pt/CienciaParaTodos/edicoes_online/diversos/potential).
- Ihlen, P., Schiellerup, H., Gautneb, H., Skar, O. (2013). Characterization of apatite resources in Norway and their REE potential – A review. *Ore Geology Reviews*. doi: 10.1016/j.oregeorev.2013.11.003.
- Inverno, C., Oliveira, D., Viegas, L., Lencastre, J., Salgueiro, R. (1998). REE-enriched Ordovician quartzites in Vale de Cavalos, Portalegre, Portugal. *Proceedings Volume of GeoCongress'98, Pretoria*. Geological Society of South Africa, Johannesburg.
- Inverno, C., Oliveira, D., Rodrigues, L. (2007). Inventariação e prospecção de terras raras nas regiões fronteiriças da Beira Baixa e do Norte Alentejo. Report, INETI, Alfragide.
- Isokangas, P. (1975). The mineral deposits in Finland. PhD Thesis, University of Helsinki.
- Ixer, R.A., Young, B., Stanley, C.J. (1996). Bismuth-bearing assemblages from the Northern Pennine Orefield. *Min. Mag.*, 60, 317–324.
- Jacquemin, D. (2020). The Phosphatic chalk of the Mons Basin, Belgium. Petrography and geo-chemistry of the Cibly Phosphatic Chalk and implications on its genesis. *Memoirs of the Geological Survey of Belgium*, 64, 46.
- Jia, Y.-H. and Liu, Y. (2020). REE enrichment during magmatic–hydrothermal processes in carbonatite-related REE deposits: A case study of the Weishan REE deposit, China. *Minerals*, 10(1), 25.
- Johnsen, O. and Grice, J.D. (1999). The crystal chemistry of the eudialyte group. *Canadian Mineralogist*, 37, 865–891.
- Johnsen, O., Petersen, O.V., Medenbach, O. (1985). The Gardiner complex, a new locality in Greenland. *Mineral. Record*, 16, 485–494.
- Johnsen, O., Grice, J.D., Gault, R.A. (2001). The eudialyte group: A review. In *The Ilímaussaq Complex, South Greenland: Status of Mineralogical Research with New Results*, Sørensen, H. (ed.). Geology of Greenland Survey Bulletin, Copenhagen.
- Jones, A.P., Wall, F., Williams, C.T. (1996). *Rare Earth Minerals: Chemistry, Origin and Ore Deposits*. Chapman & Hall, London.
- Josso, P., Pelleter, E., Pourret, O., Fouquet, Y., Etoubleau, J., Cheron, S., Bollinger, C. (2017). A new discrimination scheme for oceanic ferromanganese deposits using high field strength and rare earth elements. *Ore Geology Reviews*, 87, 3–15.
- Judge, W.D., Xiao, Z.W., Kipouros, G.J. (2017). Application of rare earths for higher efficiencies in energy conversion. In *Rare Metal Technology 2017*, Kim, H., Alam, S., Neelameggham, N.R., Oosterhof, H., Ouchi, T., Guan, X. (eds). Springer, Berlin.

- Juteau, T., Noack, Y., Whitechurch, H., Courtois, C. (1979). Mineralogy and geochemistry of alteration products in Holes 417A and 417D basement samples (Deep Sea Drilling Project Leg 51). In *Initial Reports of the Deep Sea Drilling Project*, Donnelly, T., Francheteau, J., Bryan, W., Robinson, P., Flower, M., Salisbury, M. (eds). U.S. Government Printing Office, Washington.
- Kalashnikov, A.O., Konopleva, N.G., Pakhomovsky, Y.A., Ivanyuk, G.Y. (2016). Rare earth deposits of the Murmansk Region, Russia – A review. *Economic Geology*, 111(7), 1529–1559.
- Kalatha, S., Perraki, M., Economou-Eliopoulos, M., Mitsis, I. (2017). On the origin of Bastnaesite-(La,Nd,Y) in the Nissi (Patitira) Bauxite Laterite deposit, Lokris, Greece. *Minerals*, 7(3), 19.
- Kalsbeek, F., Pulvertaft, T.C.R., Nutman, A.P. (1998). Geochemistry, age and origin of metagrey-wackes from the Palaeoproterozoic Karrat Group, Rinkian belt, West Greenland. *Precambrian Research*, 91, 383–399.
- Kärenlampi, K., Kontinen, A., Hanski, E., Huhma, H., Lahaye, Y., Krause, J., Heinig, T. (2020). Age and origin of the Nb-Zr-REE mineralization in the Paleoproterozoic A1-type granitoids at Otanmäki, central Finland. *Bulletin of the Geological Society of Finland*, 92(1), 39–71.
- Kärkkäinen, N. and Huhta, P. (1993). Korsnäsin lyijypitoisten kalkkilohkareiden selvitys v. 1989-1990. *Geological Survey of Finland*, Report no. 3577, 23.
- Kato, Y., Fujinaga, K., Nakamura, K., Takaya, Y., Kitamura, K., Ohta, J., Toda, R., Nakashima, T., Iwamori, H. (2011). Deep-sea mud in the Pacific Ocean as a potential resource for rare-earth elements. *Nature Geoscience*, 4(8), 535–539.
- Keller, J. (1981). Carbonatitic volcanism in the Kaiserstuhl alkaline complex: Evidence for highly fluid carbonatitic melts at the earth's surface. *Journal of Volcanology and Geothermal Research*, 9, 423–431.
- Keller, J. and Krafft, M. (1990). Effusive natrocarbonatite activity of Oldoinyo Lengai, June 1988. *Bulletin of Volcanology*, 52(8), 629–645.
- Kimbell, G.S., Young, B., Millward, D., Crowley, Q.G. (2010). The North Pennine batholith (Wear-dale Granite) of northern England: New data on its age and form. *Proceedings of the Yorkshire Geological Society*, 58, 107–128.
- Kirchheimer, F. (1957). *Bericht über das Vorkommen von Uran in Baden Württemberg*. Abh. des Geol. Land, Baden-Württemberg.
- Kjarsgaard, B.A. and Hamilton, D.L. (1989). The genesis of carbonatites by immiscibility. In *Genesis and Evolution Carbonatites*, Bell, K. (ed.). Unwin-Hyman, London.
- Kjarsgaard, B.A., Hamilton, D.L., Peterson, T.D. (1995). Peralkaline nephelinite/carbonatite liquid immiscibility: Comparison of phase compositions in experiments and natural lavas from Ol-doinyo Lengai. In *Carbonatite Volcanism: Oldoinyo Lengai and the Petrogenesis of Natrocarbonatites*, Bell, K. and Keller, J. (eds). Springer, Berlin.

- Kleinhanns, I.C., Fischer-Gödde, M., Hansen, B.T. (2012). Sr-Nd isotope and geochemical characterisation of the paleoproterozoic Västervik formation (Baltic Shield, SE Sweden): A southerly exposure of Svecofennian meta-siliciclastic sediments. *International Journal of Earth Sciences*, 101, 39–55.
- Knudsen, C. (1989). Pyrochlore group minerals from the Qaqarssuk carbonatite complex. In *Lanthanides, Tantalum and Niobium*, Saupé, F. (ed.). Springer-Verlag, Berlin.
- Knudsen, C. (1991). Petrology, geochemistry and economic geology of the Qaqarssuk carbonatite complex, southern West Greenland. *Monograph Series on Mineral Deposits*, 29, 110.
- Knudsen, C. and Buchardt, B. (1991). Carbon and oxygen isotope composition of carbonates from the Qaqarssuk carbonatite complex, southern West Greenland. *Chemical Geology*, 86, 263–274.
- Kogarko, L.N. (1987). Alkaline rocks of the eastern part of the Baltic Shield (Kola Peninsula). In *Alkaline Igneous Rocks*, Fitton, J.G. and Upton, B.G.J (eds). Geological Society Publications, London.
- Kogarko, L.N., Kononova, V.A., Orlova, M.P., Woolley, A.R. (1995). *Alkaline Rocks and Carbonatites of the World. Part 2: Former USSR*. Chapman and Hall, London.
- Kolb, J., Thrane, K., Bagas, L. (2013). Field relationship of high-grade Neo- to Mesoarchean rocks of South East Greenland: Tectonometamorphic and magmatic evolution. *Gondwana Research*, 23, 471–492.
- Kontio, M. and Pankka, H. (2006). Tutkimustyöselostus Savukosken kunnassa valtausalueella Jammi 1, kaiv. rek. nro 7819/1 tehdyistä malmitutkimuksista 2004-2005. Report, Geological Survey of Finland, M06/4723/2006/1/10.
- Korneliusson, A., McEnroe, S.A., Nilsson, L.P., Schiellerup, H., Gautneb, H., Meyer, G.B., Størseth, L.R. (2000). An overview of titanium deposits in Norway. *Norges geologiske undersøkelse Bulletin*, 436, 27–38.
- Korovkin, V.A., Turyleva, L.V., Rudenko, D.G., Juravlev, A.V., Kluchnikova, G.N. (2003). Mineral resources of the northwest Russian Federation. *VSEGEI Cartographic Factory*, Saint-Petersburg, 519 [in Russian].
- Korsakova, M., Krasotkin, S., Stromov, V., Iljina, M., Lauri, L., Nilsson, N.P. (2012). Metallogenic areas in Russian part of the Fennoscandian shield. In *Mineral Deposits and Metallogeny of Fennoscandia*, Eilu, P. (ed.). Geological Survey of Finland, Espoo.
- Kraemer, D., Viehmann, S., Banks, D., Sumoondur, A.D., Koeberl, C., Bau, M. (2019). Regional variations in fluid formation and metal sources in MVT mineralization in the Pennine Orefield, UK: Implications from rare earth elements and yttrium distribution, Sr-Nd isotopes and fluid inclusion compositions of hydrothermal vein fluorites. *Ore Geology Reviews*, 107, 960–972.
- Kramm, A. and Kogarko, L.N. (1994). Nd and Sr isotope signatures of the Khibina and Lovozero apatitic centres, Kola alkaline province, Russia. *Lithos*, 32, 225–242.

- Kramm, U., Kogarko, L.N., Kononova, V.A., Vartiainen, H. (1993). The Kola alkaline province of the CIS and Finland: Precise Rb-Sr ages define 380-360 Ma age range for all magmatism. *Lithos*, 30, 33–44.
- Kresten, P. and Morogan, V. (1986). Fenitization at the Fen complex, southern Norway. *Lithos*, 19, 27–42.
- Křištiak, J. and Záliš, Z. (1994). *Database of Radioactive Sites of the Czech Uranium Industry MS*. Geofond Praha, Holesovice.
- Krüger, J.C., Romer, R.L., Kämpf, H. (2013). Late cretaceous ultramafic lamprophyres and carbonatites from the Delitzsch Complex, Germany. *Chemical Geology*, 353, 140–150.
- Krumrei, T.V., Villa, I.M., Marks, M.A., Markl, G. (2006). A  $^{40}\text{Ar}/^{39}\text{Ar}$  and U/Pb isotopic study of the Ilímaussaq complex, South Greenland: Implications for the  $^{40}\text{K}$  decay constant and for the duration of magmatic activity in a peralkaline complex. *Chemical Geology*, 227, 258–273.
- Kunzendorf, H. and Secher, K. (1987). Dispersion of niobium and phosphorus in soil overlying the Qaqarsuk carbonatite complex, Southern West Greenland. *Journal of Geochemical Exploration*, 28, 285–296.
- Kusiak, M.A., Dunkley, D.J., Suzuki, K., Kachlik, V., Kedzior, A., Lekki, J., Oplustil, S. (2010). Chemical (non-isotopic) and isotopic dating of Phanerozoic zircon. A case study of durbachite from the Třebíč Pluton, Bohemian Massif. *Gondwana Research*, 17, 153–161.
- Lacan, F. and Jeandel, C. (2005). Neodymium isotopes as a new tool for quantifying exchange fluxes at the continent–ocean interface. *Earth and Planetary Science Letters*, 232(3), 245–257.
- Lacomme, A. and Fontan, F. (1971). Sur la présence de monazite dans les Pyrénées. *Comptes-Rendus de l'Académie des Sciences*, 272, 1193–1194.
- Lacomme, A., Hottin, A.M., Laval, M. (1993). La monazite grise du massif de l'Arize (Pyrénées françaises). Report, BRGM, R37041 GEO-SGN.
- Larsen, R.B. (2002). The distribution of rare-earth elements in K-feldspar as an indicator of petrogenetic processes in granitic pegmatites: Examples from two pegmatite fields in southern Norway. *Canadian Mineralogist*, 40, 137–151.
- Larsen, A.O. (ed.) (2010). *The Langesundsfjord: History, Geology, Pegmatites and Minerals*. Verlag, Berlin.
- Larsen, L.M. and Sørensen, H. (1987). The Ilímaussaq intrusion-progressive crystallization and formation of layering in an agpaitic magma. In *Alkaline Igneous Rocks*, Fitton, J.G. and Upton, B.G.J. (eds). Geological Society Publications, London.
- Larsen, L.T., Rex, D., Secher, K. (1983). The age of carbonatites, kimberlites and lamprophyres from southern West Greenland: Recurrent alkaline magmatism during 2500 million years. *Lithos*, 16, 215–221.

- Larsen, M., Piasecki, S., Surlyk, F. (2003). Stratigraphy and sedimentology of a basement-onlapping shallow marine sandstone succession, the Charcot Bugt Formation, Middle-Upper Jurassic, East Greenland. *Geological Survey of Denmark and Greenland Bulletin*, 1, 893–930.
- Larsen, B.T., Olausson, S., Sundvoll, B., Heeremans, M. (2008). The Permo-Carboniferous Oslo Rift through six stages and 65 million years. *Episodes*, 31, 52–58.
- Lauri, L.S., Eilu, P., Brown, T., Gunn, G., Kalvig, P., Sievers, H. (2018). Identification and quantification of primary CRM resources in Europe. Report, SCRREEN Deliverable 3.1.
- Laval, M. and Dromart, G. (1990). Les terres rares dans les shales noirs mésozoïques. Report, BRGM, DAM/DEX 1756.
- Laval, M., Prian, J.P., Hottin, A.M., Orgeval, J.J. (1990). Les rare earths dans les formations cambriennes des Cévennes et de la Montagne Noire (Massif central français). Report, BRGM, DAM/DEX R31672.
- Le Bas, M.J. (1981). Carbonatite magmas. *Mineralogical Magazine*, 44(334), 133–140.
- Le Maitre, R.W., Streckeisen, A., Zanettin, B., Le Bas, M., Bonin, B., Bateman, P. (2005). *Igneous Rocks: A Classification and Glossary of Terms*. Cambridge University Press.
- Lefebvre, G. (2017). Sursaut sur le marché des terres rares en 2017 [Online]. Available at: <http://www.mineralinfo.fr/ecomine/sursaut-marche-terres-rares-en-2017>.
- Lehijärvi, M. (1960). The alkaline district of Iivaara, Kuusamo, Finland. *Bulletin of the Geological Commission of Finland*, 185, 1–62.
- Lehtonen, M.I., Kujala, H., Kärkkäinen, N., Lehtonen, A., Mäkitie, H., Mänttari, I., Virransalo, P., Vuokko, J. (2005). Etelä-Pohjanmaan liuskealueen kallioperä. Summary: Pre-Quaternary rocks of the south Ostrobothnian schist belt. Report, Geological Survey of Finland.
- Lemarchand, R. (1970). Résultats des travaux de reconnaissance et premier pronostic sur les grès à zircon-rutile-monazite de Bailleul (Orne). Report, BRGM, 70-RME-011-RMM.
- Lemoine, M. (1984). *Les marges continentales actuelles et fossiles autour de la France*. Masson, Paris.
- Li, M.Y.H., Zhou, M.-F., Williams-Jones, A.E. (2020). Controls on the dynamics of rare earth elements during subtropical hillslope processes and formation of regolith-hosted deposits. *Economic Geology*, 115(5), 1097–1118.
- Lie, A. and Østergaard, C. (2011). The Fen carbonatite complex, Ulefoss, South Norway. Summary of historic work and data. *21st North in Commission for REE Minerals*, Svendborg.
- Lie, A. and Østergaard, C. (2014). The Fen rare earth element deposit, Ulefoss, South Norway. Summary of historic work and data. *21st North in Commission for REE Minerals*, Svendborg.

- Limbourg, Y. (1986). Découverte de monazite grise en nodules dans l'Eodévonien du Synclinorium de Neufchateau (Belgium). *Bulletin de la Société belge de géologie*, 95, 281–285.
- Lindberg, P.A. (1985). Fe-Ti-P mineralizations in the Larvikite-lardalite complex, Oslo Rift. In *Titaniferous Magnetite, Ilmenite and Rutile Deposits in Norway*, Korneliussen, A. and Robins, B. (eds). Norges geologiske undersøkelse Bulletin, Trondheim.
- Lindh, A. and Persson, P.O. (1990). Proterozoic granitoid rocks of the Baltic shield – Trends of development. In *Mid-Proterozoic Laurentia-Baltica*, Gower, C.F., Rivers, T., Ryan, A.B. (eds). Special Papers, Geological Association of Canada, St. John's, NL.
- Lipin, B.R. and McKay, G.A. (1989). Geochemistry and mineralogy of rare earth elements. Review in mineralogy. *Mineralogical Society of America*, 21, 348.
- Liu, H., Pourret, O., Guo, H., Bonhoure, J. (2017). Rare earth elements sorption to iron oxyhydroxide: Model development and application to groundwater. *Applied Geochemistry*, 87, 158–166.
- Lottermoser, B.G. (1990). Rare-earth element mineralization within the Mt. Weld carbonatite late-rite, Western Australia. *Lithos*, 24, 151–167.
- Lottermoser, B.G. (1992). Rare earth elements and hydrothermal ore formation processes. *Ore Geology Reviews*, 7(1), 25–41.
- Luckscheiter, B. and Morteani, G. (1980). Microthermometrical and chemical studies of fluid inclusions in minerals from Alpine veins from the penninic rocks of the central and western Tauern Window (Austria/Italy). *Lithos*, 13, 61–77.
- Luossavaara-Kiirunavaara, A.B. (2018). By Per Juntti, Mine waste will now be utilised. Press release, LKAB.
- Machacek, E. and Kalvig, P. (2016). Assessing advanced rare earth element-bearing deposits for industrial demand in the EU. *Resources Policy*, 49, 186–203.
- Maksimović, Z.J. (1976). Genesis of some Mediterranean karstic bauxite deposits. Travaux ICSOBA. Report, Comité International pour l'Étude des Bauxites, de l'Alumine et de l'Aluminium.
- Maksimović, Z.J. (1987). Trace elements in the Jurassic bauxites of Montenegro and their genetic significance. Special volume devoted to acad. *Acad. Montenegro Sci. Arts*, 47–60.
- Maksimović, Z.J. and Pantó, G. (1996). Authigenic rare earth minerals in karst-bauxites and karstic nickel deposits. In *Rare Earth Minerals: Chemistry, Origin and Ore Deposits*, Jones, A.P., Wall, F., Williams, C.T. (eds). Springer, Berlin.
- Maksimović, Z.J. and Roaldset, E. (1976). Lanthanide elements in some Mediterranean karstic bauxite deposits. Travaux ICSOBA. Report, Comité International pour l'Étude des Bauxites, de l'Alumine et de l'Aluminium.

- Maðour, J., Procházka, J., Vavóin, I. (1992). Zircon in sediments of the upper Lužnice River and its relationship to aeroradiometric anomalies. *Geol. Průzk.*, 34, 129–131.
- Marcos, A., Perez-Estaun, A., Pulgar, J.A., Bastida, F., Vargas, I. (1980). Mapa geológica de España. Scale 1:50,000 (Becerreá). *Instituto Geológico y Minero de España*, Sheet n°2.
- Marignac, C. (1880). Sur les terres de la samarskite. *Annales de Chimie et de Physique*, 5(20), 535–557.
- Marmo, V., Hoffren, V., Hytönen, K., Kallio, P., Lindholm, O., Siivola, J. (1966). On the granites of Honkamäki and Otanmäki, Finland, with special reference to the mineralogy of accessories. *Bulletin of the Geological Commission of Finland*, 221, 34.
- Marmolejo-Rodríguez, A.J., Caetano, M., de Pablo, H., Vale, C., Prego, R. (2008). Yttrium in the Vigo Ria (NW Iberian Peninsula): Sources, distribution, and background levels. *Ciencias Marinas*, 34, 399–406.
- Martens, P.N. and Seemann, U. (1973). Prospektionsbericht 1972. Traill Ø. Report, Nordisk Mineselskab A/S, Geological Survey of Denmark and Greenland archives, GEUS.
- Martinsson, O. (1997). Tectonic setting and metallogeny of the Kiruna greenstones. PhD Thesis, Luleå University of Technology.
- Martinsson, O. (2007). Apatite-iron deposits. Metallogeny and tectonic evolution of the northern Fennoscandian shield: Field trip guidebook. *Geological Survey of Finland*, 54, 113.
- McCreath, J.A., Finch, A.A., Simonsen, S.L., Donaldson, C.H., Armour-Brown, A. (2012). India-pendent ages of magmatic and hydrothermal activity in alkaline igneous rocks: The Motzfeldt Centre, Gardar Province, South Greenland. *Contribution to Mineralogy and Petrology*, 163, 967–982.
- McLennan, S.M. and Taylor, S.R. (2012). Geology, geochemistry, and natural abundances of the rare earth elements. In *The Rare Earth Elements: Fundamentals and Applications*, Atwood, D.A. (ed.). John Wiley & Sons, New York.
- Meert, J.G., Torsvik, T.H., Eide, E.A., Dahlgren, S. (1998). Tectonic significance of the Fen Province, S. Norway: Constraints from geochronology and palaeomagnetism. *Journal of Geology*, 106, 553–564.
- Meert, J.G., Walderhaug, H.J., Torsvik, T.H., Hendriks, B.W.H. (2007). Age and paleomagnetic signature of the Alnø carbonatite complex (NE Sweden): Additional controversy for the Neo-proterozoic paleoposition of Baltica. *Precambrian Research*, 154(3), 159–174.
- Melfos, V. and Voudouris, P.C. (2012). Geological, mineralogical and geochemical aspects for critical and rare metals in Greece. *Minerals*, 2, 300–317.
- Menzies, M., Seyfried, W., Blanchard, D. (1979). Experimental evidence of rare earth element immobility in greenstones. *Nature*, 282(5737), 398–399.
- Michard, A. and Albarède, F. (1986). The REE content of some hydrothermal fluids. *Chemical Geology*, 55(1), 51–60.

- Migdisov, A.A. and Williams-Jones, A.E. (2014). Hydrothermal transport and deposition of the rare earth elements by fluorine-bearing aqueous liquids. *Mineralium Deposita*, 49(8), 987–997.
- Migdisov, A.A., Williams-Jones, A.E., Wagner, T. (2009). An experimental study of the solubility and speciation of the rare earth elements (III) in fluoride- and chloride-bearing aqueous solutions at temperatures up to 300°C. *Geochimica et Cosmochimica Acta*, 73(23), 7087–7109.
- Migdisov, A.A., Guo, X., Nisbet, H., Xu, H., Williams-Jones, A.E. (2019). Fractionation of REE, U, and Th in natural ore-forming hydrothermal systems: Thermodynamic modeling. *The Journal of Chemical Thermodynamics*, 128, 305–319.
- Milodowski, A.E. and Zalasiewicz, J.A. (1991). Redistribution of rare earth elements during diagenesis of turbidite/hemipelagite mudrock sequences of Llandovery age from central Wales. *Geological Society Special Publication*, 57, 101–124.
- Mitchell, R.H. and Brunfelt, A.O. (1975). Rare earth element chemistry of the Fen alkaline complex, Norway. *Contributions to Mineralogical Petrology*, 52, 247–259.
- Mitrofanov, F.P., Zozulya, D.R., Bayanova, T.B., Levkovich, N.V. (2000). The world's oldest anorogenic alkali granitic magmatism in the Keivy structure on the Baltic Shield, *Dokl. Earth Sci.*, 374, 1145–1148.
- Moine, B., Fortuné, J.P., Moreau, P., Viguié, F. (1989). Comparative mineralogy, geochemistry, conditions of formation of two metasomatic talc and chlorite deposits: Trimouns (Pyrenees, France) and Rabenwald (eastern Alps, Austria). *Economic Geology*, 84, 1398–1416.
- Mondillo, N., Balassone, G., Boni, M., Chelle-Michou, C., Cretella, S., Mormone, A., Putzolu, F., Santoro, L., Scognamiglio, G., Tarallo, M. (2019). Rare earth elements (REE) in Al- and Fe-(oxy)-hydroxides in bauxites of Provence and Languedoc (Southern France): Implications for the potential recovery of REEs as by-products of bauxite mining. *Minerals*, 9, 504. doi: 10.3390/min9090504.
- Mongelli, G. (1997). Ce-anomalies in the textural components of Upper Cretaceous karst bauxites from the Apulian carbonate platform (southern Italy). *Chemical Geology*, 140(1), 69–79.
- Montero, P., Floor, P., Corretgé, G. (1998). The accumulation of rare-earth and high-field-strength elements in peralkaline granitic rocks: The Galiñeiro orthogneiss complex, northwestern Spain. *Canadian Mineralogist*, 36, 638–700.
- Montero, P., Bea, F., Corretgé, L.G., Floor, P., Whitehouse, M.J. (2009). U-Pb ion microprobe dating and Sr and Nd isotope geology of the Galiñeiro Igneous Complex: A model for the peraluminous/peralkaline duality of the Cambro-Ordovician magmatism of Iberia. *Lithos*, 107(3), 227–238.
- Morogan, V. (1988). Fertilization, hallmark of the ijolite-carbonatite magmatic association. PhD Thesis, Stockholm University.

- Morogan, V. and Woolley, A.R. (1988). Fenitization at the Alnö carbonatite complex, Sweden: Distribution, mineralogy and genesis. *Contributions to Mineralogy and Petrology*, 100, 169–182.
- Morteani, G. (1991). The rare earths; their minerals, production and technical use. *European Journal of Mineralogy*, 3(4), 641–650.
- Morteani, G. and Preinfalk, C. (1996). REE distribution and REE carriers in laterites formed on the alkaline complexes of Araxa and Catalao (Brazil). In *Rare Earth Minerals: Chemistry, Origin and Ore Deposits*, Jones, A.P., Wall, F., Williams, C.T. (eds). Springer, Berlin.
- Mosander, C.G. (1843). On the new metals, lanthanum and didymium, which are associated with cerium; and on erbium and terbium, new metals associated with yttria. *Philosophical Magazine*, 23(152), 241–254.
- Mott, A.V., Bird, D.K., Grove, M., Rose, N., Bernstein, S., Mackay, H., Krebs, J. (2013). Karrat Isfjord: A newly discovered Paleoproterozoic carbonatite-sourced REE deposit, central West Greenland. *Economic Geology*, 108(6), 1471–1488.
- Müller, A., Kearsley, A., Spratt, J., Seltmann, R. (2012). Petrogenetic implications of magmatic garnet in granitic pegmatites from southern Norway. *Canadian Mineralogist*, 50, 1095–1115.
- Müller, A., Spratt, J., Thomas, R., Williamson, B.J., Seltmann, R. (2018). Alkali-F-rich albite zones in evolved NYF pegmatites: The product of melt–melt immiscibility. *Canadian Mineralogist*, 56(4), 657–687.
- Mullis, J. (1996). P-T-t path of quartz formation in extensional veins of the Central Alps. *Schweiz. Mineral. Petrogr. Mitt.*, 76, 159–164.
- Mussett, A.E., Hodgson, B.N., Skehorn, R.R. (1987). Palaeomagnetism and age of the quartz-porphry intrusions, Isle of Arran, Scotland. *Scottish Journal of Geology*, 23, 9–22.
- Mutanen, T. (2011). Alkalikiviä ja appiniitteja. Raportti hankkeen “Magmatismi ja malminmuodos-tus II” toiminnasta 2002-2005. Report, Geological Survey of Finland.
- Nabyl, Z., Massuyeau, M., Gaillard, F., Tuduri, J., Iacono-Marziano, G., Rogerie, G., Le Trong, E., Di Carlo, I., Melleton, J., Bailly, L. (2020). A window in the course of alkaline magma differentiation conducive to immiscible REE-rich carbonatites. *Geochimica et Cosmochimica Acta*, 282, 297–323.
- Nadeau, O., Stevenson, R., Jébrak, M. (2016). Evolution of Montviel alkaline–carbonatite complex by coupled fractional crystallization, fluid mixing and metasomatism – Part I: Petrography and geochemistry of metasomatic aegirine–augite and biotite: Implications for REE–Nb mineralization. *Ore Geology Reviews*, 72, 1143–1162.
- Nazari-Dehkordi, T., Spandler, C., Oliver, N.H.S., Wilson, R. (2018). Unconformity-related rare earth element deposits: A regional-scale hydrothermal mineralization type of Northern Australia. *Economic Geology*, 113(6), 1297–1305.

- Nelson, D.R., Chivas, A.R., Chappell, B.W., McCulloch, M.T. (1988). Geochemical and isotopic systematics in carbonatites and implications for the evolution of ocean-island sources. *Geochimica et Cosmochimica Acta*, 52(1), 1–17.
- NGU (2013). Metallogenic map of Norway [Online]. Available at: <http://geo.ngu.no/kart/mineralressurser>.
- Nielsen, B.L. (1976). Economic minerals. In *Geology of Greenland*, Escher, A. and Watt, W.S. (eds). Geological Survey of Greenland, Copenhagen.
- Nielsen, T.F.D. (1979). The occurrence and formation of Ti-aegirines in peralkaline syenites. An example from the Tertiary ultramafic alkaline Gardiner complex, East Greenland. *Contrib. Mineral. Petrol.*, 69, 235–244.
- Nielsen, T.F.D. (1980). The petrology of a melilitolite, melteigite, carbonatite and syenite ring dike system, in the Gardiner complex, East Greenland. *Lithos*, 13, 181–197.
- Nielsen, T.F.D. (1987). Tertiary alkaline magmatism in East Greenland: A review. In *Alkaline Igneous Rocks*, Fitton, J.G. and Upton, B.G.J. (eds). Geological Society Special Publication, London.
- Nielsen, T.F.D. (1994). Alkaline dyke swarms of the Gardiner complex and the origin of ultramafic alkaline complexes. *Geochemistry International*, 31, 37–56.
- Nielsen, T.F.D. (2002). Palaeogene intrusions and magmatic complexes in East Greenland, 66 to 75°N. Report, GEUS.
- Nielsen, T.F.D. and Rosing, M.T. (1990). The Archaean Skjoldungen alkaline province, South-East Greenland. Report, Grønlands Geologiske Undersøgelse 148.
- Nielsen, B.K. and Steinfelt, A. (1979). Intrusive events at Kvanefjeld in the Ilímaussaq igneous complex. *Bulletin of the Geological Society of Denmark*, 27, 143–155.
- Nonnon, M. (1984). Découverte de monazite grise en nodules et d'or alluvionnaire dans le massif de la Croix-Scaille. *Bulletin de la Société belge de géologie*, 93, 307–314.
- Nonnon, M. (1989). Une nouvelle occurrence de monazite grise en Belgique. *Bulletin de la Société belge de géologie*, 98, 73–76.
- Notholt, A.J.G., Sheldon, R.P., Davidson, D.F. (eds) (1989). *Phosphate Deposits of the World. Volume 2: Phosphate Rocks Resources*. Cambridge University Press.
- Nuna Minerals (2010). Commercially interesting rare earth element (REE) grades at two separate projects [Online]. Available at: <http://nunaminerals.com>.
- Nykänen, J., Laajoki, K., Karhu, J. (1997). Geology and geochemistry of the early Proterozoic Kortejärvi and Laivajoki carbonatites, Central Fennoscandian Shield, Finland. *Bull. Soc. Finland*, 69(1–2), 5–30.
- Olerud, S. (1985). Metallogeny of Finnmark, North Norway. *Nor. Geol. Unders. Bull.*, 403, 183–196.

- Olerud, S. (1988). Davidite-loveringite in early Proterozoic albite felsite in Finnmark, north Norway. *Mineralogical Magazine*, 52, 400–402.
- Orris, G.J. and Grauch, R.I. (2002). Rare earth element mines, deposits, and occurrences. Report, USGS.
- Özlü, N. (1983). Trace-element content of “karst bauxites” and their parent rocks in the Mediterranean belt. *Mineralium Deposita*, 18, 469–476.
- Paarma, H. (1970). A new find of carbonatite in north Finland, the Sokli plug in Savukoski. *Lithos*, 3, 129–133.
- Papunen, H. (1986). Suomen metalliset malmiesiintymät. Suomen malmigeologia: Metalliset malmiesiintymät. *Geological Society of Finland*, 86, 49.
- Papunen, H. and Lindsjö, O. (1972). Apatite, monazite and allanite: Three rare earth minerals from Korsnäs, Finland. *Bulletin of the Geological Society of Finland*, 44, 123–129.
- Parák, T. (1973). Rare earths in the apatite iron ores of Lapland and some data about the Sr, Th and U content of these ores. *Economic Geology*, 68, 210–221.
- Parák, T. (1975). The origin of the Kiruna iron ores. *Sver. Geol. Unders.*, 8, 709.
- Parák, T. (1985). Phosphorus in different types of ore, sulfide in the iron deposit and the type and origin of ores at Kiruna. *Economic Geology*, 80, 646–665.
- Pardillo, F. and Soriano, V. (1929). Hallazgo de la monacita en las arenas de la Ría de Vigo. *Asoc. Esp. Prog. Cienc., Con. Barc.*, 4, 141.
- Parga Pondal, I. (1935). Arena monacítica de la Ría de Arosa (Galicia). *An. Soco Esp. Fís. Quím.*, 33, 466–469.
- Parseval, P. (1992). Minéralogie et géochimie du gisement de talc et chlorite de Trimouns (Pyrénées, France). PhD Thesis, Université Paul Sabatier, Toulouse.
- Parseval, P., Moine, B., Fortuné, J.P., Ferret, J. (1993). Fluid-mineral interactions at the origin of the Trimouns talc and chlorite deposit (Pyrénées, France). In *Current Research in Geology Applied to Ore Deposits*, Hach-Ali, F., Torres-Ruiz, J., Gervilla, F. (eds). Springer, Berlin.
- Parseval, P., Fontan, F., Aigouy, T. (1997). Composition chimique des minéraux de terres rares de Trimouns (France). *Comptes-Rendus de l'Académie des Sciences*, 324, 625–630.
- Pavel, C.C., Lacal-Arántegui, R., Marmier, A., Schüller, D., Tzimas, E., Buchert, M., Jenseit, W., Blagoeva, D. (2017). Substitution strategies for reducing the use of rare earths in wind turbines. *Resources Policy*, 52, 349–357.
- Pearce, N.J.G., Leng, M.J., Emeleus, C.H., Bedford, C.M. (1997). The origins of carbonatites and related rocks from the Grønnedal-Ika Nepheline Syenite complex, South Greenland: C-O-Sr isotope evidence. *Mineralogical Magazine*, 61, 515–529.
- Pearson, R.G. (1963). Hard and soft acids and bases. *Journal of the American Chemical Society*, 85(22), 3533–3539.

- Pergamalis, F., Karageorgiou, D.E., Koukoulis, A. (2001b). The location of Tl, REE, Th, U, Au deposits in the seafront zones of Nea Peramos-Loutra Eleftheron area, Kavala (N. Greece) using  $\gamma$  radiation. *Bulletin of the Geological Society of Greece*, 34, 1023–1029.
- Pergamalis, F., Karageorgiou, D.E., Koukoulis, A., Katsikis, I. (2001a). Mineralogical and chemical composition of sand ore deposits in the seashore zone Nea Peramos-Loutra Eleftheron Kavala (N. Greece). *Bulletin of the Geological Society of Greece*, 34, 845–850.
- Perissoratis, C., Moorby, S.A., Angelopoulos, I., Cronan, D.S., Papavasiliou, C., Konispoliatis, N., Sakellariadou, F., Mitropoulos, D. (1988). Mineral concentrations in the recent sediments of Eastern Macedonia, Northern Greece: Geological and geochemical considerations. In *Mineral Deposits within the European Community*, Boissonnas, J. and Omenetto, P. (eds). Springer, Berlin.
- Piilonen, P.C., McDonald, A.M., Poirier, G., Rowe, R., Larsen, A.O. (2018). The mineralogy and crystal chemistry of alkaline pegmatites in the Larvik plutonic complex, Oslo rift valley, Norway. Part 1. Magmatic and secondary zircon: Implications for petrogenesis from trace-element geochemistry. *Mineralogical Magazine*, 76(3), 649–672.
- Piret, P., Deliens, M., Pinet, M. (1990). La trimounsité-(Y), nouveau silicotitanate de terres rares de Trimouns, Ariège, France :  $(\text{TR})_2\text{Ti}_2\text{SiO}_9$ . *European Journal of Mineralogy*, 2, 725–729.
- Plant, J.A. and Jones, D.G. (1999). Development of regional exploration criteria for buried carbonate-hosted mineral deposits: A multidisciplinary approach in northern England. Report, BGS WP/91/1.
- Plant, J.A., Whittaker, A., Demetriades, A., De Vivo, B., Lexa, J. (2005). The geological and tectonic framework of Europe. In *Geochemical Atlas of Europe. Part 1: Background Information, Methodology and Maps*, Salminen, R. (ed.). FOREGS, GTK, Nottingham.
- Pourret, O. and Davranche, M. (2013). Rare earth element sorption onto hydrous manganese oxide: A modeling study. *Journal of Colloid and Interface Science*, 395, 18–23.
- Pourret, O. and Tuduri, J. (2017). Continental shelves as potential resource of rare earth elements. *Scientific Reports*, 7(1), 5857.
- Pozhilenko, V.I., Gavrilenko, B.V., Zhirov, D.V., Zhabin, S.V. (2002). *Geology of Ore Areas of the Murmansk Oblast*. KSC RAS, Apatity.
- Prego, R., Caetano, M., Vale, C., Marmolejo-Rodríguez, J. (2009). Rare earth elements in sediments of the Vigo Ria, NW Iberian Peninsula. *Continental Shelf Research*, 29(7), 896–902.
- Prego, R., Caetano, M., Bernárdez, P., Brito, P., Ospina-Alvarez, N., Vale, C. (2012). Rare earth elements in coastal sediments of the northern Galicia shelf: Influence of geological features. *Continental Shelf Research*, 35, 75–85.
- Pusstinen, K. (1971). Geology of the Siilinjärvi carbonatite complex, Eastern Finland. *Bulletin of the Geological Commission of Finland*, 249, 1–43.

- Rabiei, M., Chi, G., Normand, C., Davis, W.J., Fayek, M., Blamey, N.J.F. (2017). Hydrothermal rare earth element (xenotime) mineralization at Maw Zone, Athabasca Basin, Canada, and its relationship to unconformity-related uranium deposits. *Economic Geology*, 112(6), 1483–1507.
- Ram Resources Ltd. (2012). Ram Resources to build rare earths resource inventory at Motzfeldt with a \$3m capital raising [Online]. Available at: [www.ramresources.com.au](http://www.ramresources.com.au).
- Rasmussen, B., Buick, R., Taylor, W.R. (1998). Removal of oceanic REE by authigenic precipitation of phosphatic minerals. *Earth and Planetary Science Letters*, 164(1), 135–149.
- Rauchenstein-Martinek, K., Wagner, T., Wälle, M., Heinrich, C. (2014). Gold concentrations in metamorphic fluids: A LA-ICPMS study of fluid inclusions from the Alpine orogenic belt. *Chemical Geology*, 385, 70–83.
- Read, D., Cooper, D.C., McArthur, J.M. (1987). The composition and distribution of nodular monazite in the Lower Palaeozoic rocks of Great Britain. *Mineralogical Magazine*, 51, 271–280.
- Reed, G.C. (2013). Amended and restated technical report for Olserum REE deposit, southern Sweden. Report, Prepared for Tasman Metals Ltd. by Reed Leyton Consulting.
- Renberg, R. (2014). Recovery of Rare Earth elements from magnetic waste in the WEEE recycling industry and tailings from the iron ore industry. Project “REEcovery”, Luleå University of Technology [Online]. Available at: [www.ltu.se/research/subjects/Malmgeologi/Forskningsprojekt/REEcover?l=en](http://www.ltu.se/research/subjects/Malmgeologi/Forskningsprojekt/REEcover?l=en).
- Rillard, J., Pourret, O., Censi, P., Inguaggiato, C., Zuddas, P., Toulhoat, P., Gombert, P., Brusca, L. (2019). Behavior of rare earth elements in an aquifer perturbed by CO<sub>2</sub> injection: Environmental implications. *Science of the Total Environment*, 687, 978–990.
- Roadset, E. (1973). Rare earth elements in Quaternary clays of the Numedal area, southern Norway. *Lithos*, 6(4), 349–372.
- Rollat, A., Guyonnet, D., Planchon, M., Tuduri, J. (2016). Prospective analysis of the flows of certain rare earths in Europe at the 2020 horizon. *Waste Management*, 49, 427–436.
- Romer, R.L. and Smeds, S.A. (1994). Implications of U/Pb ages of columbite-tantalites from granitic pegmatites for the Palaeoproterozoic accretion of 1.90-1.85 Ga magmatic arcs to the Baltic Shield. *Precambrian Research*, 67(1), 141–158.
- Rosa, D., Salgueiro, R., Inverno, C., de Oliveira, D., Guimarães, F. (2010). Occurrence and origin of alluvial xenotime from Central Eastern Portugal (Central Iberian Zone/Ossa-Morena Zone). *Comunicações Geológicas*, 97, 63–72.
- Rosenblum, S. and Mosier, E.L. (1983). Mineralogy and occurrence of Europium-rich dark monazite. Report, US Geological Survey Professional Paper 1181.
- Rosing, M.T., Leshner, C.E., Thomsen, H.S., Blichert-Toft, J. (1992). Alkaline magmatism in the Archaean Skjoldungen province, East Greenland (abstract). *Eos Transactions, American Geophysical Union*, 73, 331.

- Roure, F., Brun, J.P., Colletta, B., van den Driessche, J. (1992). Geometry and kinematics of extensional structures in the Alpine Foreland Basin of southeastern France. *Journal of Structural Geology*, 14, 503–519.
- Rousseau, T.C.C., Sonke, J.E., Chmeleff, J., van Beek, P., Souhaut, M., Boaventura, G., Seyler, P., Jeandel, C. (2015). Rapid neodymium release to marine waters from lithogenic sediments in the Amazon estuary. *Nature Communications*, 6(1), 7592.
- Ryghaug, P. (1983). Geochemical exploration methods for niobium and rare earth elements at Sæteråsen, Vestfold volcanic area, Oslo Graben. *Norsk geologisk tidsskrift*, 63, 1–13.
- Sadeghi, M., Morris, G.A., Carranza, E.J.M., Ladenberger, A., Andersson, M. (2013). Rare earth elements distribution and mineralization in Sweden: An application of principal component analysis to FOREGS soil geochemistry. *Journal of Geochemical Exploration*, 133, 160–175.
- Sæther, E. (1957). *The Alkaline Rock Province of the Fen Area in Southern Norway*. Bruns Bokhandel i kommisjon, Trondheim.
- Sahlström, F., Jonsson, E., Högdahl, K., Troll, V.R., Harris, C., Jolis, E.M., Weis, F. (2019). Interaction between high-temperature magmatic fluids and limestone explains “Bastnäs-type” REE deposits in central Sweden. *Scientific Reports*, 9(1), 15203.
- Salgueiro, R., Inverno, C., de Oliveira, D.P.S., Guimarães, F., Lencastre, J., Rosa, D. (2020). Alluvial nodular monazite in Monfortinho (Idanha-a-Nova, Portugal): Regional distribution and genesis. *Journal of Geochemical Exploration*, 210, 106444.
- Sarapää, O. (1996). *Proterozoic Primary Kaolin Deposits at Virtasalmi, South-eastern Finland*. Geological Survey of Finland, Espoo.
- Sarapää, O. and Sarala, P. (2011). Mäkäräselkä REE-Au exploration target, Sodankylä, northern Finland. *25th International Applied Geochemistry Symposium 2011, 22-26 August 2011, Rovaniemi, Finland. Geochemical and Indicator Mineral Exploration Methods and Ongoing Projects in the Glaciated Terrains in Northern Finland: Excursion Guide, 26-30 August 2011: Vuorimiesyhdistys-Finnish Association of Mining and Metallurgical Engineers*, Rovaniemi.
- Sarapää, O. and Sarala, P. (2013). Rare earth element and gold exploration in glaciated terrain – Example from the Mäkärä area, Northern Finland. *Geochemistry: Exploration, Environment, Analysis*, 13, 131–143.
- Sarapää, O., Al Ani, T., Lahti, S.I., Lauri, L.S., Sarala, P., Torppa, A., Kontinen, A. (2013). Rare earth exploration potential in Finland. *Journal of Geochemical Exploration*, 133, 25–41.
- Saunders, A.D., Fitton, J.G., Kerr, A.C., Norry, M.J., Kent, R.W. (1997). The North Atlantic Igneous Province. In *Large Igneous Provinces. Geophysical Monograph*, Mahoney, J.J. and Coffin, M.F. (eds). American Geophysical Union, Washington.

- Schärer, U., de Parseval, P., Polvé, M., de Saint-Blanquat, M. (1999). Formation of the Trimouns talc-chlorite deposit (Pyrenees) from persistent hydrothermal activity between 112 and 97 Ma. *Terra Nova*, 11, 30–37.
- Schassberger, H.T. and Newall, G.C. (1980). The east Greenland molybdenum project 1979. Internal NM-report, AMAX.
- Schassberger, H.T. and Spieth, V. (1978). Molybdenum exploration in NE Greenland 1977. Internal NM-report, AMAX.
- Schaub, H.P. (1942). Zur Geologie der Traill Insel (Nordost-Grønland). *Eclogae Geol. Helv.*, 35, 1–54.
- Scherer, E., Münker, C., Mezger, K. (2001). Calibration of the lutetium-hafnium clock. *Science*, 293, 683–687.
- Scheyder, E. (2019). U.S. Army will fund rare earths plant for weapons development. *Reuters* [Online]. Available at: <https://www.reuters.com/article/us-usa-rareearths-army-exclusive-idUSKBN1YF0HU>.
- Scheyder, E. (2020). Pentagon resumes rare earths funding program after review. *Reuters* [Online]. Available at: <https://uk.reuters.com/article/us-usa-rareearths/pentagon-resumes-rare-earths-funding-program-after-review-idUSKCN24M2Z4>.
- Schilling, J., Wu, F.Y., McCammon, C., Wenzel, T., Marks, M.A.W., Pfaff, K., Jacob, D.E., Markl, G. (2011). The compositional variability of eudialyte-group minerals. *Miner. Magazine*, 75, 87–115.
- Schleicher, H., Keller, J., Kramm, U. (1990). Isotope studies on alkaline volcanics and carbonatites from the Kaiserstuhl, Federal Republic of Germany. *Lithos*, 26, 21–35.
- Schoenberg, J. and Markl, G. (2008). The magmatic and fluid evolution of the Motzfeldt intrusion in South Greenland: Insights into the formation of agpaitic and miaskitic rocks. *Journal of Petrology*, 49, 1549–1577.
- Sebastian, D., Mancheri, N., Tukker, A., Brown, T., Petavratzi, E., Espinoza, L. (2017). Report on the current use of critical raw materials. Report, Solutions for Critical Raw Materials – A European Expert Network (SCRREEN).
- Secher, K. (1976). Airborne radiometric survey between 66° and 69°N, southern and central West Greenland. *Grønlands Geologiske Undersøgelse*, 80, 65–67.
- Secher, K. (1980). Distribution of radioactive mineralization in central West Greenland. *Grønlands Geologiske Undersøgelse*, 100, 61–65.
- Secher, K. (1986). Exploration for the Sarfartoq carbonatite complex, southern West Greenland. *Grønlands geol. Unders.*, 128, 89–101.
- Secher, K. and Larsen, L.M. (1980). Geology and mineralogy of the Sarfartoq carbonatite complex, southern West Greenland. *Lithos*, 13, 199–212.

- Secher, K., Heaman, L.M., Nielsen, T.F.D., Jensen, S.M., Schjøth, F., Creaser, R.A. (2009). Timing of kimberlite, carbonatite, and ultramafic lamprophyre emplacement in the alkaline province located 64°-67° N in southern West Greenland. *Lithos*, 112S, 400–406.
- Seifert, W., Kämpf, H., Wasternack, J. (2000). Compositional variation in apatite, phlogopite and other accessory minerals of the ultramafic Delitzsch complex, Germany: Implication for cooling history of carbonatites. *Lithos*, 53, 81–100.
- Shaw, M.H. and Gunn, A.G. (1993). Rare earth elements in alkaline intrusions, North-West Scotland. Report, British Geological Survey.
- Shepherd, T.J., Darbyshire, D.P.F., Moore, G.R., Greenwood, D.A. (1982). Rare earth element and isotopic geochemistry of the North Pennine ore deposits. In *Symposium Jules Agard ; gîtes filoniens Pb-Zn-F-Ba de basse température du domaine varisque d'Europe et d'Afrique du Nord*, Anonymous (ed.). BRGM, Orléans.
- Sinisi, R. (2018). Mineralogical and geochemical features of Cretaceous bauxite from San Giovanni Rotondo (Apulia, Southern Italy): A provenance tool. *Minerals*, 8(12), 19.
- Šjöqvist, A.S.L., Cornell, D.H., Andersen, T., Erambert, M., Ek, M., Leijd, M. (2013). Three compositional varieties of rare-earth element ore: Eudialyte-group minerals from the Norra Kärr alkaline complex, southern Sweden. *Minerals*, 3, 94–120.
- Škoda, R. and Novák, M. (2007). Y, REE, Nb, Ta, Ti-oxide ( $AB_2O_6$ ) minerals from REL-REE euxenite-subtype pegmatites of the Třebíč Pluton, Czech Republic: Substitutions and fractionation trends. *Lithos*, 95, 43–57.
- Škoda, R., Novák, M., Houzar, S. (2006). Granitic NYF pegmatites of the Třebíč Pluton. *Acta Mus. Moraviae, Sci. Geol.*, 91, 129–176.
- Smeds, S.A. (1990). Regional trends in mineral assemblages of Swedish Proterozoic granitic pegmatites and their geological significance. *Geologiska Föreningens I Stockholm Förhandlingar*, 112, 227–242.
- Smirnov, V.I. (1977). *Ore Deposits of the USSR 3*. Pitman, San Francisco.
- Smith, R.T., Cooper, D.C., Bland, D.J. (1994). The occurrence and economic potential of nodular monazite in south-central Wales. Mineral Reconnaissance Programme Report 130. British Geological Survey Technical Report WF/94/1.
- Sørensen, H. (2001). The Ilímaussaq complex, South Greenland: Status of mineralogical research with new results. *Geology of Greenland Survey Bulletin*, 190, 55–64.
- Sørensen, L.L. and Kalvig, P. (2011). The rare earth element potential in Greenland. *Geology and Ore*, 20(2011).
- Sørensen, H., Hansen, J., Bondam, J. (1969). Preliminary account of the geology of the Kvanefjeld area of the Ilímaussaq intrusion, South Greenland. *GEUS*, 18, 1–40.
- Sørensen, H., Bailey, J.C., Rose-Hansen, J. (2011). The emplacement and crystallization of the U-Th-REE rich agpaitic and hyperagpaitic lujavrites at Kvanefjeld, Ilímaussaq alkaline complex, South Greenland. *Bulletin of the Geological Society of Denmark*, 59, 69–92.

- Steenfelt, A. (2012). Rare earth elements in Greenland: Known and new targets identified and characterised by regional stream sediment data. *Geochemistry: Exploration, Environment, Analysis*, 12, 313–326.
- Steenfelt, A., Hollis, J.A., Secher, K. (2006). The Tikiusaaq carbonatite: A new Mesozoic intrusive complex in southern West Greenland. *GEUS Bulletin*, 10, 41–44.
- Steensgaard, B.M., Kolb, J., Nielsen, T.F.D., Olsen, S.D., Pilbeam, L., Lieber, D., Clausen, A. (2010). The mineral resource assessment project, South-East Greenland: Year one. *Geological Survey of Denmark and Greenland Bulletin*, 20, 59–62.
- Steensgaard, B.M., Stendal, H., Kalvig, P., Hanghøj, K. (2016). Review of potential resources for critical minerals in Greenland. MiMa Report 2016/3.
- Stembera, J. (2012). Exploration projects in East Greenland. Oral presentation, Greenland Day Congress, CRGR (Czech Geological Research Group), Perth.
- Stendal, H. (2014). Critical minerals in Greenland. Oral presentation, Mines and Money Congress [Online]. Available at: [www.minesandmoney.com/hongkong](http://www.minesandmoney.com/hongkong).
- Stewart, J.W. (1970). Precambrian alkaline-ultramafic/carbonatite volcanism at Qagssiarssuk, South Greenland. *Bulletin Grønlands Geologiske Undersøgelse*, 84, 70.
- Sturesson, U. (1995). Llanvirnian (Ord.) iron ooids in Baltoscandia: Element mobility, REE distribution patterns, and origin of the REE. *Chemical Geology*, 125, 45–60.
- Sulovský, P. (2000). Comparison of chemistry of the Třebíč durbachite and other durbachites. *Geol. Vězk. Morave Slez. v r.*, 1999, 135–140.
- Tanbreez Mining Greenland A/S (2014). Tanbreez [Online]. Available at: <http://tanbreez.com>.
- Tasman Metals Ltd. (2010a). Tasman expands Otanmäki REE Project in Finland [Online]. Available at: [www.tasmanmetals.com](http://www.tasmanmetals.com).
- Tasman Metals Ltd. (2010b). Tasman expands rare earth element portfolio with the Bastnäs Project, Sweden [Online]. Available at: [www.tasmanmetals.com](http://www.tasmanmetals.com).
- Tasman Metals Ltd. (2010c). Tasman acquires the past producing Korsnäs REE-Pb Mine, Finland [Online]. Available at: [www.tasmanmetals.com](http://www.tasmanmetals.com).
- Tasman Metals Ltd. (2012). Tasman expands rare earth element project portfolio in Finland [Online]. Available at: [www.tasmanmetals.com](http://www.tasmanmetals.com).
- Tasman Metals Ltd. (2013). Tasman submits mining lease application over Olserum heavy rare earth element project, Sweden [Online]. Available at: [www.tasmanmetals.com](http://www.tasmanmetals.com).
- Tegner, C., Duncan, R.A., Bernstein, S., Brooks, C.K., Bird, D.K., Storey, M. (1998).  $^{40}\text{Ar}$ - $^{39}\text{Ar}$  geochronology of tertiary mafic intrusions along the East Greenland rifted margin: Relation to flood basalts and the Iceland hotspot track. *Earth and Planetary Science Letters*, 156, 75–88.

- Tegner, C., Brooks, C.K., Duncan, R.A., Heister, L.E., Bernstein, S. (2008).  $^{40}\text{Ar}$ - $^{39}\text{Ar}$  ages of intrusions in East Greenland: Rift-to drift transition over the Iceland hotspot. *Lithos*, 101, 480–500.
- Teisseyre, W. (1903). Der Paleozoische Horst von Podolien und die ihn umgehenden Senkungsfelder. Beiträge zur Paleontologie und Geologie Österreichs-Ungarn und d. Orients, 15, 29.
- Thirlwall, M.F. (1988). Geochronology of Late Caledonian magmatism in northern Britain. *Journal of the Geological Society of London*, 145, 951–967.
- Thomassen, B. (1988). The Motzfeldt 87 project. Report, Grønlands Geologiske Undersøgelse, 88/1.
- Thompson, P., Mussett, A.E., Dagley, P. (1987). Revised  $^{40}\text{Ar}$ - $^{39}\text{Ar}$  age for granites of the Mourne Mountains, Ireland. *Scottish Journal of Geology*, 23, 215–220.
- Thorpe, R.S., Potts, P.J., Sarre, M.B. (1977). Rare earth evidence concerning the origin of granites of the Isle of Skye, northwest Scotland. *Earth and Planetary Science Letters*, 36, 111–120.
- Thybo, H., Pharaoh, T., Guterch, A. (eds) (1999). Geophysical investigations of the trans-European suture zone. *Tectonophysics*, 314(1), 1–5.
- Thybo, H., Pharaoh, T., Guterch, A. (eds) (2002). The trans European suture zone II. *Tectonophysics*, 360, 314.
- Tichomirowa, M., Whitehouse, M.J., Gerdes, A., Götze, J., Schulz, B., Belyatsky, B.V. (2013). Different zircon recrystallization types in carbonatites caused by magma mixing: Evidence from U-Pb dating, trace element and isotope composition (Hf and O) of zircons from two Precambrian carbonatites from Fennoscandia. *Chemical Geology*, 353, 173–198.
- Tornquist, A.J.H. (1908). Die Feststellung des Südwestrandes des Baltisch Russischen Schildes. *Schriften der Physikalisch-Ökonomische Gesellschaft zu Königsberg*, 49, 1–12.
- Trägårdh, J. (1991). Metamorphism of magnesium-altered felsic volcanic rocks from Bergslagen, central Sweden. A transition from Mg-chlorite to cordierite-rich rocks. *Ore Geology Reviews*, 6, 485–497.
- Tuduri, J., Pourret, O., Chauvet, A., Barbanson, L., Gaouzi, A., Ennaciri, A. (2011). Rare earth elements as proxies of supergene alteration processes from the giant Imiter silver deposit (Morocco). In *Proceeding of the 11th Biennial SGA Meeting*, Barra, F., Reich, M., Campos, E., Tornos, F. (eds). Ediciones Universidad Católica del Norte, Antofagasta.
- Tuduri, J., Chevillard, M., Colin, S., Gloaguen, E., Gouin, J., Potel, S., Pourret, O. (2013). Formation of monazite-(MREE) from Paleozoic shales: Role of host rock chemical composition and organic material. *Mineral. Mag.*, 77, 2362.
- Tuduri, J., Charles, N., Guyonnet, G., Melleton, J., Pourret, P., Rollat, A. (2015). Project ANR ASTER. Rapport de Tâche 4. Potentialité de stocks géologiques de terres rares en Europe et au Greenland. Report, BRGM, RP-64910-FR.

- Tuduri, J., Lefebvre, G., Charles, N., Nabyl, Z., Gaillard, F., Pourret, O. (2020). Lumière sur la géologie des terres rares, pourquoi tant d'attraits ? *Géologues*, 204, 48–54.
- Tuisku, P. and Huhma, H. (2006). Evolution of migmatitic granulite complexes: Implications from Lapland Granulite Belt, Part II: Isotopic dating. *Bulletin of the Geological Society of Finland*, 78, 143–175.
- Tukiainen, T. (1986). Pyrochlore in the Motzfeldt centre of the Igaliko nepheline syenite complex, South Greenland. *Grønlands Geologiske Undersøgelse*, 86, 3.
- Tukiainen, T. (1988). Niobium-Tantalum mineralization in the Motzfeldt centre of the Igaliko nepheline syenite complex, South Greenland. In *Mineral Deposits within European Community*, Boissonnas, J. and Omenetto, P. (eds). Springer-Verlag, Berlin.
- Tukiainen, T., Bradshaw, C., Emeleus, C.H. (1984). Geological and radiometric mapping of the Motzfeldt Centre of the Igaliko Complex, South Greenland. *Grønlands Geologiske Undersøgelse*, 120, 78–83.
- Upton, B.G.J. (2013). Tectono-magmatic evolution of the younger Gardar southern rift, South Greenland. *Geological Survey of Denmark and Greenland Bulletin*, 29, 128.
- Upton, B.G.J. and Emeleus, C.H. (1987). Mid-Proterozoic alkaline magmatism in southern Greenland: The Gardar province. In *Alkaline Igneous Rocks*, Fitton, J.G. and Upton, B.G.J. (eds). Geological Society of London.
- Upton, B.G.J., Emeleus, C.H., Heaman, L.M., Goodenough, K.M., Finch, A.A. (2003). Magmatism of the mid-Proterozoic Gardar Province, South Greenland: Chronology, petrogenesis and geological setting. *Lithos*, 68, 43–65.
- Van Wambeke, L., Brinck, J.W., Deutzmann, W., Gonfiantini, R., Hubaux, A., Métais, D., Omenetto, P., Tongiorgi, E., Verfaillie, G., Weber, K. et al. (1964). *Les roches alcalines et les carbonatites du Kaiserstuhl*. European Atomic Energy Community, Rome.
- Vanhänen, E. (2001). Geology, mineralogy and geochemistry of the Fe-Co-Au(U) deposits in the Paleoproterozoic Kuusamo Schist Belt, northeastern Finland. *Geological Survey of Finland Bulletin*, 399, 283.
- Vaquero, C. (1979). Descubrimiento, por primera vez en España, de una monacita de facies aberrantes portado de Europa: Spain. *Boletín Geológico y Minero*, 90–4, 374–379.
- Vartiainen, H. (1980). The petrography, mineralogy and petrochemistry of the Sokli carbonatite massif, northern Finland. *Geological Survey of Finland Bulletin*, 313, 126.
- Vartiainen, H. (2001). Sokli carbonatite complex, northern Finland. Res Terrae. PhD Thesis, University of Oulu.
- Vartiainen, H. and Vitikka, A. (1994). The late stage dykes of the Sokli massif and their tectonic control. *Geochemistry International*, 31, 103–106.
- Vartiainen, H. and Woolley, A.R. (1974). The age of the Sokli carbonatite, Finland, and some relationships of the North Atlantic alkaline igneous province. *Bulletin of the Geological Society of Finland*, 46, 81–91.

- Vartiainen, H. and Woolley, A.R. (1976). The petrography, mineralogy and chemistry of the fenites of the Sokli carbonatite intrusion, Finland. *Geological Survey of Finland Bulletin*, 280, 89.
- Vazquez-Lopez, R. and Jézéquel, P. (2002). Expertise géologique des anomalies radioactives des plages de Camargue : plage de l’Espiquette et les Saintes Maries de la Mer Ouest. Report, BRGM, RP-51754-FR.
- Verhulst, A., Balaganskaya, E., Kirnarsky, Y., Demaiffe, D. (2000). Petrological and geochemical (trace elements and Sr-Nd isotopes) characteristics of the Paleozoic Kovdor ultramafic, alkaline and carbonatite intrusion (Kola Peninsula, NW Russia). *Lithos*, 51, 1–25.
- Verplanck, P.L., Mariano, A.N., Mariano, A.J. (2016). Rare earth element ore geology of carbonatites. In *Rare Earth and Critical Elements in Ore Deposits*, Verplanck, P.L. and Hitzman, M.W. (eds). Society of Economic Geologists, Littleton.
- Vidal-Legaz, B., Mancini, L., Blengini, G.A., Pavel, C., Marmier, A., Blagoeva, D., Latunussa, C., Nuss, P., Dewulf, J., Nita, V. et al. (2016). Raw Materials Scoreboard: European Innovation Partnership on Raw Materials. Report, Office of the European Union, Luxembourg.
- Vlasov, K.A., Kuz'menko, M.V., Yes'kova, Y.M. (1966). *The Lovozero Alkali Massif*. Hafner, New York.
- Vuotovesi, T. (1974). A new find of carbonatite in West Greenland, the Qaqarsuk ring dike. PhD Thesis, University of Helsinki.
- Wagner, T., Boyce, A.J., Erzinger, J. (2010). Fluid-rock interaction during formation of metamorphic quartz veins: A REE and stable isotope study from Rhenish massif, Germany. *American Journal of Science*, 310, 645–682.
- Waight, T., Baker, J., Willigers, B.W. (2002). Rb isotope dilution analyses by MC-ICPMS using Zr to correct for mass fractionation: Towards improved Rb-Sr geochronology? *Chemical Geology*, 186, 99–116.
- Walter, B.F., Parsapoor, A., Braunger, S., Marks, M.A.W., Wenzel, T., Martin, M., Markl, G. (2018). Pyrochlore as a monitor for magmatic and hydrothermal processes in carbonatites from the Kaiserstuhl volcanic complex (SW Germany). *Chemical Geology*, 498, 1–16.
- Walters, A.S. (2011). A reconnaissance investigation of REE concentrations in the North Pennine Orefield. BGS Report IR/11/050.
- Walters, A.S., Lusty, P., Hill, A. (2011). Rare earth elements. Report, BGS NERC.
- Walters, A.S., Hughes, H.S.R., Goodenough, K.M., Gunn, A.G., Lacinska, A. (2012). Rare earth mineralization in the Cnoc nan Cuilean intrusion of the Loch Loyal syenite Complex, northern Scotland. *Geophysical Research Abstracts*, 14, EGU2012 4587.
- Weidendorfer, D., Schmidt, M.W., Mattsson, H.B. (2017). A common origin of carbonatite magmas. *Geology*, 45, 507–510.

- Weihed, P., Eilu, P., Kolb, J., Sandstad, J.S. (2013). Metallic minerals deposits in Fennoscandia, Greenland and NW Russia. *SGA News Bulletin*, 33, 9–14.
- Weisenberger, T.B., Spürgin, S., Lahaye, Y. (2014). Hydrothermal alteration and zeolitization of the Fohberg phonolite, Kaiserstuhl Volcanic Complex, Germany. *International Journal of Earth Sciences*, 103, 2273–2300.
- Welin, E. (1980). Tabulation of recalculated radiometric ages published 1960–1979 for rocks and minerals in Sweden. *GFF*, 101, 309–320.
- Weng, Z.H., Jowitt, S.M., Mudd, G.M., Haque, N. (2013). Assessing rare earth element mineral deposit types and links to environmental impacts. *Applied Earth Science*, 122(2), 83–96.
- Weng, Z.H., Jowitt, S.M., Mudd, G.M., Haque, N. (2015). A detailed assessment of global rare earth element resources: Opportunities and challenges. *Economic Geology*, 110(8), 1925–1952.
- Wimmenauer, W. (1963). Beitriffe zur Petrographie des Kaiserstuhls. Teile VI–VII. *Neues Jahrb. Mineral., Abh.*, 99, 231–276.
- Wimmenauer, W. (1974). The alkaline province of Central Europe and France. In *The Alkaline Rocks*, Søensen, H. (ed.). Wiley, London.
- Windle, S. and Nesbitt, R. (1993). The genesis of grey monazites: Textural and geochemical evidence from Central Spain. In *Mineral Deposits Studies Group Annual Meeting 1993, Abstracts Volume*. The Natural History Museum, London.
- Wood, S.A. (1990a). The aqueous geochemistry of the rare-earth elements and yttrium 1: Review of available low-temperature data for inorganic complexes and the inorganic REE speciation of natural waters. *Chemical Geology*, 82, 159–186.
- Wood, S.A. (1990b). The aqueous geochemistry of the rare-earth elements and yttrium 2: Theoretical predictions of speciation in hydrothermal solutions to 350°C at saturation water vapor pressure. *Chemical Geology*, 88(1), 99–125.
- Woolley, A.R. (1987). *Alkaline Rocks and Carbonatites of the World. Part 1: North and South America*. Cambridge University Press.
- Woolley, A.R. and Kjarsgaard, B.A. (2008). Paragenetic types of carbonatites as indicated by the diversity and relative abundances of associated silicate rocks: Evidence from a global database. *Canadian Mineralogist*, 46(4), 741–752.
- Zepf, V. (2013). *Rare Earth Elements: A New Approach to the Nexus of Supply, Demand and Use: Exemplified along the Use of Neodymium in Permanent Magnets*. Springer, Berlin.
- Zhou, B., Li, Z., Chen, C. (2017). Global potential of rare earth resources and rare earth demand from clean technologies. *Minerals*, 7(11), 203.
- Zozulya, D.R., Bayanova, T.B., Eby, G.N. (2005). Geology and age of the late Archean Keivy alkaline province, northeastern Baltic Shield. *J. Geol.*, 113, 601–608.

- Zozulya, D.R., Bayanova, T.B., Serov, P.N. (2007). Age and isotopic geochemical characteristics of Archean carbonatites and alkaline rocks of the Baltic Shield. *Doklady Akademii Nauk*, 415, 383–388.
- Zozulya, D.R., Lyalina, L.M., Eby, N., Savchenko, Y.E. (2012). Ore geochemistry, zircon mineralogy, and genesis of the Sakharjok Y-Zr deposit, Kola Peninsula, Russia. *Geology of Ore Deposits*, 54, 81–98.
- Zozulya, D.R., Eby, N., Bayanova, T., Lyalina, L. (2013). Archean alkaline magmatism of OIB-type on the Baltic Shield. *30th International Conference on “Ore Potential of Alkaline, Kimberlite and Carbonatite Magmatism”*. GEOKHI RAS, Moscow.